University of Alberta

Mechanistic Investigations of *trans*-Ru-(diphosphine)H_2(diamine) Ketone Hydrogenation Catalysts

by

Robin James Hamilton ©

A thesis submitted to the Faculty of Graduate Studies and Research
in partial fulfillment of the requirements for the degree of

Doctor of Philosophy

Department of Chemistry

Edmonton, Alberta
Fall, 2008

Library and
Archives Canada

Published Heritage
Branch

395 Wellington Street
Ottawa ON K1A 0N4
Canada

Bibliothèque et
Archives Canada

Direction du
Patrimoine de l'édition

395, rue Wellington
Ottawa ON K1A 0N4
Canada

Your file Votre référence
ISBN: 978-0-494-46328-4
Our file Notre référence
ISBN: 978-0-494-46328-4

NOTICE:
The author has granted a non-exclusive license allowing Library and Archives Canada to reproduce, publish, archive, preserve, conserve, communicate to the public by telecommunication or on the Internet, loan, distribute and sell theses worldwide, for commercial or non-commercial purposes, in microform, paper, electronic and/or any other formats.

The author retains copyright ownership and moral rights in this thesis. Neither the thesis nor substantial extracts from it may be printed or otherwise reproduced without the author's permission.

AVIS:
L'auteur a accordé une licence non exclusive permettant à la Bibliothèque et Archives Canada de reproduire, publier, archiver, sauvegarder, conserver, transmettre au public par télécommunication ou par l'Internet, prêter, distribuer et vendre des thèses partout dans le monde, à des fins commerciales ou autres, sur support microforme, papier, électronique et/ou autres formats.

L'auteur conserve la propriété du droit d'auteur et des droits moraux qui protège cette thèse. Ni la thèse ni des extraits substantiels de celle-ci ne doivent être imprimés ou autrement reproduits sans son autorisation.

In compliance with the Canadian Privacy Act some supporting forms may have been removed from this thesis.

While these forms may be included in the document page count, their removal does not represent any loss of content from the thesis.

Conformément à la loi canadienne sur la protection de la vie privée, quelques formulaires secondaires ont été enlevés de cette thèse.

Bien que ces formulaires aient inclus dans la pagination, il n'y aura aucun contenu manquant.

Canada

To my loving family whose continual support made this possible.

Abstract

The putative intermediate *trans*-[Ru((*R*)-BINAP)(H)(η^2-H_2)((*R*,*R*)-dpen)]$^+$ (**1**, BINAP = 2,2'-bis(diphenylphosphino)-1,1'-binaphthyl, **2**, dpen = 1,2-diphenylethylenediamine, **3**) was synthesized in high yield at low temperature in 2-PrOH-d_8 rich solutions without H-D exchange of the hydride and η^2-H_2 ligands. Compound **1** has the highest H-D coupling constant of a η^2-H_2 ligand to date. Further, **1** was not catalytically active (4 atm H_2, 30 °C, 2000 equiv acetophenone, **4**) in the absence of base. Stoichiometric amounts of either *t*-BuOK or $NaBH_4$ activated **1** towards the hydrogenation to afford 1-phenylethanol (**5**) in 78, and 81% *ee* (*S*), respectively. Compound **1**, however, does not react with base in 2-PrOH-d_8 to form the expected dihydride, *trans*-[Ru((*R*)-BINAP)$(H)_2$((*R*,*R*)-dpen)] (**6**), but rather the 2-propoxide *trans*-[Ru((*R*)-BINAP)(H)(2-PrO)((*R*,*R*)-dpen)] (**7**).

Compound **1** decomposes in 2-PrOH-d_8 upon removal of H_2, and does not form the expected solvento compound *trans*-[Ru((*R*)-BINAP)(H)(2-PrOH-d_8)((*R*,*R*)-dpen)] (**8**). If **1** is prepared in THF-d_8, H_2 can be removed to form the solvento compound *trans*-[Ru((*R*)-BINAP)(H)(THF-d_8)((*R*,*R*)-dpen)] (**9**). Further, **9** reacts with H_2 to regenerate **1**. Compounds **1** and **9**, react with one equiv of *t*-BuOK in *wet* THF-d_8 to form the Ru-hydroxide compound *trans*-[Ru((*R*)-BINAP)(H)(OH)((*R*,*R*)-dpen)] (**10**), not the expected dihydride **6** and amide [Ru((*R*)-BINAP)(H)((*R*,*R*)-NH(CH(Ph))$_2$$NH_2$)] (**11**), respectively.

Compounds **7** and **10** are stable, and can be isolated and studied independently. Neither **7** nor **10** react with H_2 in THF-d_8 to form the expected dihydride **6**. Compounds **7** and **10**, however, react with *t*-BuOK in THF at -80 °C to form the hydrogen bonded species *trans*-[Ru((*R*)-BINAP)(H)(2-PrO)((*R*,*R*)-$NH_2(CH(Ph))_2NH{\bullet}{\bullet}{\bullet}H{\bullet}{\bullet}{\bullet}{}^{-}O$-*t*-Bu)] (**12**) and *trans*-[Ru((*R*)-BINAP)(H)(OH)((*R*,*R*)-($NH_2(CH(Ph))_2NH{\bullet}{\bullet}{\bullet}H{\bullet}{\bullet}{\bullet}{}^{-}O$-*t*-Bu)] (**13**), respectively. Compounds **12** and **13** react cleanly with H_2 to form the dihydride **6**. Further, **9** and **10** react with the stronger base, $((CH_3)_3Si)_2NK$, THF at -80 °C to form the amide **11** in high yields. Compound **11** reacts reversibly with H_2 to form the dihydride **6**.

Compound **6** reacts with one equivalent of **4** in THF-d_8 to form the alkoxide species *trans*-[Ru((*R*)-BINAP)(H)($PhCH(CH_3)O$)((*R*,*R*)-dpen)] (**14**), not the expected amide and 1-phenylethanol (**5**). The *ee* of the liberated 1-phenylethanol was 83% (*S*). Thus, the absolute configuration of the 1-phenylethoxide ligand in the major diastereomer of **14** is *S*, and the minor diastereomer of **14** was present in ~8.5 % abundance. Further, intermolecular trapping experiments indicate that **11** and **5** do not form as distinct species in solution. Additionally, compounds **6** and **11** racemize (*R*)-1-phenylethanol (**5'**) in THF. This result indicates the reduction is reversible. 2-PrOH solvent inhibits the racemization of **5**, maintaining the high *ee*.

Acknowledgement

I would like to express my gratitude to my supervisor Professor Steven H. Bergens for advice, teachings, and for providing me with an interesting, thought provoking research project. I would also like to thank him for knowing when to be a boss, and when to be a friend.

I would also like to thank all the great friends I have made during my Ph. D. studies. Specifically I would like to thank the members of the Bergens group, past and present. I would also like to thank Drs. Ross Witherell, Aaron Skelhorne, and Myrlene Gee for being truly great friends.

I would like to thank all the technical staff in the NMR, MS, Spectral Services, and the Glass Shop. I would specifically like to thank Mark Miskolzie and Glen Bigam. Their expertise was crucial to the characterization of many of the compounds presented in this dissertation.

Finally, I would like to thank my parents and brother for the support they have given me. I would also like to express my sincere thanks to my wife Tracy, and my children, Trent and Chantal. Their smiling faces at the end of a long day made the entire process worth the sacrifices that had to be made.

Table of Contents

Chapter 1: Introduction to Asymmetric Ketone Hydrogenation.

Enantioselective catalysis 1

Metal catalyzed carbonyl hydrogenation mechanisms 3

H_2–hydrogenation of ketones by the inner-sphere mechanism without ligand assistance (HI) 6

H_2–hydrogenation of ketones by the inner-sphere mechanism with ligand assistance (HIL) 10

H_2–hydrogenation of ketones by the outer-sphere mechanism without ligand assistance (HO) 11

H_2–hydrogenation of ketones by the outer-sphere mechanism with ligand assistance (HOL) 13

Transfer-hydrogenation of ketones by the inner-sphere mechanism without ligand assistance (TI) 16

Transfer-hydrogenation of ketones by the inner-sphere mechanism with ligand assistance (TIL) 18

Transfer-hydrogenation of ketones by the outer-sphere mechanism without ligand assistance (TO) 20

Transfer-hydrogenation of ketones by the outer-sphere mechanism with ligand assistance (TOL) 21

Summary 22

References 24

Chapter 2: A Ruthenium-Dihydrogen Putative Intermediate in Ketone Hydrogenation. 27
Introduction 27
Results and Discussion 33
Conclusions 40
Materials and Methods 41
References 45
Chapter 3: An unexpected possible role of base in asymmetric catalytic hydrogenations of ketones. Synthesis and characterization of several key catalytic intermediates. 48
Introduction 48
Results and Discussion 58
Conclusions 69
Materials and Methods 70
References 83
Chapter 4: Direct Observations of the Bifunctional Ligand-Assisted Addition Step in an Enantioselective Ketone Hydrogenation. 85
Introduction 85
Results and Discussion 110
Conclusions 125
Materials and Methods 128
References 143

Chapter 5: Summary and future work. 146

Summary 146

Future Work 154

References 160

Appendix 1: NMR spectra. 163

List of Tables

Chapter 1

No tables

Chapter 2

Table 2.1: Noyori *et al.*'s hydrogenation results. 29

Table 2.2: Hydrogenation of acetophenone using *trans*-[Ru((*R*)-BINAP)(H)(η^2-H_2)((*R*,*R*)-dpen)]$^+$ in the presence and absence of base. 40

Chapter 3

No tables

Chapter 4

No tables

Chapter 5

No tables

Appendix 1

No tables

List of Figures

Chapter 1

Figure 1.1: Hypothetical enantioselective catalytic mechanisms with different enantioselective steps. 2

Figure 1.2: Classification of the different mechanisms for the reduction of polar bonds. 4

Chapter 2

Figure 2.1: Representative list of ligands used in Noyori *et al.*'s catalyst system. 27

Figure 2.2: Examples of substrates hydrogenated by Noyori *et al.*'s Ru(diphosphine)X_2(diamine) catalysts systems. 28

Figure 2.3: Proposed hydrogen exchange mechanism in *cis*-[(phosphine)$_2$Ru(H)(η^2-H_2)(diamine)]$^+$compounds. 35

Figure 2.4: Orbital interactions and the relationship between H-H bond distance and lability. 37

Chapter 3

Figure 3.1: Preparation of model amide compounds. 53

Figure 3.2: Deuterium exchange reactions in model compounds. 53

Figure 3.3: Stoichiometric addition of acetophenone to a model dihydride catalyst. 54

Figure 3.4: Reaction between acetophenone and a model amide. 55

Figure 3.5: Reaction of 1-phenylethanol and a model amide. 56

Figure 3.6: Proposed mechanism of akoxide formation. 57

Figure 3.7: Proposed intramolecular hydrogen bonding in the 2-propoxide compound. 61

Figure 3.8: Proposed intramolecular hydrogen bonding in the hydroxide compound. 63

Chapter 4

Figure 4.1: Formation of Ru-diphenylmethoxide. 87

Figure 4.2: KIE for the reduction of benzaldehyde by Shvo's catalyst. 88

Figure 4.3: KIE for the oxidation of 1-(4-fluorophenyl)ethanol. 88

Figure 4.4: Comparison of Bäckvall's (bottom) and Casey's (top) intramolecular trapping experiments. 96

Figure 4.5: Pseudo-symmetric imine and the symmetrical diamine produced upon hydrogenation. 98

Figure 4.6: Potential trapping products and their expected ratios. 100

Figure 4.7: Reduction of acetophenone by model compounds in the absence of hydrogen. 102

Figure 4.8: Noyori *et al.*'s proposed mechanism for Ru-methoxide formation. 103

Figure 4.9: Meijer *et al.*'s proposed solvent assisted mechanism. 104

Figure 4.10: Morris *et al.*'s proposed alcohol assisted mechanisim. 106

Figure 4.11: Morris *et al.*'s theoretical study on the metal-ligand bifunctional mechanism. 108

Figure 4.12: Brandt *et al.*'s theoretical energies in the alcohol-assisted heterolytic cleavage of H_2. 109

Figure 4.13: ^{1}H NMR assignments for 1-phenylethoxide **14**. 112

Figure 4.14: Observed NOE's in the 1-phenylethoxide **14**. 113

Figure 4.15: Morris *et al.*'s preparation of the model 1-phenylethoxide. 115

Figure 4.16: Reaction of a model amide with 1-phenylethanol. 116

Figure 4.17: Intra- and intermolecular hydrogen bonding of the 1-phenylethoxide **14**. 117

Figure 4.18: Different pathways for the formation of 1-phenylethoxide **14**. 119

Chapter 5

No figures.

Appendix 1

Figure A1.1: ^{1}H NMR Ru–η^2-H_2 and Ru–H signals for complex **1**. 163

Figure A1.2: (A) ^{1}H NMR Ru–H signal trans to η^2–H_2 in complex **1**. (B) ^{1}H NMR Ru–H signal trans to η^2–D_2 in complex **89**, prepared by bubbling D_2 through solutions of **1** at -60 °C. 164

Figure A1.3: ^{31}P{^{1}H} NMR spectrum of **6** at –60 °C. 165

Figure A1.4: ^{1}H NMR spectrum (hydride region) of **6** at –60 °C. 166

Figure A1.5: ^{1}H NMR spectrum (0 to 10 ppm) of **6** at –60 °C. 167

Figure A1.6: ^{31}P{^{1}H} NMR spectrum of **11** at –60 °C. 168

Figure A1.7: ^{1}H NMR spectrum (hydride region) of **11** at –60 °C. 169

Figure A1.8: ^{1}H NMR spectrum (1 to 10 ppm) of **11** at –60 °C. 170

Figure A1.9: ^{1}H NMR spectrum (-1 to 10 ppm) of **14** at –80 °C. 171

Figure A1.10: ^{1}H NMR spectrum (hydride region) of **14** in the presence of ~1.5 equiv of excess base at –80 °C. 172

Figure A1.11: $^{31}P\{^1H\}$ NMR spectrum of **14** at –80 °C.

List of Schemes

Chapter 1

Scheme 1.1: General HI mechanism for the hydrogenation of ketones. 7

Scheme 1.2: HI mechanism for the hydrogenation of dialkly 3,3-dimethyloxaloacetate ketone substrates. 9

Scheme 1.3: Proposed hydrogenation of acetophenone *via* the HIL mechanism. 11

Scheme 1.4: Hydrogenation of ketones *via* the HO mechanism. 12

Scheme 1.5: Proposed HO mechanism for the hydrogenation of imminium ions. 13

Scheme 1.6: Proposed HOL mechanism using the Noyori-type catalyst. 14

Scheme 1.7: Proposed HOL mechanism using Shvo's catalyst. 15

Scheme 1.8: Proposed TI mechanism using a Ru-H catalyst. 16

Scheme 1.9: Proposed TI mechanism using a H-Ru-H catalyst. 17

Scheme 1.10: Bäckvall *et al.*'s proposed mechanism for the oxidation of acetophenone. 18

Scheme 1.11: Proposed TIL mechanism for ketone hydrogenation. 20

Scheme 1.12: Proposed TO mechanism for ketone hydrogenation. 21

Scheme 1.13: Proposed TOL mechanism for ketone hydrogenation. 22

Chapter 2

Scheme 2.1: Noyori *et al.*'s proposed base-free hydrogenation mechanism. 31

Chapter 3

Scheme 3.1: Noyori *et al.*'s proposed base-assisted hydrogenation mechanism. 49

Scheme 3.2: Summary of the putative intermediates reactivity. 69

Chapter 4

Scheme 4.1: Bäckvall *et al.*'s proposed mechanism for imine and ketone reduction. 90

Scheme 4.2: Casey *et al.*'s proposed mechanism for imine and ketone reduction. 91

Scheme 4.3: Proposed pathway for the formation of intermolecular trapping products. 94

Scheme 4.4: Proposed trapping experiments for the interception of the amide. 120

Scheme 4.5: Observed reactivity of the key intermediates in the catalytic cycle. 125

Scheme 4.6: Observed reactivity of the putative intermediates. 125

Chapter 5

Scheme 5.1: Observed reactivity of the putatuive intermediates. 149

Scheme 5.2: Possible route for the formation of 1-phenylethoxide **14**. 151

Scheme 5.3: Proposed route for the formation of observed intermediates. 152

Scheme 5.4: Proposed intramolecular trapping experiments. 154

Scheme 5.5: Proposed reactivity for the oxidation of deuterium-labeled 1-phenylethanol. 157

List of Equations

Chapter 1

Equation 1.1: Molecular hydrogen hydride source. 5
Equation 1.2: Donor molecule hydride source. 5
Equation 1.3: Inner-sphere hydride transfer. 5
Equation 1.4: Outer-sphere hydride transfer. 6
Equation 1.5: Ligand-assisted inner-sphere hydride transfer. 6
Equation 1.6: Ligand-assisted outer-sphere hydride transfer. 6

Chapter 2

Equation 2.1: Metal-ligand bifunctional mechanism. 30
Equation 2.2: Reaction of [Ru((*R*)-BINAP)(1-5-η-C_8H_{11})]$^+$ and hydrogen. 33
Equation 2.3: Reaction of *fac*-[Ru((*R*)-BINAP)(H)(2-PrOH)$_3$]$^+$ and (*R*, *R*)-dpen. 34
Equation 2.4: Reaction of *trans*-[Ru((*R*)-BINAP)(H)(η^2-H_2)((*R*,*R*)-dpen)]$^+$ and deuterium. 35
Equation 2.5: Reaction of *trans*-[Ru((*R*)-BINAP)(H)(η^2-H_2)((*R*,*R*)-dpen)]$^+$ and argon. 37
Equation 2.6: Reaction of *trans*-[Ru((*R*)-BINAP)(H)(η^2-H_2)((*R*,*R*)-dpen)]$^+$ and acetophenone. 38

Equation 2.7: Reaction of *trans*-[Ru((*R*)-tol-BINAP)(H)(η^2-H_2)((*R*,*R*)-dpen)]$^+$ and $NaBH_4$. 39

Chapter 3

Equation 3.1: Reaction of *trans*-Ru((*R*)-BINAP)(H)(Cl)(tmen) and base. 52

Equation 3.2: Reaction of *trans*-[Ru((*R*)-BINAP)(H)(η^2-H_2)((*R*,*R*)-dpen)]$^+$ and base in 2-PrOH. 59

Equation 3.3: Reaction of [Ru(H)(CNN)(dppb)] and benzophenone. 60

Equation 3.4: Generation of *trans*-[Ru((*R*)-BINAP)(H)(THF)((*R*,*R*)-dpen)]$^+$. 62

Equation 3.5: Generation of *trans*-[Ru((*R*)-BINAP)(H)(OH)((*R*,*R*)-dpen)]. 63

Equation 3.6: Intermolecular hydrogen bonding in a ruthenium-amine compound. 64

Equation 3.7: Intermolecular hydrogen bonding in a ruthenium-alkoxide and ruthenium-hydroxide compound. 65

Equation 3.8: Reaction of ruthenium-alkoxide and ruthenium-hydroxide compounds with base. 66

Equation 3.9: Equilibria between ruthenium-alkoxide or ruthenium-hydroxide with the ruthenium-amide. 67

Equation 3.10: Reaction of ruthenium-amide with D_2. 69

Equation 3.11: Reaction of *trans*-[Ru((*R*)-BINAP)(H)(η^2-H_2)((*R*,*R*)-dpen)]$^+$ and $((CH_3)_3Si)_2NK$ in THF. 69

Chapter 4

Equation 4.1: Metal-ligand bifunctional addition. 85

Equation 4.2: Reaction of [2,5-Ph_2-3,4-Tol_2(η^5-C_4COH)Ru$(CO)_2$(H)] and H_2N-Ph. 92

Equation 4.3: Reaction of [2,5-Ph_2-3,4-Tol_2(η^5-C_4COH)Ru$(CO)_2$(H)] and H_2N-*p*-$C_6H_4N{=}CHPh$. 95

Equation 4.4: Reaction of [2,3,4,5-Ph_4(η^5-C_4COH)Ru$(CO)_2$(H)] and 1,4-NH(CH_2Ph)(*c*-C_6H_{10})=NPh. 97

Equation 4.5: Reaction of [2,5-Ph_2-3,4-Tol_2(η^5-C_4COH)Ru$(CO)_2$(H)] and 1,4-($PhCH_2$)N=(*c*-C_6H_{10})^{15}NH(CH_2Ph). 99

Equation 4.6: Reaction of *trans*-[Ru((*R*)-BINAP)(H)(η^2-H_2)((*R*,*R*)-dpen)]$^+$ and base in THF. 110

Equation 4.7: Reaction of *trans*-[Ru((*R*)-BINAP)(H)(PhCH(CH_3)O)((*R*,*R*)-dpen)] and H_2. 111

Equation 4.8: Reaction of *trans*-[Ru((*R*)-BINAP)(H)(PhCH(CH_3)O)((*R*,*R*)-dpen)] and 2-PrOH. 122

Equation 4.9: Reaction of *trans*-[Ru((*R*)-BINAP)$(H)_2$((*R*,*R*)-dpen)] and acetophenone in the presence of 5 equiv of 2-PrOH. 123

Equation 4.10: Reaction of [Ru((*R*)-BINAP)(H)((*R*,*R*)-NH(CH(Ph))$_2$NH$_2$)] and a mixture of 2-PrOH, 5 equiv, and 1-phenylethanol, 1 equiv. 124

Chapter 5

Equation 5.1: Metal-ligand bifunctional addition. 146

Appendix 1

No equations

List of Abbreviations and Symbols

2-PrOH	2-propanol
2-Pr	2-propyl
BINAP	2,2'-bis(diphenylphosphino)-1,1'-binaphthyl
COSY	correlation spectroscopy
Cy	cyclohexyl
dpen	1,2-diphenylethylenediamine
dppe	1,2-diphenylphosphinoethane
dppb	1,4-bis(diphenylphosphino)butane
ee	enantiomeric excess
equiv	equivalent
ESI-MS	electrospray ionization mass spectroscopy
gc	gas chromatography
HCNN	6-(4'-methylphenyl)-2-pyridylmethylamine
HI	H_2-hydrogenation inner-sphere
HIL	H_2-hydrogenation inner-sphere ligand-assisted
HMQC	heteronuclear multiple-quantum coherence spectroscopy
HMRS	high-resolution mass spectrometry
HO	H_2-hydrogenation outer-sphere
HOL	H_2-hydrogenation outer-sphere ligand-assisted
Hz	hertz
KIE	kinetic isotope effect

LRMS	low-resolution mass spectrometry
MeOH	methanol
NMR	nuclear magnetic resonance
NOE	Nuclear Overhauser effect
NOESY	Nuclear Overhauser enhancement spectroscopy
om	overlapping multiplets
pica	α-picolylamine
Ph	phenyl
ppm	parts per million
t-Bu	*tert*-butyl
t-BuOH	*tert*-butanol
t-BuOK	potassium *tert*-butoxide
THF	tetrahydrofuran
TI	transfer-hydrogenation inner-sphere
TIL	transfer-hydrogenation inner-sphere ligand-assisted
TLS	turnover limiting step
tmen	1,2-tetramethylethylenediamine
TMS	tetramethylsilane
TO	transfer-hydrogenation outer-sphere
TOF	turnover frequency
TOL	transfer-hydrogenation outer-sphere ligand-assisted
tol-BINAP	2,2'-bis(di-p-tolylphosphino)-1,1'-binaphthyl
TON	turnover number

Ts-dpen	N-(*p*-toluenesulfonyl)-1,2-diphenylethylenediamine
α	alpha
β	beta
η	eta
λ	lambda
σ	sigma

Chapter 1: Introduction to Asymmetric Ketone Hydrogenation.

Enantioselective catalysis

The synthesis of optically pure chiral compounds is an integral component of the fine chemical industry. The biological activity of the enantiomers can be drastically different. As such, obtaining these chiral compounds in their optically pure form is essential for pharmaceutical, agrochemical, and the flavour and fragrance industries.[1,2] Traditionally these chemicals were produced *via* multistep non-catalytic processes that required multiple purification steps. Enantioselective catalysis, however, can produce the chiral compound faster, with less waste, and in very high enantiomeric excess (*ee*).

Enantioselective catalysis is the transformation of a prochiral compound preferentially into one enantiomer over the other using an optically pure catalyst. As enantiomers are equal in energy, there is no *thermodynamic* preference for a specific enantiomer. Enantioselective catalysis is thus a kinetic phenomenon, and the origins of catalytic enantioselection can only be determined from a thorough understanding of a reaction mechanism. Diastereomers differ in energy. If the prochiral substrate reacts with the optically pure catalyst to form different diastereomers, there will potentially be a kinetic preference for the formation of one enantiomer over the other. It is the relative rates of the first irreversible steps in the different pathways involving diastereomeric transition states that determines the *ee* of the catalytic cycle.

Figure 1.1 shows three different hypothetical enantioselective catalytic reaction mechanisms, differing only in the enantioselective step. In the top example, the enantioselective step is the formation of the catalyst-substrate adduct. The (*S*)-product is therefore the major product enantiomer since k_1 is greater than k_2, even if k_3 is less than k_4. In the middle example the (*R*)-product

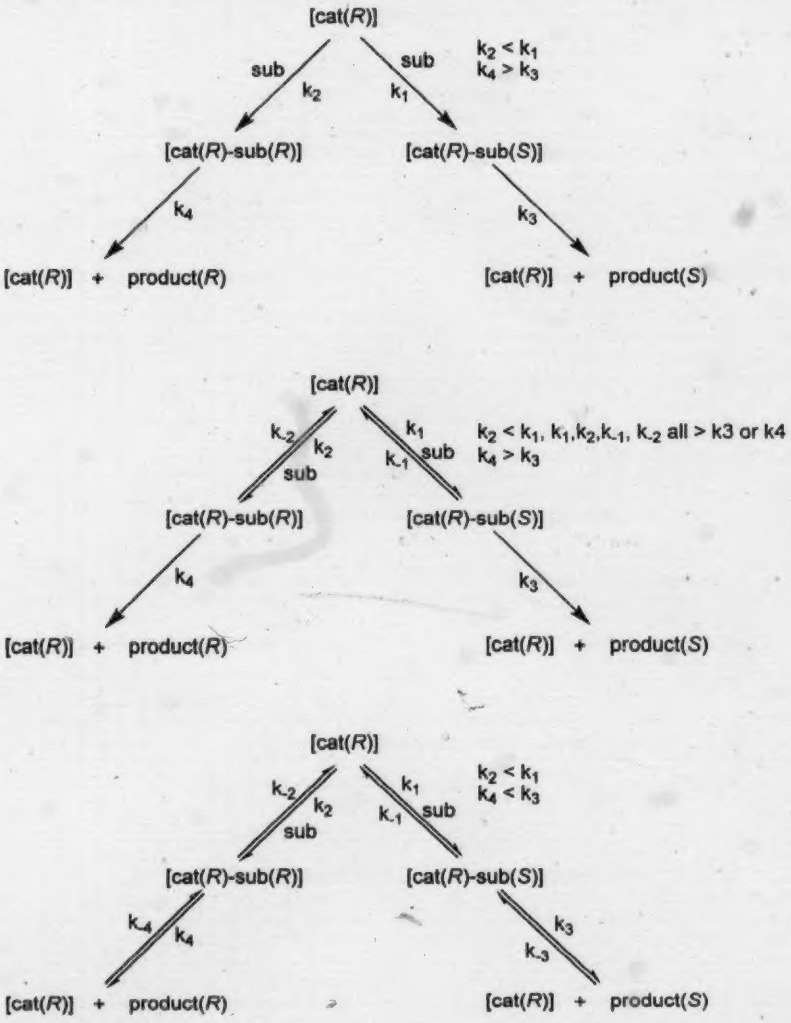
[cat(R)]
sub
k2
sub
k1
k2 < k1
k4 > k3
[cat(R)-sub(R)]
[cat(R)-sub(S)]
k4
k3
[cat(R)] + product(R)
[cat(R)] + product(S)
[cat(R)]
k-2
k2
sub
k1
k-1
sub
k2 < k1, k1,k2,k-1, k-2 all > k3 or k4
k4 > k3
[cat(R)-sub(R)]
[cat(R)-sub(S)]
k4
k3
[cat(R)] + product(R)
[cat(R)] + product(S)
[cat(R)]
k-2
k2
sub
k1
k-1
sub
k2 < k1
k4 < k3
[cat(R)-sub(R)]
[cat(R)-sub(S)]
k-4
k4
k3
k-3
[cat(R)] + product(R)
[cat(R)] + product(S)

Figure 1.1: Hypothetical enantioselective catalytic mechanisms with different enantioselective steps.

is the major product enantiomer since the first irreversible step is the product formation step. If the equilibrium is rapid, *i.e.* k_1, k_{-1}, k_2, and k_{-2} all > k_3 or k_4, then (*R*)-product is formed preferentially since k_4 is greater than k_3. In the bottom example, there is no enantioselective step since all the steps are reversible. There would be an initial kinetic product mixture where one enantiomer is in excess, but the eventual thermodynamic mixture would be racemic. The rate at which the product racemizes will depend, in part, on the relative rates of the reverse reactions *i.e.* k_{-1}, k_{-2}, k_{-3}, and k_{-4}.

Metal catalyzed carbonyl hydrogenation mechanisms

The mechanisms of homogeneous hydrogenations are extensively studied.[3] In a recent review, Morris *et al.* classified the mechanisms of catalytic hydrogenation of polar double bonds, *e.g.* ketones, based on three criteria: the hydrogen source for generation of a metal–hydride ([M]-H), the hydride transfer step, and the presence or absence of ancillary ligands that can assist the hydride transfer step (Figure 1.2).[4]

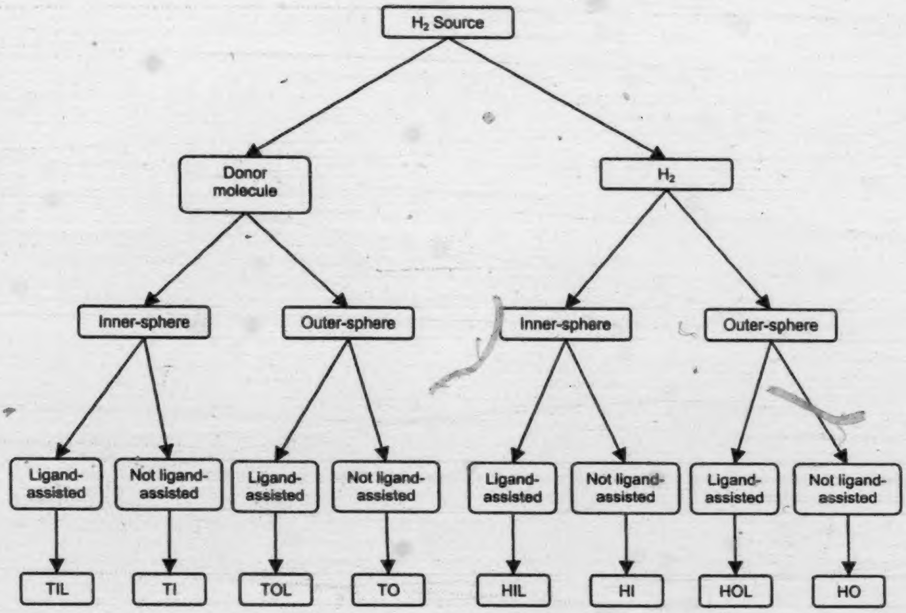
H_2 Source
Donor molecule
H_2
Inner-sphere
Outer-sphere
Inner-sphere
Outer-sphere
Ligand-assisted
Not ligand-assisted
Ligand-assisted
Not ligand-assisted
Ligand-assisted
Not ligand-assisted
Ligand-assisted
Not ligand-assisted
TIL
TI
TOL
TO
HIL
HI
HOL
HO

Figure 1.2: Classification of the mechanism of reduction of polar bonds based on hydrogen source (H or T), hydride transfer step (I or O) and the presence of ancillary ligand assistance (L).

The active catalyst contains a metal-hydride (*e.g.* [Ru-H]) generated from molecular hydrogen (H, Equation 1.1) or a donor hydrogen molecule (e.g. 2-propanol, T, Equation 1.2) to reduce, in this case, a ketone to an alcohol.[4]

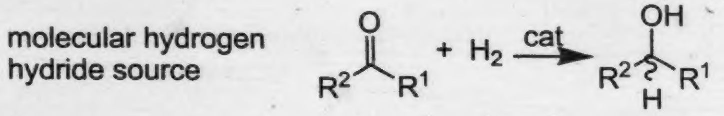
molecular hydrogen
hydride source
O
R2
R1
+ H2
cat
OH
R2
R1
H

Equation 1.1

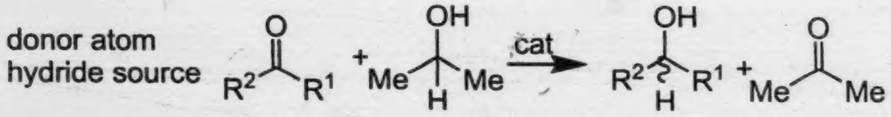
donor atom
hydride source
O
R2
R1
+
OH
Me
Me
H
cat
OH
R2
R1
H
+
O
Me
Me

Equation 1.2

The hydride transfer step can be classified as either inner (I) or outer (O) sphere.[4] In the inner-sphere mechanism, the carbonyl oxygen of the ketone coordinates to a vacant site on the metal. This activates the carbonyl carbon towards nucleophilic attack such that a *cis* hydride on the metal can migrate to the β-carbon (Equation 1.3). In the outer-sphere mechanism, a hydride on the metal is transferred to the carbonyl carbon without coordination of the ketone. The carbonyl carbon is typically activated towards nucleophilic attack by a Lewis acid (Equation 1.4).[4]

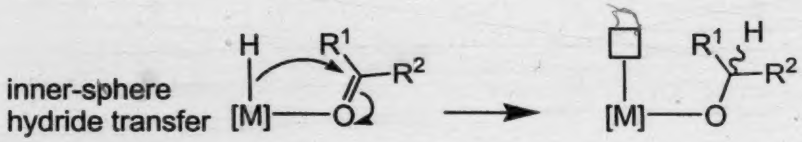
inner-sphere
hydride transfer
H
R1
R2
[M]
O
R1
H
R2
[M]
O

Equation 1.3

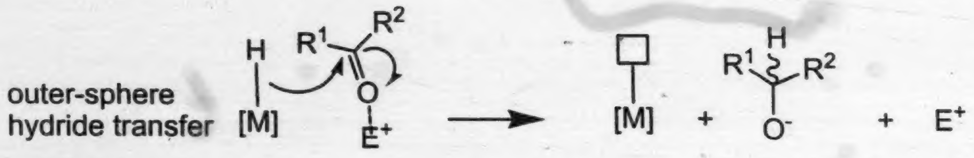
outer-sphere
hydride transfer
H
[M]
R1
R2
O
E+
[M]
+
H
R1
R2
O-
+
E+

Equation 1.4

Certain ancillary ligands can activate the carbonyl carbon towards nucleophilic attack. Ligands that contain an electrophile (typically H^+) that can interact with the carbonyl oxygen facilitate hydride transfer to the carbonyl carbon in both the inner and outer sphere mechanisms (Equations. 1.5 and 1.6).[4]

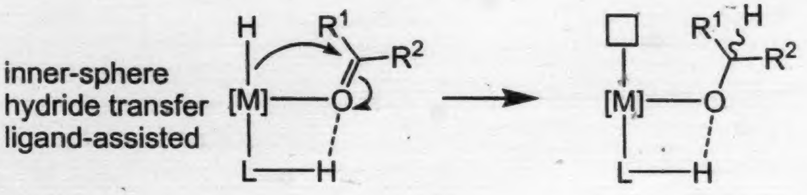
inner-sphere
hydride transfer
ligand-assisted
H
R1
R2
[M]
O
L
H
R1
H
R2
[M]
O
L
H

Equation 1.5

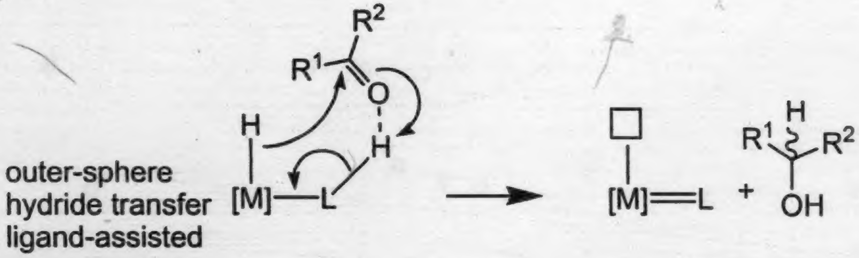
outer-sphere
hydride transfer
ligand-assisted
R2
R1
O
H
H
[M]
L
[M]
L
+
H
R1
R2
OH

Equation 1.6

H_2–hydrogenation of ketones by the inner sphere mechanism without ligand assistance (HI).

The active [M]-H species in the HI mechanism is typical prepared *in situ* from a suitable catalyst precursor. The [M]-H species must contain vacant coordination sites, or weakly bound ligands (e.g. solvent), to allow for substrate coordination, thereby activating the carbonyl carbon towards nucleophilic attack (Scheme 1.1). Hydride migration to the β-carbon forms a metal-alkoxide species with a vacant coordination site. H_2 then coordinates to the vacant site. Product elimination can occur *via* two pathways.[4] Simple protonation of the alkoxide oxygen by coordinated H_2 will liberate product alcohol and regenerate the active

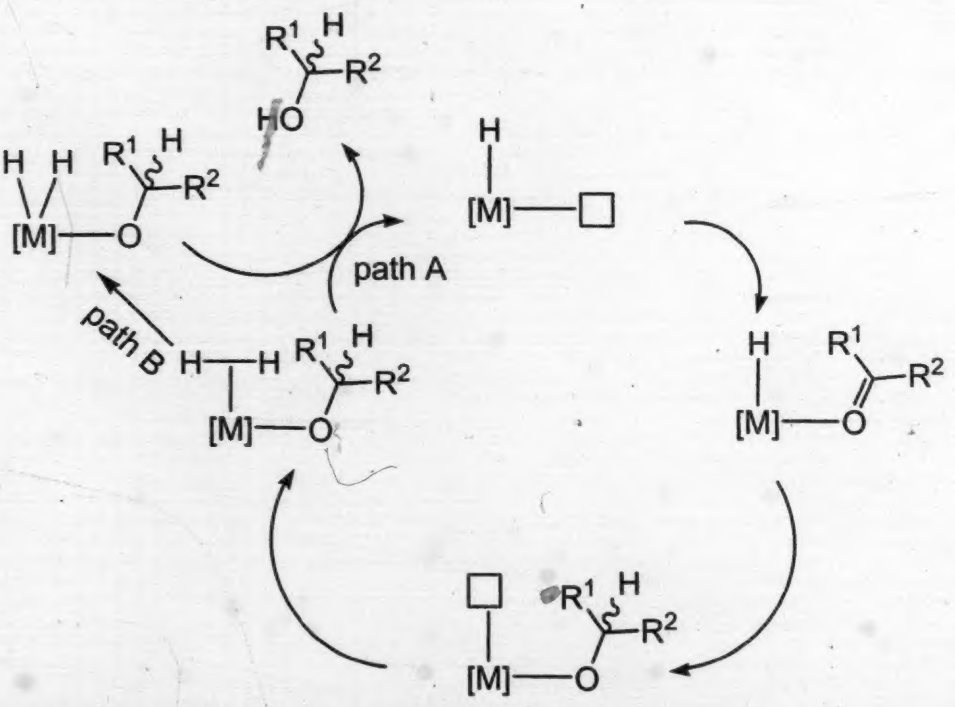

Scheme 1:1: General HI mechanism for the hydrogenation of ketones. Liberation of product alcohol can occur *via* protonation of the alkoxide (path A) or reductive elimination from a ruthenium-dihydride (path B).

[M]-H species. Alternatively, H_2 can undergo oxidative addition to generate a transient dihydride species that then reductively eliminates the product alcohol to regenerate the active catalyst.

Bergens *et al.* reported the first unambiguous ruthenium-alkoxide intermediate in ketone hydrogenation *via* the HI mechanism.[5] The required coordinatively unsaturated [Ru]-H species was generated *in situ* from the precursor [Ru((*R*)-BINAP)(MeCN)(η^5-C_8H_{11})]BF_4 (**15**). Compound **15** reacts with H_2 in coordinating solvents (THF, MeOH or Acetone = sol) to form [Ru((*R*)-BINAP)(H)(MeCN)$_n$(sol)$_{3-n}$]BF_4 (**16**) and cyclooctane. The labile solvento ligands rapidly furnish vacant coordination sites. The corresponding ruthenium-deuteride [Ru((*R*)-BINAP)(D)(MeCN)$_n$(sol)$_{3-n}$]BF_4 (**17**) is likewise formed when under a D_2 atmosphere. In either case, there is rapid (complete at –30 °C) formation of [Ru((*R*)-BINAP)(MeCN)(κ^3-OCHR^{1}R^2)]BF_4 (**18**) or [Ru((*R*)-BINAP)(MeCN)(κ^3-OCDR^{1}R^2)]BF_4 (**18''**). R^1 and R^2 contain ester functional groups that coordinate to Ru making the alkoxide tridentate (Scheme 1.2). Since the Ru–alkoxide is a coordinatively saturated 18–electron species, there is either desolvation of MeCN, or dissociation of a coordinated ester prior to coordination of H_2.[5] Alcohol is produced either by protonation of the alkoxide by coordinated H_2, or by oxidative addition of H_2 followed by reductive elimination of alcohol concomitant with regeneration of the active catalyst.

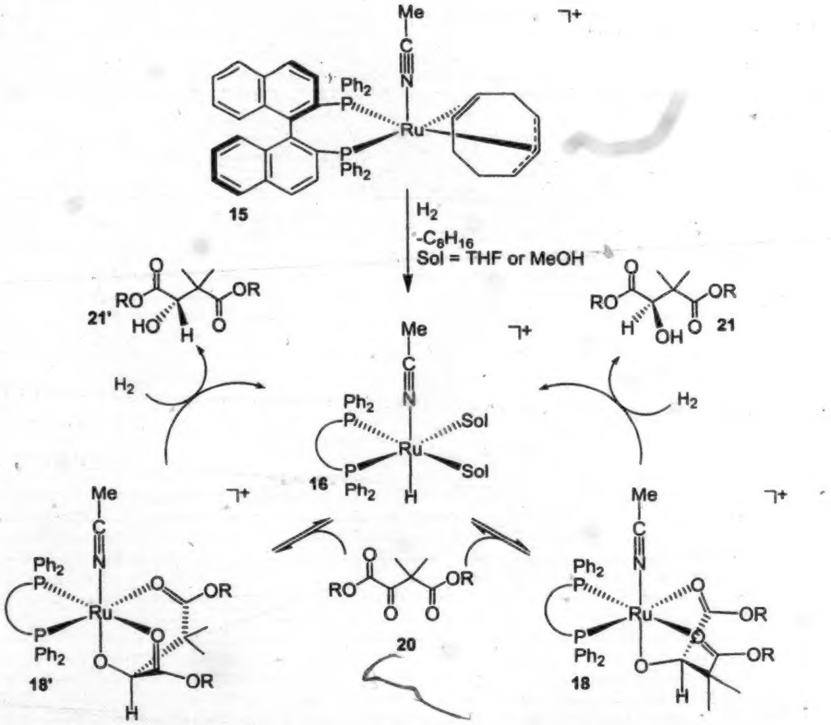

Scheme 1.2: HI mechanism for the hydrogenation of dialkly 3,3-dimethyloxaloacetate ketone substrates. R = Me, 2-Pr and ^{t}Bu.

The Ru–alkoxide species does not react stoichiometrically with H_2 unless elevated pressures and temperatures are employed (50 atm H_2, 50 °C).[5] The sole detectable product from the catalytic hydrogenation of di-*tert*-butyl 3,3-dimethyloxaloacetate (when R = ^{t}Bu) interrupted after four turnovers was the Ru–alkoxide species resulting from ketone–hydride insertion. Additionally, the rates of stoichiometric hydrogenolysis of the Ru–alkoxides are comparable to the turnover frequencies (TOF) of the catalytic hydrogenations (~ 1 turnover/h in THF or MeOH).[5] This result indicates that the reaction between Ru–alkoxide and H_2 to form the H_2 adduct is likely the TLS, and that subsequent product formation steps are rapid. Further, Ru–alkoxide formation is a reversible process.[5] When the deuterium labeled Ru–alkoxide reacts with H_2 (50 atm, 50

°C), there is H–D exchange at the alkoxide carbon in the product. The extent of exchange (~10-40%) depends on the ketone substrate and the solvent. Given that there is incomplete H–D exchange, the rate of β–hydride elimination is slower than the rate of hydrogenolysis of the Ru–alkoxide bond. The *ee*'s of the resulting alcohols (**21**) from catalytic hydrogenations were similar to the diasteriomeric excesses (*de*) of the Ru–alkoxide species. Additionally, the *ee*'s of the alcohols obtained from stoichiometric hydrogenolyses of the Ru–alkoxides at 50 atm of H_2 and 50 °C were nearly identical to the *ee* obtained from catalytic hydrogenation under the same conditions.[5]

H_2–Hydrogenation of ketones by the inner sphere mechanism with ligand assistance (HIL).

To the best of my knowledge, there are no confirmed reports of a ketone hydrogenation proceeding *via* the HIL mechanism. There are, however, several examples in which the HIL mechanism may be possible.

Noyori and coworkers observed that [Ru((*R*)-xyl-BINAP)(acetate)$_2$] (**22**, xyl-BINAP = 2,2′-bis(dixylylphosphino)-1,1′-binaphthyl, **23**) undergoes ligand exchange reactions with carboxylic acids, sodium or potassium salts of carboxylic acids, amino acids, phosphoric acids and hydroxyl phosphonic acids to make suitable catalyst precursors for the hydrogenation of ketones. The best results were obtained using **22** with phenylphosphonic acid present in a 1:2 ratio. Noyori proposed that a Ru–diphosphonate (**24**) forms *in situ* and then reacts with H_2 to form the active catalyst (Scheme 1.3).[1a] The oxygen of the coordinated ketone can interact with the OH group of the phosphonate ligand, thereby activating it towards nucleophilic attack. The reaction, however, requires harsh conditions (100 atm H_2, 100 °C, 18 h) to proceed to completion.[1a]

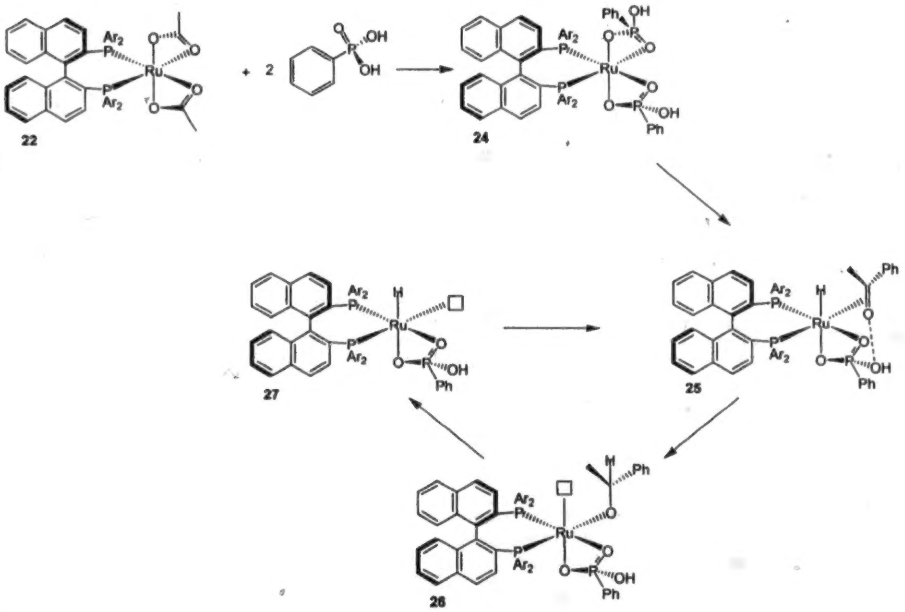

Scheme 1.3: Proposed hydrogenation of acetophenone *via* the HIL mechanism where Ar = xylyl.

H_2–Hydrogenation of ketones by the outer sphere mechanism without ligand assistance (HO).

There are relatively few examples of a hydrogenation catalyst operating *via* a HO type mechanism. In most cases, the carbonyl carbon is activated internally prior to nucleophilic attack from the metal hydride. Dihydrides of Mo and W (**28**) were proposed to first act as an acid, protonating the carbonyl oxygen and making the carbonyl carbon cationic (**29**, Scheme 1.4).[6] The metal–hydride (**30**) then attacks the activated carbon producing product alcohol. The metal dihydride is regenerated by reacting with H_2 in solution.

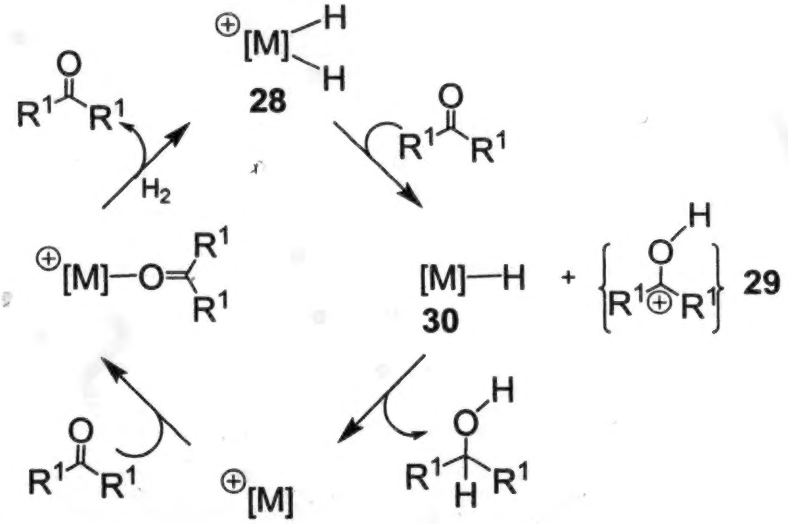

Scheme 1.4: Hydrogenation of ketones *via* the HO mechanism. [M] = [Cp(CO)$_2$(PR$_3$)Mo] or [Cp(CO)$_2$(PR$_3$)W] where R = Me, Ph, or Cy, R^1 = Et.

Magee *et al.* developed a ruthenium catalyst (**31**, Scheme 1.5) that is believed to hydrogenate iminium ions *via* a similar mechanism.[7] The substrate (**32**) itself carries an overall positive charge, activating the iminium carbon towards nucleophilic attack. Hydride transfer from ruthenium generates a basic amine (**33**) and **35** which then yields a new [Ru]–η^2–H_2 species (**34**) under an atmosphere of H_2. The coordinated H_2 ligand is sufficiently acidic to be deprotonated by the generated amine, resulting in a net hydrogenation of the iminium ion.[7]

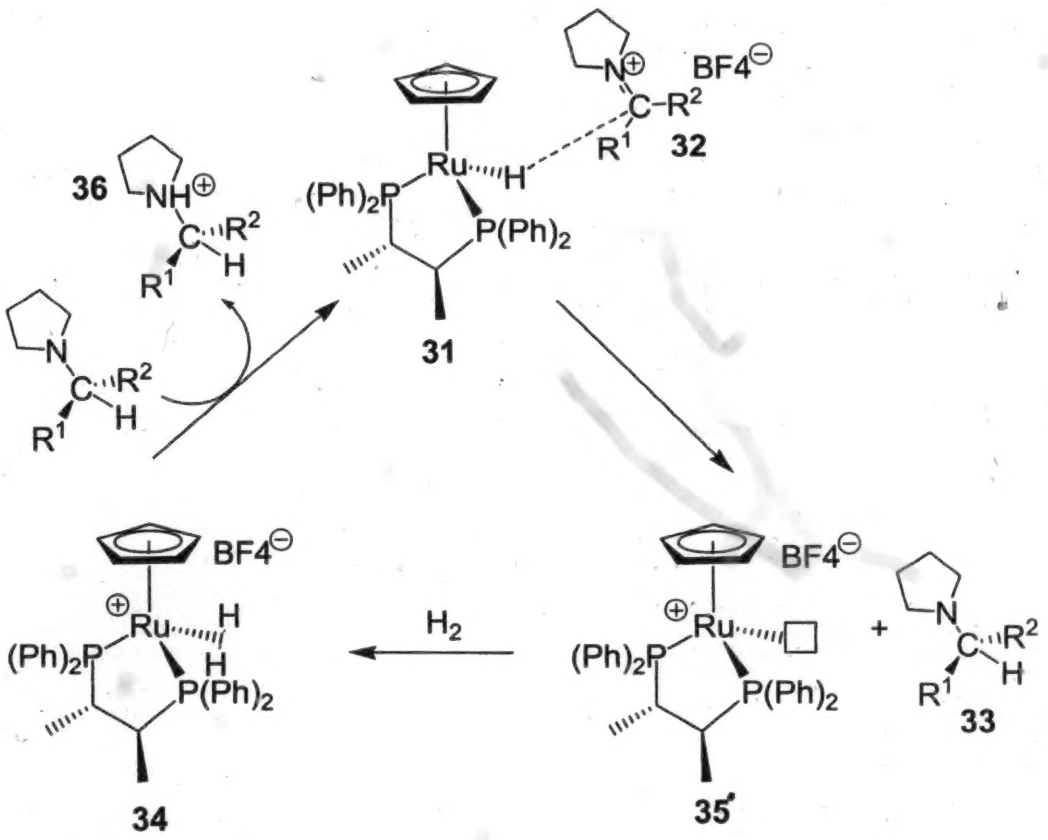

Scheme 1.5: Proposed HO mechanism of imminium hydrogenation.

H_2–Hydrogenation of ketones by the outer sphere mechanism with ligand assistance (HOL).

Catalysts operating *via* the HOL mechanism are amongst the most significant developments in ketone hydrogenation. Noyori *et al.* developed the catalyst systems *trans*-Ru(diphosphine)Cl_2(diamine) plus base in 2-PrOH that hydrogenate aryl-alkyl, vinyl-alkyl, and even several alkyl-alkyl ketones with high *ee*, turnover numbers and frequencies.[1,8] These catalysts contain a Ru–H/N–H motif and are proposed to operate *via* what Noyori termed the metal-ligand bifunctional mechanism. The active catalyst is *trans*-

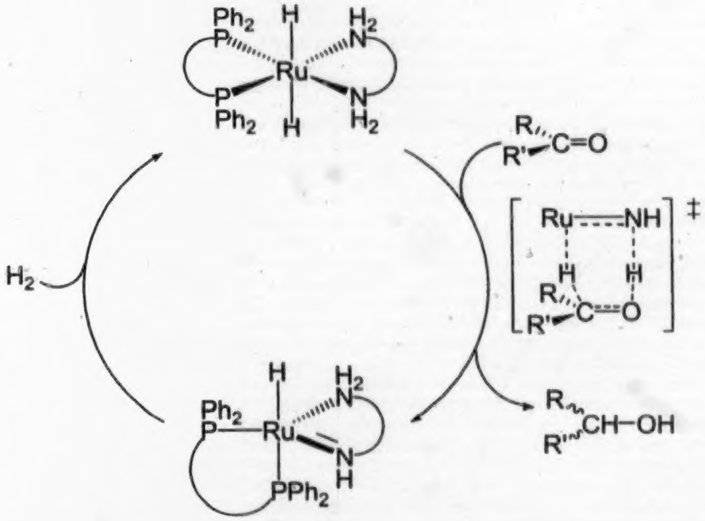

Scheme 1.6: Proposed HOL mechanism using the Noyori-type catalyst.

Ru(diphosphine)H_2(diamine) generated *in situ* (Scheme 1.6). Noyori proposed that the enantioselective step is a bifunctional addition of a nucleophilic hydride on Ru and a protic hydrogen on nitrogen to the carbon- and oxygen atoms, respectively, of the ketone through a pericyclic 6-membered transition state.[8c] The simultaneous transfer of the hydride and protic hydrogenation generates the product alcohol and a Ru(diphosphine)(amide) complex. Heterolytic cleavage of H_2 by Ru(diphosphine)(amide) regenerates the active catalyst. The interaction between the amine ancillary ligand and the oxygen atom of the ketone characterize these systems as HOL catalysts by Morris' classification.

Recent studies by Casey's group suggest that Shvo's catalyst, [(2,5-Ph_2-3,4-Tol_2(η^5-C_4COH))Ru$(CO)_2$H] (**37**), may hydrogenate ketones *via* a HOL mechanism rather than HIL as originally proposed (Scheme 1.7).[9] With the

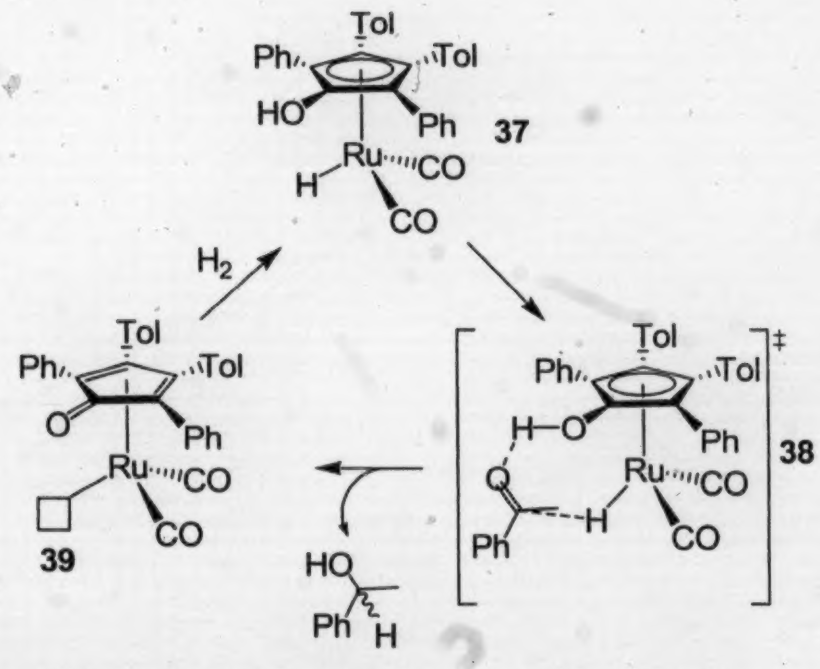

Scheme 1.7: Proposed HOL mechanism using Shvo's catalyst.

Shvo catalyst, a hydrogen bond between the hydroxyl proton and the oxygen on the ketone activates the carbonyl carbon towards nucleophilic attack. The proposed product formation step is very similar to that proposed for the Ru(diphosphine)H_2(diamine) catalysts. In the proposed mechanism, there is a pericyclic 6-membered transition state (**38**) with simultaneous transfer of the hydroxyl proton and the hydride on ruthenium to the oxygen and carbon of the ketone, respectively. This creates an oxygen-carbon double bond on the Cp ring resulting in dearomatization, and creating a vacant coordination site on ruthenium. Heterolytic cleavage of H_2 then regenerates the hydride catalyst. In the Noyori system there is no formal change in oxidation state of the metal. In the Shvo system there is a formal change in oxidation state, and is perhaps better classified as a HOL-redox mechanism.

Transfer-hydrogenation of ketones by the inner sphere mechanism without ligand assistance (TI).

The product formation step in transfer hydrogenation mechanisms is typically very similar to that of H_2-hydrogenation catalysts. The difference lies in how the metal hydride is regenerated to complete the catalytic cycle. One of the most common ketone transfer hydrogenation catalyst systems is $RuH_2(PPh_3)_4$ (**40**).[10] The catalyst must contain a hydride *cis* to a vacant coordination site. Therefore, one of PPh_3 ligands must first dissociate to generate the active catalyst (**41**, Scheme 1.8). The ketone substrate then coordinates at oxygen (**42**) and hydride migration to the carbonyl carbon of the ketone occurs to form a metal-alkoxide compound (**43**) with a vacant coordination site. A hydrogen donor (*e.g.* 2-PrOH) then protonates the alkoxide to liberate the product alcohol, and form a new coordinatively unsaturated 2-propoxide compound (**44**). β-

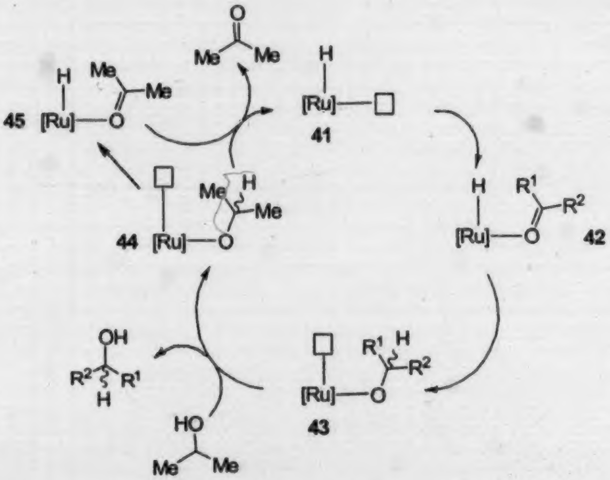

Scheme 1.8: Proposed TI mechanism using a Ru-H catalyst.

Hydride elimination of the 2-propoxide ligand and liberation of the resulting acetone regenerates the hydride catalyst. Even though the metal contains two hydride ligands, it was proposed that hydrogenation occurs *via* a mono-hydridic route.[10]

The transfer hydrogenation catalyst $RuCl_2(PPh_3)_3$ (**46**) reacts with base to form the same active catalyst species as $RuH_2(PPh_3)_4$. There is an alternate mechanistic proposal that involves both hydrides on ruthenium for the hydrogenation of ketones (Scheme 1.9).[11] The ketone coordinates to the ruthenium at oxygen, again activating the carbonyl carbon towards nucleophilic attack. Hydride migration then forms a metal-alkoxide species with a vacant coordination site. It is proposed that the alkoxide and hydride ligands reductively eliminate to form product alcohol and a Ru(0) species (**47**). Oxidative addition of 2-PrOH generates the new metal-hydride/alkoxide

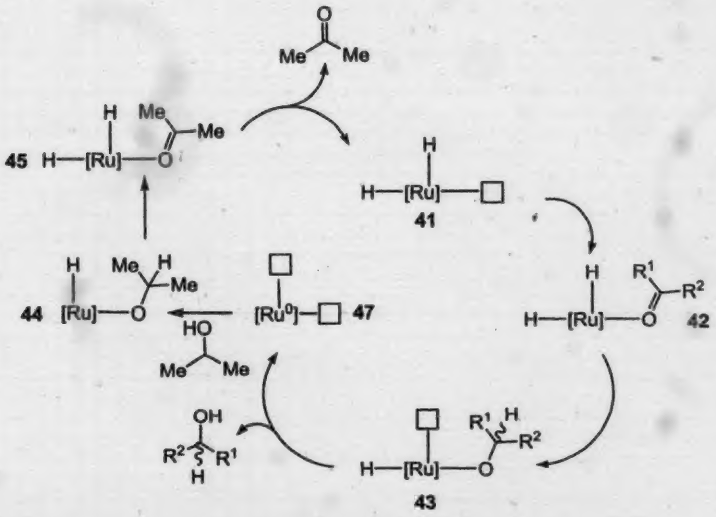

Scheme 1.9: Proposed TI mechanism using a H-Ru-H catalyst.

species. β-Hydride elimination regenerates the dihydride catalyst. Bäckvall *et al.* used deuterium labeling experiments to investigate this mechanism (Scheme 1.10).[11b] The catalyst precursor **46** plus base was used to racemize (*S*)-PhMeDCOH (**48**). It was proposed that the reduced metal species **47** forms in solution and oxidatively adds the alcohol to form Ru(H)(OCDMePh)$(PPh_3)_3$ (**49**). β-Deuteride elimination would give Ru(H)(D)(OCMePh)$(PPh_3)_3$ (**50**). It is possible that either the deuteride or the hydride could transfer to the carbonyl carbon of acetophenone and therefore there should be roughly a 50:50 mixture of PhMeDCOH and PhMeHCOD.[11b] As predicted, there was approximately 50% deuteration on the alpha carbon but OD was not detected due to exchange with protic species in solution.

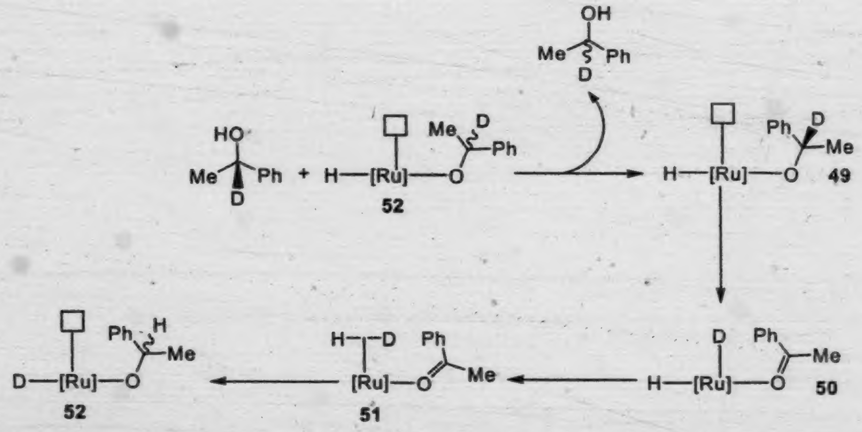

Scheme 1.10: Bäckvall *et al.*'s proposed mechanism for the oxidation of 1-phenylethanol.

Transfer-hydrogenation of ketones by the inner sphere mechanism with ligand assistance (TIL).

The catalyst system Ru(H)(NHCOMe)(2-PrOH)$(PCy_3)_2$(CO) (**53**) in 2-PrOH is the best example of hydrogenation catalyst operating under a TIL mechanism.[12] Decoordination of a PCy_3 ligand creates a vacant coordination site *cis* to the 2-propanol ligand. The acetamido ligand then deprotonates the coordinated 2-PrOH to form a 2-propoxide compound (**55**, Scheme 1.11). β-Hydride elimination would then generate a ruthenium-hydride *cis* to an acetone ligand (**56**). The ketone substrate then displaces the acetone, and is protonated by the iminol hydroxyl proton (**58**). Hydride transfer to the activated carbonyl carbon then generates product alcohol coordinated to ruthenium. 2-PrOH displaces the product alcohol and β-hydride elimination regenerates the active catalyst.[12]

It is possible that the catalyst simply operates under a TOL type mechanism where there is simultaneous transfer of the iminol proton and the ruthenium hydride to the oxygen and carbon of the ketone, respectively. Deuterium labeling experiments, however, indicate that the stepwise TIL mechanism is most likely.[12] When 2-PrOD was used as a hydrogen donor rather than 2-PrOH, the active catalyst would contain an iminol OD. An inverse kinetic isotope effect (KIE, $k_{OH}/k_{OD} = 0.7 \pm 0.1$) was found which is typically observed for stepwise hydrogen transfer reactions involving a rapid and reversible proton transfer process.[13] A normal KIE ($k_{CH}/k_{CD} = 1.9 \pm 0.2$) was found when $(CH_3)_2CDOH$ was used for a hydrogen donor rather than $(CH_3)_2CHOH$. If the hydrogenation occurred through a concerted TOL type mechanism then the overall KIE should be a product of the individual KIE's

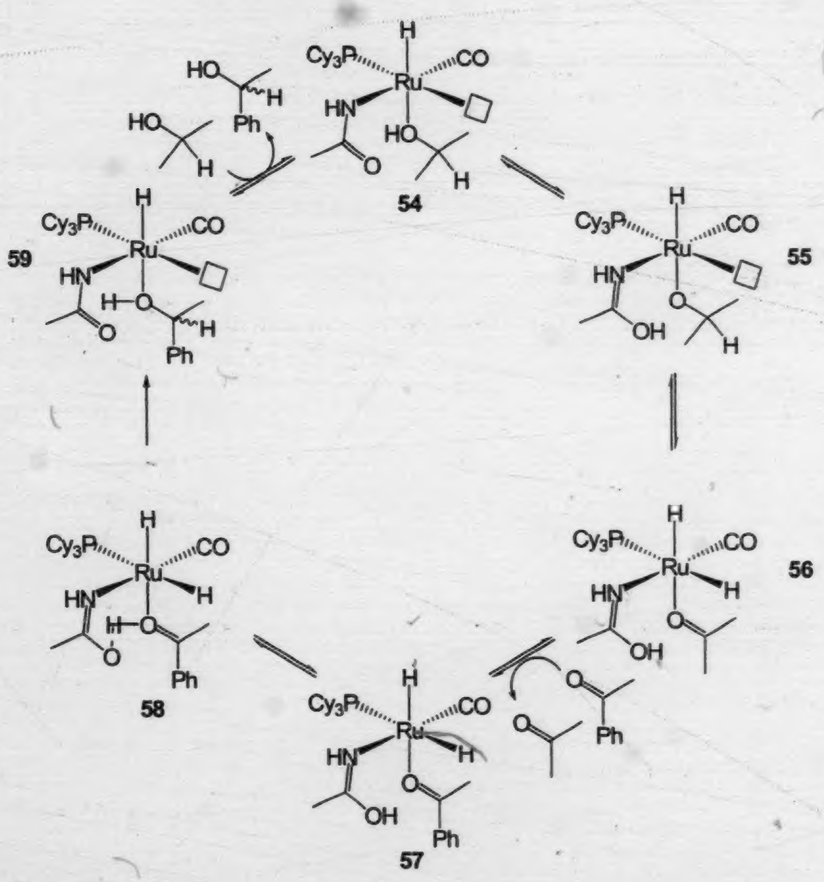

Scheme 1.11: Proposed TIL mechanism for ketone hydrogenation.

($k_{CH/OH}/k_{CD/OD}$ = ~ 1.3). Yi *et al.*, however, found that the combined KIE was $k_{CH/OH}/k_{CD/OD} = 0.7 \pm 0.2$, which is proof of a stepwise TIL type mechanism.[13]

Transfer-hydrogenation of ketones by the outer sphere mechanism without ligand assistance (TO).

Ogo *et al.* developed a ruthenium catalyst that hydrogenates ketones *via* the TO mechanism under aqueous conditions (Scheme 1.12).[14] The hydrogenation must occur under slightly acidic conditions since protons in solution are the source of the hydroxyl hydrogen of the product alcohol. Further, the carbonyl carbon is activated towards nucleophilic attack by the metal-hydride *via* hydrogen bonding between protons in solution (**60**), and the carbonyl oxygen. Formate is typically used as the hydride source. The formate, however, cannot displace a hydroxide ligand on the metal.[15] Therefore, the pH of the solution must be kept below the pKa of the aqua compound (**61**) to

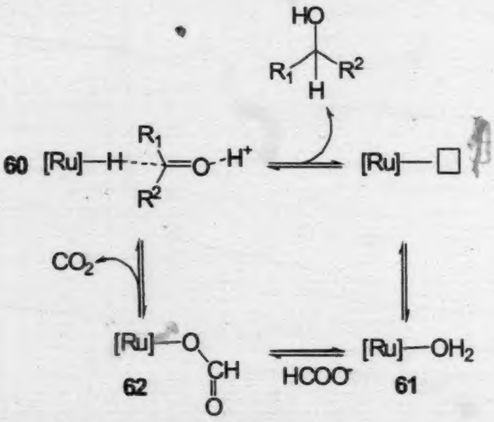

Scheme 1.12: Proposed TO mechanism for ketone hydrogenation.

ensure that a metal-hydroxide is not formed. Under these slightly acidic conditons, a ruthenium-formate complex forms (**62**) and undergoes β-hydride elimination to regenerate the catalyst.[14]

Transfer-hydrogenation of ketones by the outer sphere mechanism with ligand assistance (TOL).

Noyori *et al.* discovered that an ancillary ligand can greatly affect the activity of the catalyst.[1] Specifically, catalyst systems that contain ligands with

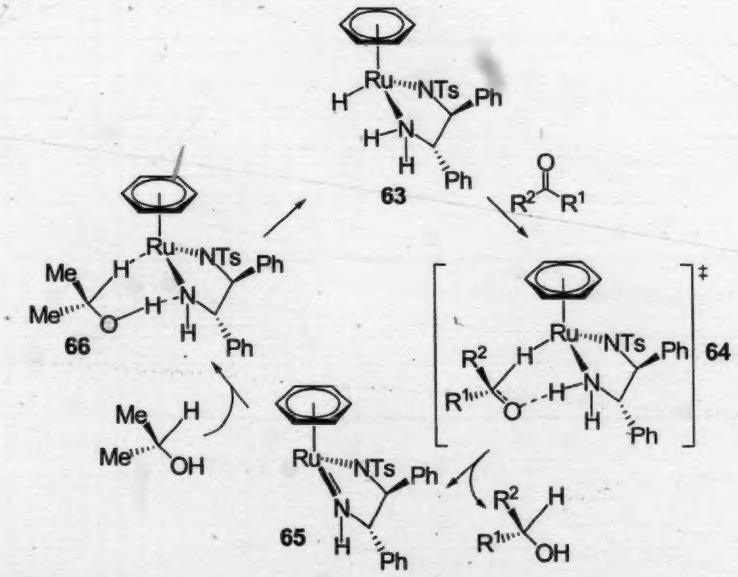

Scheme 1.13: Proposed TOL mechanism for ketone hydrogenation.

protic hydrogens such as NH's hydrogenate ketones *via* a mechanism very similar to that of the HOL mechanism (Scheme 1.13). The protic hydrogen on the ancillary ligand activates the carbonyl carbon of the ketone towards nucleophilic attack by hydrogen bonding to the oxygen of the ketone. Additionally, it acts as the hydrogen source of the hydroxyl proton of the product alcohol. Hydrogenation is proposed to occur *via* a 6-membered pericyclic transition state (**64**), similar to that of the HOL mechanism, resulting in product alcohol and a metal-amide species (**65**).[1] Oxidation of a donor alcohol (*e.g.* 2-PrOH) regenerates the active hydride catalyst, rather than heterolytic cleavage of H_2 as is the case in the HOL mechanism.

Summary

Mechanistic investigation is a fundamental component of catalyst development. Through mechanistic investigations, more is learned about the reactivity of the catalyst. As such, it may be possible to predict catalytic behavior, and modify the catalyst to increase performance. Further, if the catalyst resting state can be determined, heterogeneous versions of the catalyst may be developed leading to highly reusable heterogeneous catalysts, thereby increasing the economic and environmental viability of the catalytic process. The following chapters describe the synthesis and reactivity studies of the putative intermediates in the metal-ligand bifunctional mechanism, and their significance to the catalytic reaction.

References

(1) (a) Noyori, R.; Ohkuma, T. *Angew. Chem., Int. Ed.* **2001**, *40*, 40-73. (b) Noyori, R. *Angew. Chem., Int. Ed.* **2002**, *41*, 2008–2022.

(2) Blaser, H.-U.; Spindler, F.; Thommen, M. In *The Handbook of Homogeneous Hydrogenation*; de Vries, J. G., Elsevier, C. J., Eds.; Wiley-VCH: Weinheim, 2007; Vol. 3, p 1279.

(3) For reviews see *The Handbook of Homogeneous Hydrogenation*; de Vries, J. G., Elsevier, C. J., Eds.; Wiley-VCH: Weinheim, 2007; Vol. 1-3.

(4) Clapham, S. E.; Hadzovic, A.; Morris, R. H. *Coord. Chem. Rev.* **2004**, *248*, 2201-2237.

(5) Daley, C. J. A.; Bergens, S. H. *J. Am. Chem. Soc.* **2002**, *124*, 3680-3691.

(6) Bullock, R. M.; Voges, M. H. *J. Am. Chem. Soc.* **2000**, *122*, 12594-12595.

(7) Magee, M. P.; Norton, J. R. *J. Am. Chem. Soc.* **2001**, *123*, 1778-1779.

(8) For reviews and related systems see (a) Noyori, R.; Yamakawa, M.; Hashiguchi, S. *J. Org. Chem* **2001**, *66*, 7931-7944. (b) Abdur-Rashid, K.; Clapham, S. E.; Hadzovic, A.; Harvey, J. N.; Lough, A. J.; Morris, R. H. *J. Am. Chem. Soc.* **2002**, *124*, 15104-15118. (c) Sandoval, C. A.; Ohkuma, T.; Muniz, K.; Noyori, R. *J. Am. Chem. Soc.* **2003**, *125*, 13490-13503. (d) Noyori, R.; Kitamura, M.; Ohkuma, T. *Proc. Natl. Acad. Sci U.S.A* **2004**, *101*, 5356-5362. (e) Noyori, R.; Sandoval, C. A.; Muñiz, K.; Ohkuma, T. *Phil. Trans. R. Soc. A.* **2005**, *363*, 901-912. (f) Muñiz, K. *Angew. Chem. Int. Ed.* **2005**, *44*, 6622-6627.

(g) Ohkuma, T.; Sandoval, C. A.; Srinivasan, R.; Lin, Q.; Wei, Y.; Muniz, K.; Noyori, R. *J. Am. Chem. Soc.* **2005**, *127*, 8288-8289. (h) Abbel, R.; Abdur-Rashid, K.; Faatz, M.; Hadzovic, A.; Lough, A. J.; Morris, R. H. *J. Am. Chem. Soc.* **2005**, *127*, 1870-1882. (i) Gladiali, S.; Alberico, E. *Chem. Soc. Rev.* **2006**, *35*, 226-236. (j) Samec, J. S. M.; Bäckvall, J.-E.; Andersson, P. G.; Brandt, P. *Chem. Soc. Rev.* **2006**, *35*, 237-248. (k) Ikariya, I.; Blacker, A. J. *Acc. Chem. Res.* **2007**, *44*, 1300-1308. (l) Ito, M.; Ikariya, T. *Chem. Commun.* **2007**, *48*, 5134-5142. (m) Morris, R. H. In *Handbook of Homogeneous Hydrogenation*; de Vries, J. G., Elsevier, C. J., Eds.; Wiley-VCH: Weinheim, 2007; Vol. 1, p 45. (n) Ohkuma, T.; Noyori, R. In *Handbook of Homogeneous Hydrogenation*; de Vries, J. G., Elsevier, C. J., Eds.; Wiley-VCH: Weinheim, 2007; Vol. 3, p 1105. (o) Hadzovic, A.; Song, D.; MacLaughlin, C. M.; Morris, R. H. *Organometalics* **2007**, *26*, 5987-5999.

(9) (a) Casey, C. P.; Singer, S. W.; Powell, D. R.; Hayashi, R. K.; Kavana, M. *J. Am. Chem. Soc.* **2001**, *123*, 1090-1100. (b) Casey, C. P.; Johnson, J. B. *J. Org. Chem.* **2003**, *68*, 1998-2001. (c) Casey, C. P.; Johnson, J. B. *Can. J. Chem.* **2005**, *83*, 1339-1346. (d) Casey, C. P.; Johnson, J. B. *J. Am. Chem. Soc.* **2005**, *127*, 1883-1894. (e) Casey, C. P.; Johnson, J. B.; Singer, S. W.; Cui, Q. *J. Am. Chem. Soc.* **2005**, *127*, 3100-3109. (f) Casey, C. P.; Bikzhanova, G. A.; Cui, Q.; Guzei, I. A. *J Am. Chem. Soc.* **2005**, *127*, 14062-14071. (g) Casey, C. P.; Bikzhanova, G. A.; Guzei, I. A. *J Am. Chem. Soc.* **2006**, *128*, 2286-2293. (h) Casey, C. P.; Clark, T. B.; Guzei, L. A. *J. Am. Chem. Soc* **2007**,

129, 11821-11827. (i) Casey, C. P.; Beetner, S. E.; Johnson, J. B. *J. Am. Chem. Soc.* **2008**, *130*, 2285-2295.

(10) Mizushima, E.; Yamaguchi, M.; Yamagishi, T. *J. Mol. Catal. A: Chem.* **1999**, *148*, 69-75.

(11) (a) Pàmies, O.; Bäckvall, J.-E. *Chem.–Eur. J.* **2001**, *7*, 5052–5057. (b) Backvall, J. -E. *J. Organomet. Chem.* **2002**, *652*, 105-111.

(12) Yi, C. S.; He, Z. *Organometallics* **2001**, *20*, 3641-3643.

(13) Bullock, R. M. In *Transition Metal Hydrides*; Dedieu, A., Ed.; VCH: Weinheim, Germany, 1992; Chapter 8.

(14) Ogo, S.; Abura, T.; Watanabe, Y. *Organometallics* **2002**, *21*, 2964-2969.

Chapter 2: A Ruthenium-Dihydrogen Putative Intermediate in Ketone Hydrogenation.[§]

Introduction

Noyori *et al.*'s catalyst systems comprised of *trans*-(diphosphine)$RuCl_2$(diamine) and a base (*e.g.* 2-propoxide, or *tert*-butoxide) are amongst the most successful catalysts for the hydrogenation of polar bonds.[1] A wide range of phosphines and amines (Figure 2.1) can be incorporated into this highly tailorable catalyst. Further, these catalyst systems display remarkable functional group tolerance and chemioselectivity to different

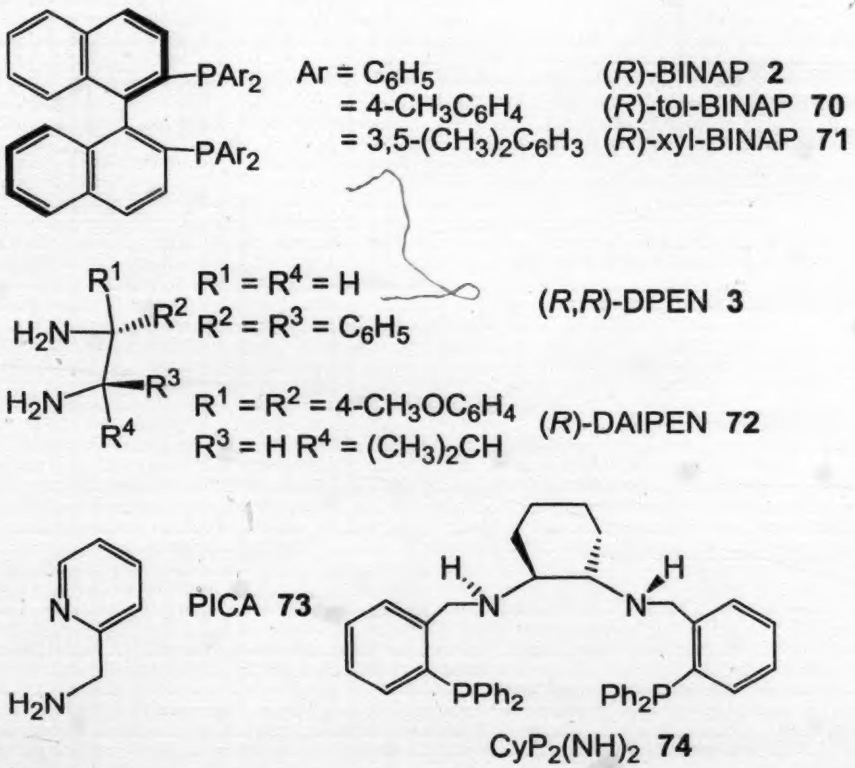

-PAr$_2$
-PAr$_2$
Ar = C_6H_5 (*R*)-BINAP **2**
= $4\text{-}CH_3C_6H_4$ (*R*)-tol-BINAP **70**
= $3,5\text{-}(CH_3)_2C_6H_3$ (*R*)-xyl-BINAP **71**
R^1
H_2N
R^2
H_2N
R^3
R^4
$R^1 = R^4 = H$
$R^2 = R^3 = C_6H_5$
(*R*,*R*)-DPEN **3**
$R^1 = R^2 = 4\text{-}CH_3OC_6H_4$
$R^3 = H$ $R^4 = (CH_3)_2CH$
(*R*)-DAIPEN **72**
N
H_2N
PICA **73**
H
N
H
N
PPh_2
Ph_2P
$CyP_2(NH)_2$ **74**

Figure 2.1: Representative list of ligands used in Noyori *et al.*'s catalyst system.

[§] A version of this chapter has been published. *J. Am. Chem. Soc.* **2005**, 127, 4152-4153.

substrates (Figure 2.2). A wide range of chiral alcohols are accessible when using these catalysts.[1] For example, tertiary-alkyl ketones and β-keto esters, which are typically difficult to hydrogenate for steric reasons, can be converted to the alcohol with high rates and enantiomeric *ee*'s under relatively mild conditions.[1f] Further, base sensitive substrates such as the β-amino ketone **76**, and the keto benzoate **81**, are hydrogenated to alcohols with high *ee* without the formation of 1-phenyl-1-propanol, or transesterification, respectively.[1d] The common test substrate acetophenone can be hydrogenated with high *ee* and turnover numbers. In fact, 100,000 turnovers and *ee*'s greater than 99 % have

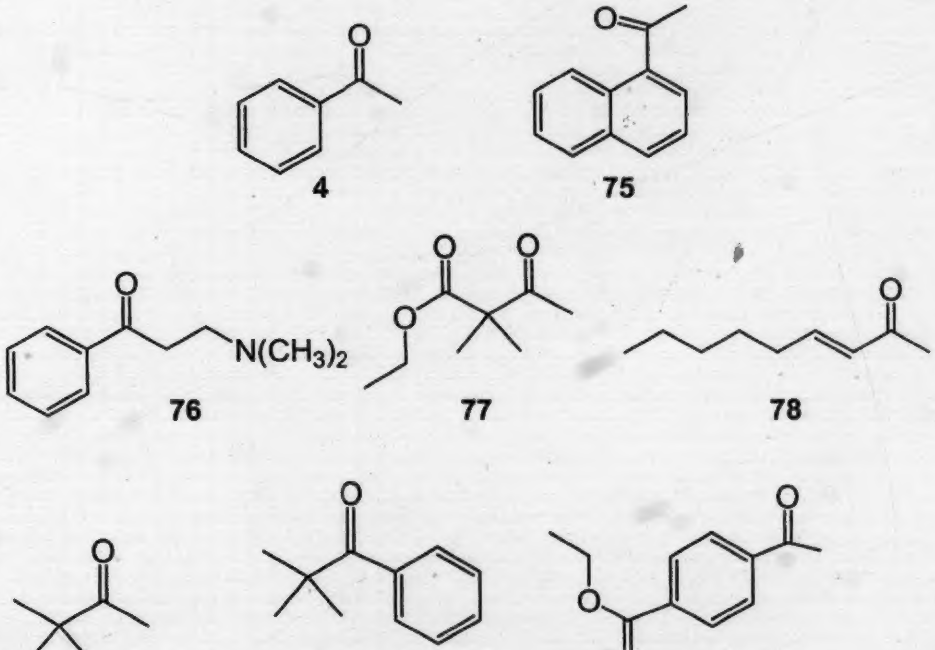

Figure 2.2: Examples of ketones hydrogenated by Noyori *et al.*'s Ru(diphosphine)X_2(diamine) catalyst systems.

been achieved with these catalysts (Table 2.1).[1b,e]

The mechanisms of these and related hydrogenations have been studied by the groups of Noyori, Morris, Casey, and others.[1e,2-4] The predominant consensus of these studies is that the enantioselective step is a concerted bifunctional addition of a nucleophilic hydride ligand on Ru, and an acidic

Table 2.1: Noyori *et al.*'s hydrogenation results.

Ketone	*Catalyst Precursor*	*Sub/Cat*	*H_2 (atm)*	*Time (h)*	*% yield*	*% ee*
4	*trans*-Ru((*R*)-tol-BINAP)(H)(η^1-BH_4)((*R*,*R*)-dpen)	100,000	8	6	99.9	82 (*S*)
4	*trans*-Ru((*S*)-xyl-BINAP)(H)(η^1-BH_4)((*S*,*S*)-dpen)	100,000	8	7	100	99 (*R*)
4	*trans*-Ru((*S*)-xyl-BINAP)(H)(η^1-BH_4)((*S*,*S*)-dpen)	4000	8	12	99.9	99 (*R*)
76	*trans*-Ru((*S*)-xyl-BINAP)(H)(η^1-BH_4)((*S*,*S*)-dpen)	4000	8	12	100	97 (*R*)
81	*trans*-Ru((*S*)-xyl-BINAP)(H)(η^1-BH_4)((*S*,*S*)-dpen)	4000	8	15	100	99 (*R*)
77	*trans*-Ru((*S*)-tol-BINAP)(Cl_2)((*S*)-pica)	2000	5	5	100	97 (*S*)
78	*trans*-Ru((*S*)-xyl-BINAP)(H)(η^1-BH_4)((*S*,*S*)-dpen)	4000	8	16	95	99 (*R*)
79	*trans*-Ru((*S*)-tol-BINAP)(Cl_2)((*S*)-pica)	2000	5	5	100	97 (*S*)
80	*trans*-Ru((*S*)-tol-BINAP)(Cl_2)((*S*)-pica)	2000	5	12	100	97 (R)

hydrogen on nitrogen to the carbon, and oxygen atoms of the ketone group, respectively (Equation 2.1). The interaction between the hydrogen on nitrogen

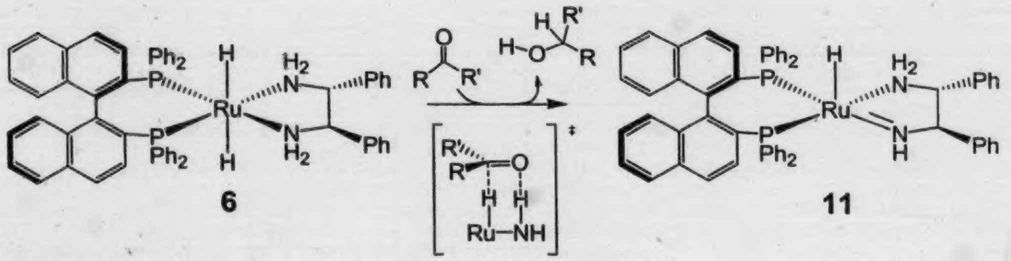

Equation 2.1

and the oxygen atom creates a partial positive charge on the carbonyl carbon, activating it towards nucleophilic attack. Although *cis* dihydride compounds were active, Morris *et al.* found that the *trans* dihydrides species that are the most active towards this addition (e.g. compound 6 in Scheme 2.1).[2b,2f] Hydrides are strong sigma donors and consequently have a strong trans influence. The mutually trans disposition of the hydride ligands in *trans*-(diphosphine)Ru$(H)_2$(diamine) thereby activates them towards nucleophilic addition to the carbon center of the ketone.

Noyori *et al.* recently reported that the catalyst precursors *trans*-Ru((*R*)-tol-BINAP)(H)(η^1-BH_4)((*R*,*R*)-dpen) (**82**, tol-BINAP = 2,2'-bis(ditolylphosphino)-1,1'-binaphthyl **70, 82'** is the BINAP analogue of **82**), and analogues thereof hydrogenate ketones in 2-PrOH with high rates and *ee* in the absence of added base.[1b,e] This is in contrast to the dichloride precursors, *trans*-Ru((*R*)-tol-BINAP)$(Cl)_2$((*R*,*R*)-dpen) (**83**), that require a strong base to activate the catalyst, presumably *via* the formation of a ruthenium-alkoxide group by chloride

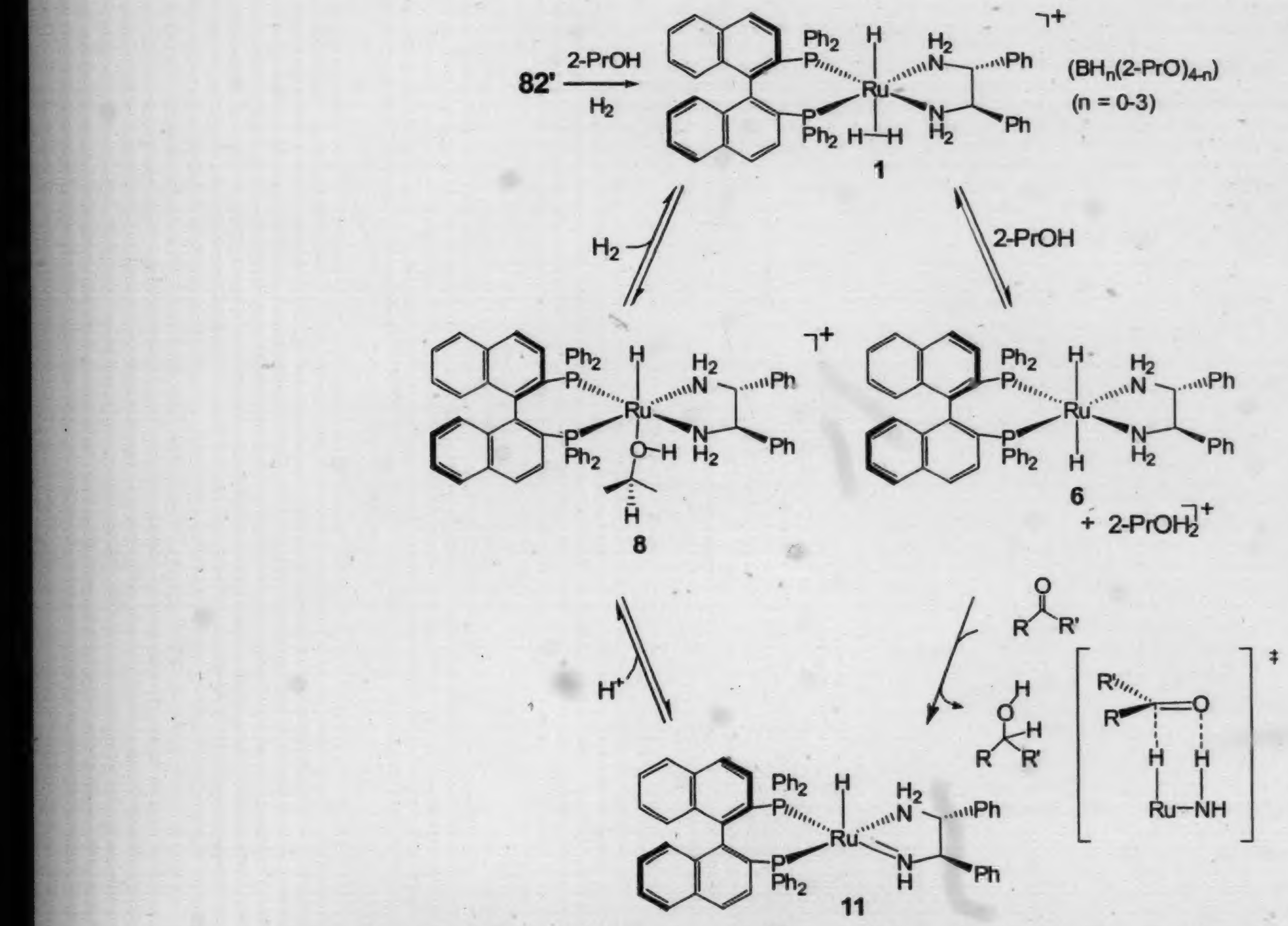

Scheme 2.1: Noyori *et al.*'s proposed base-free hydrogenation mechanism.

displacement, followed by β-hydride elimination to form the active *trans* dihydride. Noyori *et al.* suggested that these base-free hydrogenations in 2-PrOH proceed through the cationic dihydrogen intermediate *trans*-[Ru((*R*)-tol-BINAP)(H)(η^2-H_2)((*R*,*R*)-dpen)]$^+$ (**84**).[1e] Scheme 2.1 shows the proposed catalytic cycle with **1** (the BINAP analogue of **84**) as a catalytic intermediate.

Noyori *et al.* proposed that in the absence of base, compound **1** dissociates a BH_4^- anion to form the solvento-Ru complex *trans*-[Ru((*R*)-BINAP)(H)(2-PrOH)((*R*,*R*)-dpen)]$^+$ (**8**).[1e] Further, Noyori proposed that the BH_4^-

anion reacts with alcohol solvent to form H_2, RO^- and $B(OR)_3$. Compound **8** is in equilibrium with the 16 e^- species *trans*-[Ru((*R*)-BINAP)(H)((*R*,*R*)-dpen)]$^+$ (**85**), paired with either RO^- or $[BH_n(OR)_{4-n}]^-$ as anion, that then reacts with H_2 to form the cationic dihydrogen intermediate **1**. Noyori *et al.*'s kinetic studies show that in the absence of base, the rate of alcohol production does not depend on H_2 pressure.[1e] Further, there is a significant incubation period. Noyori *et al.* therefore propose that **1** is the resting state of the catalyst in the absence of base, and that deprotonation of **1** to form **6** is the turnover limiting step. It was proposed that the dihydrogen ligand in **1** is sufficiently acidic to protonate 2-PrOH, generating the *trans*-dihydride compound **6** and 2-$PrOH_2^+$.[1e,5] Once formed, the *trans*-dihydride **6** then hydrogenates the ketone *via* the metal-ligand bifunctional mechanism to form product alcohol and the neutral Ru-amide compound **11**. The amide **11** is then protonated at nitrogen to regenerate the solvento complex **8**, which reacts with H_2 to regenerate the dihydrogen intermediate **1** and complete the cycle.

Although 2-PrOH is typically the optimum solvent for activity and enantioselectivity with these catalytic hydrogenations, it is not the optimum solvent for the observation of active catalytic intermediates. H-D exchange between 2-PrOH-d_8 and the hydride/dihydrogen ligands on the active Ru species prevent comprehensive NMR observations of putative catalytic intermediates and steps.[1e] In fact, the only species conclusively identified was the catalyst precursor **82**. The published ^1H NMR mechanistic studies of these hydrogenations, including the key concerted bifunctional addition step, are usually carried out either in non protic solvents,[2c] or in solvent mixtures containing only small amounts of 2-PrOH. Additionally, only model species, not the actual proposed catalytic intermediates, could be fully characterized. For example, despite Noyori *et al.*'s kinetic evidence for its existence (*vide supra*), the putative cationic dihydrogen intermediate **84** could not be directly observed and studied by ^{1}H NMR.[1e] This chapter describes the synthesis, characterization and reactivity study of the dihydrogen complex **1** without H-D exchange in 2-PrOH-d_8 solvent.

Results and Discussion

Bergens *et al.* reported that the catalyst precursor [Ru((*R*)-BINAP)(1-5-η-C_8H_{11})](BF_4) (**86**) reacts under 1 atm H_2 in weak oxygen donor solvents (e.g. acetone, THF) to produce cyclooctane and the labile, active olefin hydrogenation catalysts *fac*-[Ru((*R*)-BINAP)(H)(solvent)$_3$]$^+$.[6a] When the solvent is either acetone or THF, the resulting solvento compound is stable at room temperature. In 2-PrOH, *fac*-[Ru((R)-BINAP)(H)(2-PrOH)$_3$]$^+$ (**87**) rapidly decomposes at room temperature, but can be prepared without significant decomposition at ~ -60 °C (Equation 2.2).[6b] Further, there is no evidence of H-D exchange between the hydride ligand in *fac*-[Ru((*R*)-BINAP)(H)(2-PrOH-d_8)$_3$](BF_4) (**88**) and 2-PrOH-d_8 at -60 °C, permitting the use of ^{1}H NMR to study

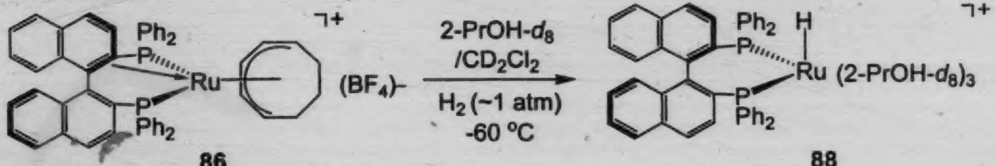

86 **88**

Equation 2.2

its reactivity. For the present study, **88** was prepared in mixtures of 2-PrOH-d_8/CD_2Cl_2 (between 4:1 and 2:1) and reacted with (*R*,*R*)-dpen under H_2 at -60 °C, to quickly form **1** (BF_4) in ~ 95 % yield (Equation 2.3). This result is the first

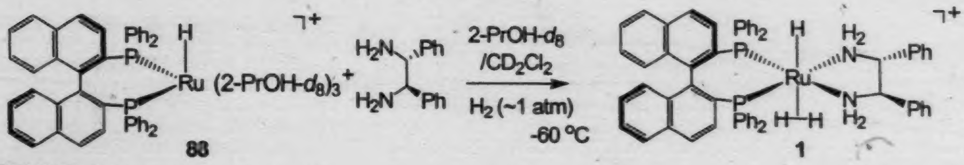

Equation 2.3

conclusive identification of a putative intermediate in hydrogenations with *trans*-(diphosphine)RuH_2(diamine) catalysts. Compound **1** was identified by the hydride signal at -8.5ppm (1H) and the η^2-H_2 signal at -0.66 ppm (2H) in the ^1H NMR spectrum, and the signals from the BINAP and dpen ligands (see appendix A for NMR spectra of **1**). The geometry of **1** was established as follows. The hydride signal appears as an apparent broad triplet with $^2J_{P\text{-}H}$ ~ 22 Hz, showing that the hydride occupies a coordination site *cis*-to both phosphine groups. Typically $^2J_{P\text{-}H}$ coupling constants for a hydride *trans* to a phosphine are

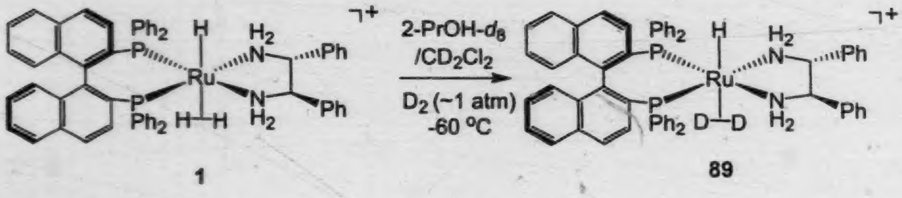

Equation 2.4

larger than those in a *cis* arrangement.[2f] The η^2-H_2 ligand can be completely exchanged with η^2-D_2 to form *trans*-[Ru((*R*)-BINAP)(H)(η^2-D_2)((*R*,*R*)-dpen)]$^+$ (**89**) by flushing D_2 gas (1 atm) through the solution for several min at -60 °C (Equation 2.4). There is no H-D exchange between the hydride and η^2-D_2 groups of **89** detectable by ^1H or ^2H-NMR at -60 °C. Hydrogen atom exchange between the H and η^2-H_2 ligands is extremely facile at low temperatures for the cationic Ru(II) complexes *cis*-[(phosphine)$_2$Ru(H)(η^2-H_2)(diamine)]$^+$.[7] The proposed mechanism for this exchange in *cis* compounds is shown in Figure 2.3. The absence of H-D exchange in **89** is conclusive evidence for a *trans*-disposition of the H and η^2-D_2 ligands. Further evidence for this *trans*-disposition is that the hydride ^1H NMR signal in **1** sharpens significantly, and shifts downfield by ~0.16 ppm upon exchange of η^2-H_2 for η^2-D_2. Morris *et al.* observed a similar sharpening, albeit with a smaller shift, when η^2-H_2 is

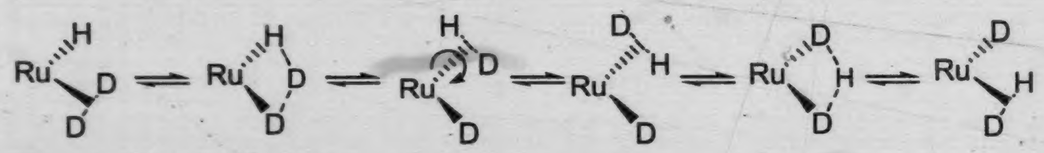

Figure 2.3: Proposed hydrogen exchange mechanism in *cis*-[(phosphine)$_2$Ru(H)(η^2-H_2)(diamine)]$^+$compounds.

exchanged for η^2-D_2 in $[Ru(dppe)_2(H)(H_2)]^+$ (**90**, dppe = 1,2-bis(diphenylphosphino)ethane) and related compounds.[8] This shift in peak position results from differences between the *trans* influence of η^2-H_2 and η^2-D_2.[8,9] The η^2-D_2 ligand has a stronger *trans* influence than η^2-H_2. Morris *et al.* showed that there is a nearly linear correlation between the hydride chemical shift, as well as the Ru-H vibrational frequency, with the electronegativity of the atom *trans* to the hydride. The Ru-H bond lengthened, while the hydride chemical shift, and Ru-H vibrational frequency, shifted downfield and to lower wavenumbers, respectively, with decreasing electronegativity of the *trans* atom.[9] This indicates that the hydride chemical shift moves downfield when *trans* to a ligand with a stronger *trans* influence. The sharpening of the hydride peak likely results from higher *trans* coupling with η^2-H_2 than η^2-D_2.[10]

The H-H bond distance in a coordinated η^2-H_2 varies with the degree of back bonding to the σ^* antibonding orbital. The greater the degree of back bonding the longer the H-H bond distance, and eventually oxidative addition of H_2 to form a dihydride (Figure 2.4) occurs. The lability of η^2-H_2 ligand also decreases with increasing back bonding. The ^{1}H NMR signal for free H_2 is approximately 4.5 ppm whereas coordinated η^2-H_2 is typically in the range of -2 to -8 ppm. The η^2-H_2 ligand in **1** is at higher frequencies (-0.66 ppm) than most. The $^1J_{H\text{-}D}$ of the η^2-H-D ligand in **1** is large (~ 37Hz) in comparison to other η^2-H_2 compounds.[11-13] In fact, it is the largest $^1J_{H\text{-}D}$ of a coordinated η^2-H-D ligand reported to date. The relatively downfield chemical shift and large $^1J_{H\text{-}D}$ shows that the η^2-H_2 ligand in **1** retains an unusually high degree of free H_2

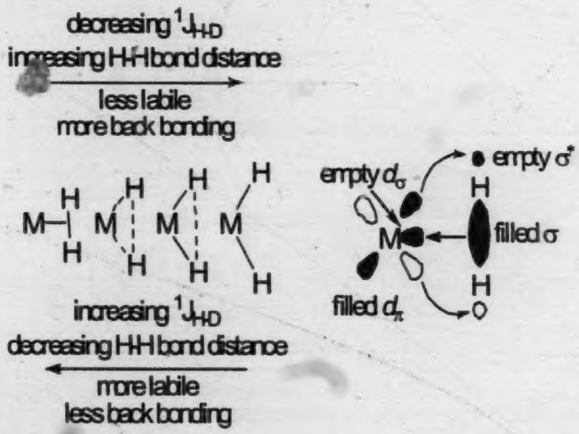
decreasing ¹J_H-D
increasing H-H bond distance
less labile
more back bonding
M
H
H
empty d_σ
empty σ*
filled σ
filled d_π
increasing ¹J_H-D
decreasing H-H bond distance
more labile
less back bonding

Figure 2.4: Orbital interactions and the relationship between H-H bond distance and lability.

character.[11-13] Further, as shown by the facile exchange with D_2 gas at -60 °C, the η^2-H_2 ligand in **1** is labile. Flushing the hydrogen atmosphere with argon at -60 °C also resulted in loss of η^2-H_2 from the complex. Rather than form the expected solvento complex **8** (Equation 2.5), however, flushing the hydrogen atmosphere with argon also resulted in loss of the hydride ligand, presumably as H_2, and formation of an unidentified Ru species. The loss of the η^2-H_2 and H ligands from **1** is not reversed by replenishing the atmosphere with hydrogen.

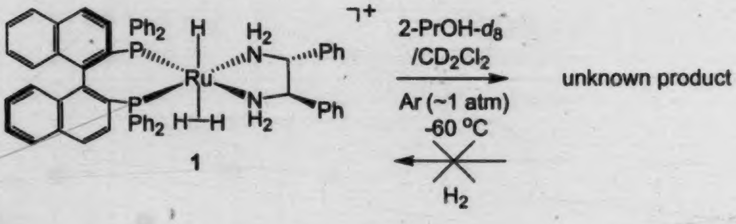
Ph₂
P
Ru
H
H₂
N
Ph
H—H
1
+
2-PrOH-d₈
/CD₂Cl₂
Ar (~1 atm)
-60 °C
H₂
unknown product

Equation 2.5

Morris *et al.* reported that β-hydride elimination occurs in the dpen ligand in benzene solutions of the dihydride **4**.[2b,13] Perhaps a similar process occurs in 2-PrOH solutions of **8**. Another possibility is loss of a protic hydrogen on nitrogen with the hydride ligand to generate H_2. Thus, these and related hydrogenations should be kept saturated with H_2 to avoid decomposition of the catalyst. Compound **1** is stable under H_2 at room temperature for periods of minutes.

The putative catalytic sequence **1**→**6**→**11** was investigated as follows. The neutral dihydride **6** compound was not detected by NMR in solutions of **1**. The thermodynamic acidity of the dihydrogen ligand in **1** is therefore not sufficient to protonate 2-PrOH-d_8 to a detectable extent at -60 °C. H-D exchange occurred between 2-PrOH-d_8 and the Ru-H and η^2-H_2 groups occurs at an appreciable rate upon warming to ~ -20 °C. This result suggests that the kinetic acidity of the dihydrogen ligand in **1** is sufficient enough to reversibly protonate 2-PrOH-d_8 to form $[(CD_3)_2CD\text{-}OHD]^+$ to a small extent at higher temperatures. To investigate whether this deprotonation is significant to ketone hydrogenation, a stoichiometric reaction was carried out between **1** and the common ketone substrate acetophenone (Equation 2.6). There was no reaction between acetophenone and **1** mixed at -60 °C and then warmed to room temperature. Thus if the dihydride compound **6** did form, it was not present in

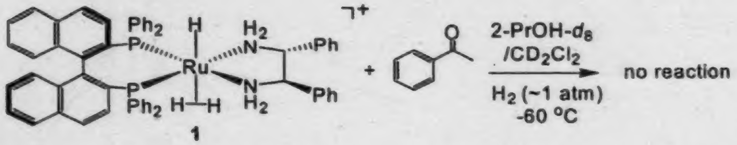

Equation 2.6

sufficient amounts to reduce acetophenone under these conditions. To investigate the behavior of this system under catalytic conditions, the hydrogenation of acetophenone using **1** as catalyst was attempted in 2-PrOH solvent (4 atm H_2, 30 °C, 2000 equiv ketone, no base). The reaction produced miniscule amounts (~ 0.1 %) of 1-phenylethanol product after 3 h, and little further product after 24 h (Table 2.2). Reaction of **84** with $NaBH_4$ displaces the η^2-H_2 ligand upon warming to room temperature to generate the η^1-BH_4 adduct **82** (Equation 2.7). Therefore the catalytic hydrogenation of acetophenone using **1** and $NaBH_4$ as added base (Ru:B ~ 1:1) was tested. The hydrogenation was dramatically faster in the presence of $NaBH_4$. 32 % Conversion (640 turnovers) was achieved after 3 h. The *ee* of the catalytic hydrogenation (81% (*S*)) with BH_4^- present is in line with Noyori *et al.*'s reported *ee* using the BH_4^- adduct **82'** as catalyst precursor.[1b,e] The catalytic hydrogenation was also rapid (500 turnovers in 3h, 78% (*S*)) using **1** and *t*-BuOK (1 equiv). The cationic dihydrogen compound **1** thus requires added base or BH_4^- to be active towards this catalytic hydrogenation.

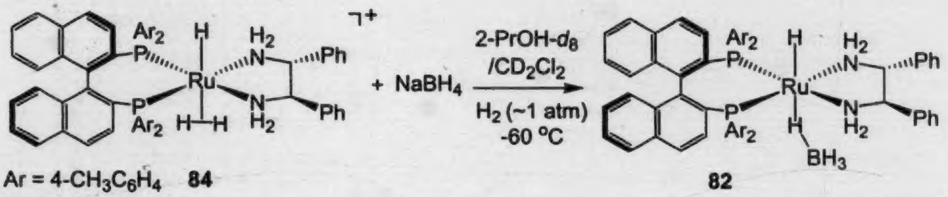

Ar = 4-$CH_3C_6H_4$ **84** **82**

Equation 2.7

Table 2.2: Hydrogenation of acetophenone using *trans*-[Ru((*R*)-BINAP)(H)(η^2-H_2)((*R*,*R*)-dpen]$^+$ in the presence and absence of base.

Base	*Sub/Cat*	*H_2 (atm)*	*Time (h)*	*% yield*	*% ee*
NA	2000	4	3	0.1	NA
1 equiv *t*-BuOK	2000	4	3	25	78 (*S*)
1 equiv $NaBH_4$	2000	4	3	32	81 (*S*)

Conclusions

The catalyst species that contain the active hydrogen ligands, namely the hydride and η^2-H_2, in **1** can be prepared at low temperatures in 2-PrOH-d_8-rich solutions without H-D exchange, thereby allowing their conclusive ^{1}H NMR characterization and study. The η^2-H_2 in **1** has largest $^1J_{H\text{-}D}$ coupling constant to date. Noyori *et* al proposed a solvento species in the catalytic cycle. There was no evidence, however, for the solvento species, even though the η^2-H_2 ligand is very labile. There is rapid H-D exchange with the solvent at room temperature which suggests that **1** is weakly acidic. The dihydride, however, was not detected in NMR experiments. Further, compound **1** does not generate sufficient active catalyst for rapid ketone hydrogenations under the base free conditions used for this study. Traces of base (stoichiometric in Ru, either $NaBH_4$ or *t*-BuOK) are required to convert **1** into the active catalyst. There are three types of active hydrogen atoms in **1**, the dihydrogen ligand, the hydride, and the hydrogen atoms bonded to nitrogen. Chapter 3 will discuss how the active hydrogen atoms in **1** react with added base to form the active catalyst.

Materials and Methods

All operations were carried out under an argon atmosphere using standard Schlenk and glovebox techniques unless stated otherwise. The solvents were dried and distilled under a dinitrogen atmosphere using standard drying agents. All common chemicals and solvents were obtained from Aldrich. The acetophenone was distilled, washed with 0.1 M KOH_{aq}, and distilled again before use. (*R,R*)-Dpen was obtained from Strem Chemicals. All solids were recrystallized before use. *fac*-$[Ru((R)\text{-BINAP})(H)(2\text{-PrOH-}d_8)_3]^+$ (**88**) was prepared using a procedure published previously.[6b] The 1-phenylethanol (Fluka) was used without further purification. The hydrogen gas was ultra high purity grade purchased from Praxair. The glass pressure reactor used for the catalytic hydrogenations was silanized by reaction with chlorotrimethylsilane that was then removed by heating under vacuum. ^1H, ^{13}C, and ^{31}P, NMR spectra were measured with a Varian Inova-400 spectrometer. ^1H and ^{13}C NMR chemical shifts are reported in parts per million (δ) relative to TMS with the solvent as the internal reference. ^{31}P NMR chemical shifts are reported in parts per million (δ) relative to an 85% H_3PO_4 external reference. Gas chromatography was performed using a Hewlett Packard 5890 chromatograph equipped with a flame ionization detector, a 3392A integrator, and a Beta Dex™ 120 fused silica capillary column (30m × 0.25mm × 0.25μm thickness, Supelco) using 20.5 psi He as carrier gas.

?

Typical Preparation of Ruthenium-Dihydrogen Putative Intermediate 1. *fac*-[Ru((*R*)-BINAP)(H)(sol)$_3$]BF$_4$ (sol = 2-PrOH-d_8) (**88**) was prepared at –60 °C under H_2 in an NMR tube (6 mg in 0.5 mL 2-PrOH-d_8 and 0.1 mL CD_2Cl_2) as previously described.[6b] One equiv (*R,R*)-dpen was dissolved in CD_2Cl_2 (0.1 mL) in an NMR tube under argon, cooled to –60 °C, and canulated using H_2 into the tube containing **88** at –60 °C. The $^{31}P\{^1H\}$ indicated the yield of **1** was ~ 95 %. The remaining species were unidentified. Figure 1 shows the ^1H NMR of the hydride and dihydrogen region for **1**. ^1H NMR (399.98 MHz, 2-PrOH-d_8/CD_2Cl_2, –60 °C): δ –8.57 (1H, t, $^2J_{P\text{-}H}$ = 21.6 Hz, Ru–H), –0.66 (2H, br, Ru–η^2-H_2), 3.82 (C*H*NH$_2$, doublet partially obscured by solvent signal), 3.98 (1H, d, $^3J_{H\text{-}H}$ = 12 Hz, C*H*NH$_2$), 6-8.9 (44H, om, aromatic). $^{13}C\{^1H\}$ NMR (100.6 MHz, 2-PrOH-d_8/CD_2Cl_2, –60 °C): δ ~62.6 (CHNH$_2$, obscured by solvent signal), 68.7 (CHNH$_2$), 123-141 (aromatic). $^{31}P\{^1H\}$ NMR (161.9 MHz, 2-PrOH-d_8/CD_2Cl_2, –60 °C). δ 69.77 (d, $^2J_{P\text{–}P}$ = 33 Hz), 72.17 (d, $^2J_{P\text{–}P}$ = 33 Hz). ^{13}C–^1H HMQC 2D NMR aided in making these assignments. Bubbling D_2 gas at 1 atm through solutions of **1** at –60 °C resulted in the loss of Ru–η^2-H_2 signal with an upfield shift and sharpening of the Ru–H signal (Figure 2). The N*H* signals could not be detected in 2-PrOH-d_8 presumably due to H-D exchange. Preparation of **1** from THF-d_8 allowed detection of the N*H* signals. The chemical shift of N*H* signals varied with temperature and with the amount of residual H_2O in the solvent. At –60 °C the N*H* signals were observed at: δ 1.89 (1H), 3.85 (overlapping with C*H*NH$_2$), 4.3 (1H), and 4.87(1H). The tol-BINAP analogue **84** can be made using the same procedure. Adding ~1 equiv of $NaBH_4$ in 2-PrOH at –60 °C and warming to room temperature displaces the η^2–H_2 ligand, generating the η^1-BH_4 adduct, with identical NMR data to those reported by Noyori *et al.*[1e]

Representative Hydrogenation of Acetophenone using 1 as Catalyst. A silanized glass pressure reactor equipped with a magnetic stir bar was fitted with a rubber septum, charged with acetophenone (1.17 g, 9.73×10^{-3} mol, 2000 equiv) in dry, distilled 2-PrOH (11 mL), and then flushed with H_2. Additives (1 equiv of KPF_6, *t*-C_4H_9OK, or $NaBH_4$ (1 equiv B)) were canulated into the reactor as 2-PrOH solutions (1 mg/mL). **1** (1 equiv) was prepared as described above and canulated into the reactor using H_2. Hydrogen gas was bubbled through the solution with stirring for 1 min, the septum was replaced with a hydrogen line, and the reactor was pressurized to 40 psi (gauge). The mixture was rapidly stirred at 30 °C for the 3 h. The reactor was then depressurized, and the solution was concentrated under reduced pressure. An aliquot was passed through a Florisil plug using ethyl acetate as eluent to remove any catalyst residues. The ethyl acetate was removed under reduced pressure, and the enantiomeric excess (ee) and % conversion were measured by chiral GC analysis carried out in house. The absolute configuration of the major product enantiomer was determined by comparison to an authentic sample of (*R*)-(+)-1-phenylethanol. The sample was injected as a dichloromethane solution with concentration = 1 mg/mL. Initial oven temperature: 70 °C increased at 1 °C/min to 120 °C; held at 120 °C for 10 min. The retention times were (*R*)-(+)-1-

phenylethanol, $t_R(R)$ = 43.5 min; (*S*)-(-)-1-phenylethanol, $t_R(S)$ = 45.6 min; acetophenone, t_R = 29.9 min. The ee measurements were confirmed against racemic 1-phenylethanol.

References

(1) (a) Ohkuma, T.; Ishii, D.; Takeno, H.; Noyori, R. *J. Am. Chem. Soc.* **2000**, *122*, 6510-6511. (b) Noyori, R.; Ohkuma, T. *Angew. Chem., Int. Ed.* **2001**, *40*, 40-73. (c) Noyori, R.; Yamakawa, M.; Hashiguchi, S. *J. Org. Chem.* **2001**, *66*, 7931-7944. (d) Ohkuma, T.; Koizumi, M.; Muniz, K.; Hilt, G.; Kabuto, C.; Noyori, R. *J. Am. Chem. Soc.* **2002**, *124*, 6508-6509. (e) Sandoval, C. A.; Ohkuma, T.; Muniz, K.; Noyori, R. *J. Am. Chem. Soc.* **2003**, *125*, 13490-13503. (f) Ohkuma, T.; Sandoval, C. A.; Srinivasan, R.; Lin, Q.; Wei, Y.; Muniz, K.; Noyori, R. *J. Am. Chem. Soc.* **2005**, *127*, 8288-8289.

(2) (a) Abdur-Rashid, K.; Lough, A. J.; Morris, R. H. *Organometallics* **2000**, *19*, 2655-2657. (b) Abdur-Rashid, K.; Faatz, M.; Lough, A. J.; Morris, R. H. *J. Am. Chem. Soc.* **2001**, *123*, 7473-7474. (c) Abdur-Rashid, K.; Clapham, S. E.; Hadzovic, A.; Harvey, J. N.; Lough, A. J.; Morris, R. H. *J. Am. Chem. Soc.* **2002**, *124*, 15104-15118. (d) Rautenstrauch, V.; Hoang-Cong, X.; Churlaud, R.; Abdur-Rashid, K.; Morris, R. H. *Chem. Eur. J.* **2003**, *9*, 4954-4967. (e) Clapham, S. E.; Hadzovic, A.; Morris, R. H. *Coord. Chem. Rev.* Available online **2004**. (f) Abbel, R.; Abdur-Rashid, K.; Faatz, M.; Hadzovic, A.; Lough, A. J.; Morris, R. H. *J. Am. Chem. Soc.* **2005**, *127*, 1870–1882.

(3) Alonso, D. A.; Brandt, P.; Nordin, S. J. M.; Andersson, P. G. *J. Am. Chem. Soc.* **1999**, *121*, 9580-9588.

(4) Casey, C. P.; Singer, S. W.; Powell, D. R.; Hayashi, R. K.; Kavana, M. *J. Am. Chem. Soc.* **2001**, *123*, 1090-1100.

(5) Abdur-Rashid, K.; Fong, T. P.; Greaves, B.; Gusev, D. G.; Hinman, J. G.; Landau, S. E.; Lough, A. J.; Morris, R. H. *J. Am. Chem. Soc.* **2000**, *122*, 9155-9171.

(6) (a) Wiles, J. A.; Bergens, S. H.; Vanhessche, K. P. M.; Dobbs, D. A.; Rautenstrauch, V. *Angew. Chem., Int. Ed.* **2001**, *40*, 914-919. (c) Wiles, J. A.; Daley, C. J. A.; Hamilton, R. J.; Leong, C. G.; Bergens, S. H. *Organometallics* **2004**, 23; 4564-4568.

(7) Heinekey, D. M.; Mellows, H.; Pratum, T. *J. Am. Chem. Soc.* **2000**, *122*, 6498-6499.

(8) (a) Earl, K. A.; Jia, G.; Maltby, P. A.; Morris, R. H. *J. Am. Chem. Soc.* **1991**, *113*, 3027-3039. (b) Bautista, M. T.; Cappellani, E. P.; Drouin, S. D.; Morris, R. H.; Schweitzer, C. T.; Sella, A.; Zubkowski, J. *J. Am. Chem. Soc.* **1991**, *113*, 4876-4887.

(9) Clapham, S. E.; Guo, R.; Zimmer-De Iuliis, M.; Rasool, N.; Lough, A.; Morris, R. H. *Organometallics* **2006**, *25*, 5477–5486.

(10) Crabtree, R. H.; Habib, A. *Inorg. Chem.* **1986**, 25, 3698-3699.

(11) Jessop, P. G.; Morris, R. H. *Coord. Chem. Rev.* **1992**, *121*, 155-284.

(12) (a) Heinekey, D. M.; Oldham, W. J., Jr. *Chem. Rev.* **1993**, *93*, 913-926. (b) Heinekey, D. M.; Lledós, A.; Lluch, J. M. *Chem. Soc. Rev.* **2004**, *33*, 175-182.

(13) (a) Kubas, G. J.; Ryan, R. R.; Swanson, B. I.; Vergamini, P. J.; Wassermann, H. *J. Am. Chem. Soc.* **1984**, *106*, 451-2. (b) Kubas, G. J.; Nelson, J. E.; Bryan, J. C.; Eckert, J.; Wisniewski, L.; Zilm, K. *Inorg. Chem.*

1994, *33*, 2954-60. (c) Kubas, G. J. *J. Organomet. Chem.* **2001**, *635*, 37-68. (d) G. J. Kubas, *Metal Dihydrogen and Sigma-Bond Complexes: Structure, Theory and Reactivity*. Kluwer Academic/Plenum Publishers, NY, 2001.

(14) Morris, R. H.; Song, D. *Organometallics* **2004**, 23, 4406-4413.

Chapter 3: An unexpected possible role of base in asymmetric catalytic hydrogenations of ketones. Synthesis and characterization of several key catalytic intermediates.[§]

Introduction

Noyori *et al.* developed the catalyst precursor, *trans*-Ru((*R*)-tol-BINAP)(H)(η^1-BH_4)((*R*,*R*)-dpen) (**82, 82'** is the BINAP analogue of **82**), that is catalytically active both in the presence and absence of added base (Scheme 3.1).[1] Compound **82'**, therefore, can be used to hydrogenate base-sensitive substrates. The proposed mechanism under base-free conditions is discussed in chapter 2. Using model compounds, Morris *et al.* established that one role of the added base is to generate the active, dihydride catalysts *trans*-Ru(diphosphine)$(H)_2$(diamine).[2a] Noyori *et al.* proposed that **82'** can be activated towards hydrogenation *via* two pathways depending on the concentration of base.[1b] It was proposed that when low concentrations of base are used, **82'** is activated towards hydrogenation *via* a slightly different pathway than under base-free conditions. Specifically it is proposed that added base will deprotonate one of the amine N-H's to form the anionic species [Ru((*R*)-BINAP)(H)(η^1-BH_4)((*R*,*R*)-$NH(CH(Ph))_2NH_2$)]$^-$ (**97**, Scheme 3.1, left). Dissociation of the η^1-BH_4 generates the amide **11**, which is protonated as in the base free pathway to form the 16 e^- species **85**. As discussed in Chapter 2, compound **85** is in equilibrium with the dihydrogen compound **1** when under an atmosphere of H_2. The η^2-H_2 ligand is then deprotonated by added base, rather than by added solvent as proposed when under base-free conditions, to form the active dihydride catalyst **6** (Scheme 3.1, top right). Hydrogenation of the ketone results in product alcohol and the amide **11** which is then protonated to complete the cycle (Scheme 3.1, middle right). When higher concentrations of base are used, it is proposed that **82'** enters the catalytic cycle *via* the same sequence as with low concentrations of base, i.e. dissociative conjugate base elimination of BH_4^- to form the amide. It is proposed, however, that generation of the dihydride proceeds through a different pathway.[1b] Under strongly basic conditions, the amide **11** is not protonated to generate the 16 e^- species **85**. Instead it is proposed that hydrogen coordinates to the amide to form [Ru((*R*)-BINAP)(H)(η^2-H_2)((*R*,*R*)-NH(CH(Ph))$_2$NH$_2$)] (**98**, Scheme 3.1, bottom middle). Heterolytic cleavage of the the η^2-H_2 ligand in **98** generates the dihydride **6**

[§] A version of this chapter has been published. *J. Am. Chem. Soc.* **2006**, *128*, 13700-13701.

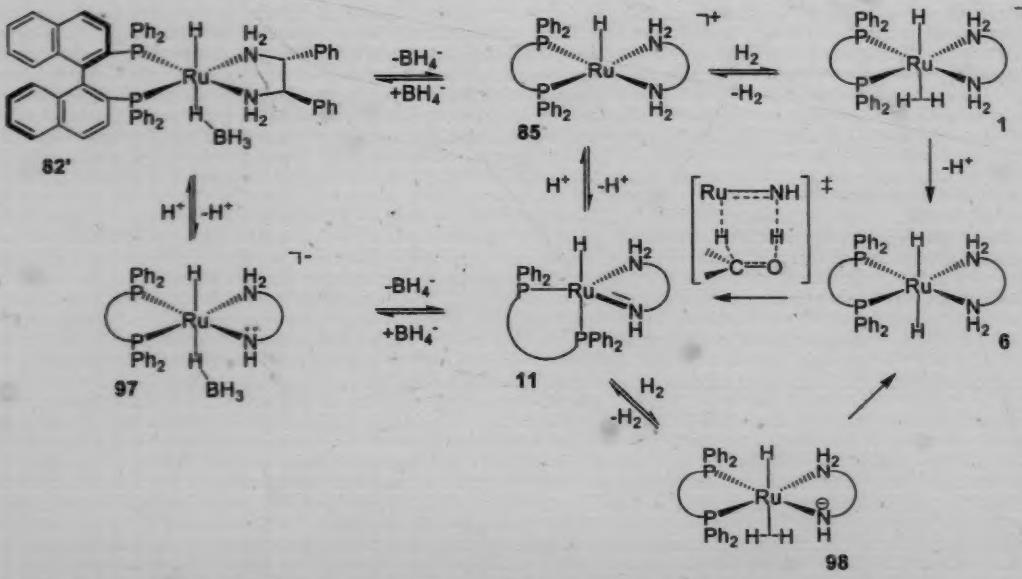

Scheme 3.1: Noyori *et al.*'s proposed base-assisted hydrogenation mechanism using the *trans*-Ru(diphosphine)(H)$_2$(diamine) catalyst system.

which then hydrogenates the ketone to form product alcohol and the amide **11**. Coordination of H_2 to form **98** completes the cycle. As is the case with most of these catalytic hydrogenations, the rate of reaction using **82'** increases, peaks, and then decreases as base is added in increasing concentrations. Noyori *et al.* proposed that the initial increase in rate with added base was due to faster deprotonation of the η^2-H_2 compound **1** to generate the active dihydride **6**.[1b] The catalytic cycle still proceeds through **11→85→1→6→11**, and the rate continues to increase with increasing concentrations of base until the solution is sufficiently basic such that the amide **11** is not protonated to form **85**. Noyori *et al.* proposed that when high base concentrations are used, hydrogenation proceeds through the catalytic cycle **11→98→6→11**. It is proposed that the rate decreases because deprotonation of **1** to form **6** when using low concentrations of base is faster than heterolytic cleavage of the η^2-H_2 ligand in **98** to form **6** when using high concentrations of base.

The concentration of base also had a profound effect on the dependence of hydrogen pressure.[1b] The rate of hydrogenation remained constant when the hydrogen pressure was increased from 1 to 16 atm in the absence of added base. Noyori *et al.* proposed that deprotonation of **1** to form **6** is slower than the formation of **1** from **85**. At lower concentrations of base (8.2 mM *t*-BuOK), however, the rate increased by a factor of 11 when the hydrogen pressure was increased from 1 to 16 atm. Under these conditions it was proposed that deprotonation of **1** to form **6** is faster than the formation of **1** from **85**, thus the dependence on H_2 pressure. Under highly basic conditions (82 mM *t*-BuOK) the rate of hydrogenation increased by a factor of 4.5 when the hydrogen pressure was increased from 1 to 16 atm. The catalytic cycle is proposed to be **11→98→6→11** under these conditions and to be less sensitive to hydrogen pressure since the turnover limiting step is proposed to be the heterolytic cleavage of the η^2-H_2 ligand (**98→6**), not the coordination of H_2 (**11→98**).[1b]

Morris *et al.* used model compounds and, in some cases, aprotic solvents to circumvent the problems associated with studying the catalytic cycle (*vide supra*).[2a-b] The diamine tmen (tmen = 1,2-tetramethylethylenediamine), which does not have hydrogens α to the amino groups, was used to prevent thermal decomposition *via* β-hydride elimination. This allowed for the synthesis and reactivity study of several relevant model compounds in the metal-ligand bifunctional mechanism. In some cases, however, only hydride ^1H and ^{31}P NMR data are provided and in others no data are provided for characterization .

Morris *et al.* prepared the dihydride model compounds *trans*-Ru((*R*)-BINAP)$(H)_2$(tmen) (**99**) and its PPh_3 analog *trans*-Ru$(PPh_3)_2(H)_2$(tmen) (**96**).[2a-b] These model compounds contain the *cis*-Ru-H/N-H motif which is proposed to be of fundamental importance in the metal-ligand bifunctional mechanism. As such, Morris *et al.*'s reactivity study of these *trans* dihydrides provide insight to how the actual catalyst may behave. Compounds **96** and **99** are prepared by reacting the corresponding hydridochloro compounds with a strong base under hydrogen in THF or benzene (Equation 3.1). Single crystal X-ray structure determination showed that **99** is an octahedral complex with the hydrides occupying axial positions.[2a-b] The *trans* disposition of the hydride ligands for

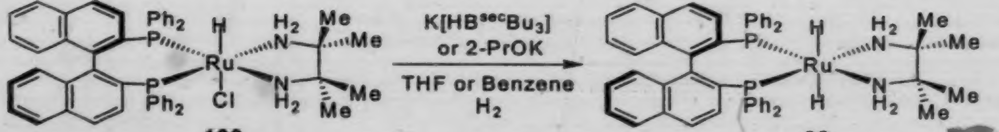

100

99

Equation 3.1

compounds **99** in solution was assigned based on ^{1}H and ^{31}P NMR spectrum. The ^{1}H NMR spectrum of **99** shows that there is one signal each for the two N-H_{axial}, the two N-$H_{equatorial}$, and the two hydride hydrogens, at 3.13, 0.95, and a triplet at -4.8 ppm, respectively. The $^{31}P\{^1H\}$ shows that there is one singlet for the BINAP phosphorus nuclei at 89.9 ppm which, along with the ^{1}H NMR data, proves that the dihydride is C_2-symmetrical. The *trans* disposition of the hydride ligands for compounds **96** in solution was assigned based on similarities to the ^{1}H and ^{31}P NMR spectra of **99**. There is only one signal for the 4 N-H's in **96**. The hydride ^{1}H (triplet, -5.5 ppm) and the $^{31}P\{^1H\}$ (singlet, 87.8 ppm) NMR signals, however, are similar to those in **99**. Using deuterium exchange experiments, Morris *et al.* provided further evidence for the *trans* disposition of the hydride ligands. In the absence of hydrogen, the dihydrides **99,** and **96,** readily lose H_2 to form the amide species **101,** and **102**, respectively (Figure 3.1). Additionally **99** reacts with D_2 gas to form to produce various isotopomers (**99'**, Figure 3.2).[2b] This result demonstrates that **99**, and **96**, may be in equilibrium with **101**, and **102**, respectively. Compounds **101** and **102** can also be prepared independently by either refluxing the corresponding dihydride in THF under Ar, or by reacting the hydridochloro compounds with a strong base in THF. The amide species react with D_2 to form isotopomers similar to when

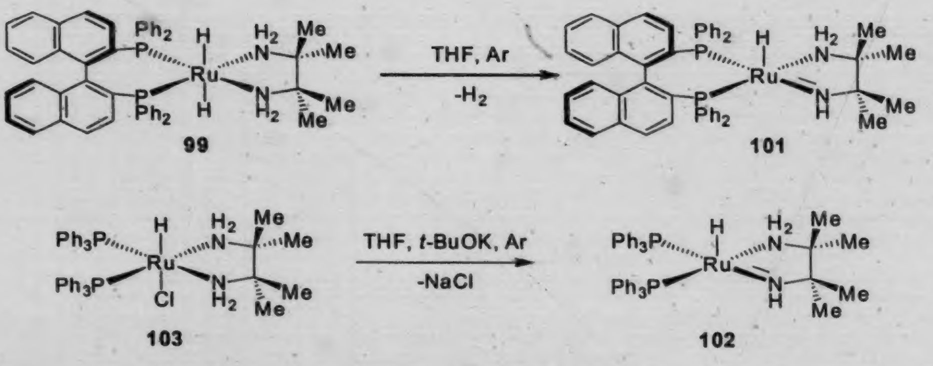
THF, Ar
$-H_2$
99
101
THF, t-BuOK, Ar
-NaCl
103
102

Figure 3.1: Preparation of model amide compounds.

the dihydride is reacted with D_2 (**96'**, Figure 3.2). In either case, there is a large downfield shift of the hydride with respect to the undeuterated dihydride compounds. The large shift is conclusive evidence for the hydride being *trans* to a deuteride based on the larger *trans* influence of deuterium versus hydrogen.[2a]

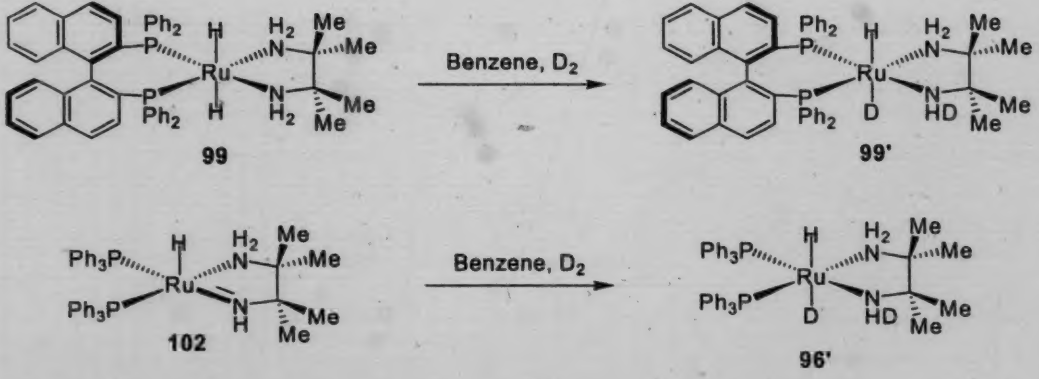
Benzene, D_2
99
99'
Benzene, D_2
102
96'

Figure 3.2: Deuterium exchange reactions in model compounds.

Morris *et al.* observed that the dihydrides **99**, and **96**, react with 1 equiv of acetophenone in benzene in the absence of H_2 to form 1-phenylethanol and the amide species **101**, and **102**, respectively (Figure 3.3 shows the reaction with the BINAP analogue).[2a-b] This proposal was based on the ^{1}H NMR signals associated with the dihydride disappearing concomitant with ^{1}H NMR consistent with the amide appearing. It was proposed that product alcohol reversibly binds to the amide to form an amide-alcohol adduct (**103**). The presence of the amide-alcohol adduct, however, was based solely on a broadening of the amide NMR resonances, with no characterization for **103**. Morris *et al.* observed that the amides will also react with excess acetopheonone to form oxygen-bound enolate compounds (**104**, Figure 3.4). It was proposed that ketone coordinates to the amide to form an amide-ketone adduct (**105**).[2b] This would increase the basicity of the amido nitrogen such that it could deprotonate the methyl group of

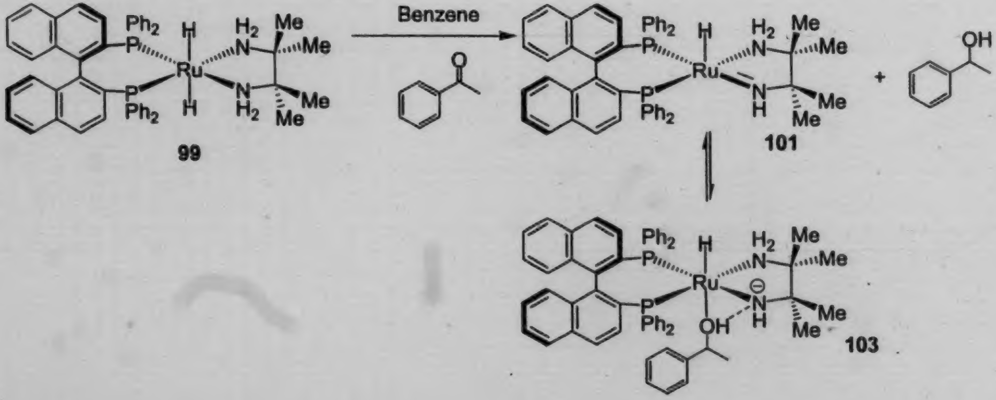

Figure 3.3: Stoichiometric addition of acetophenone to a model dihydride catalyst.

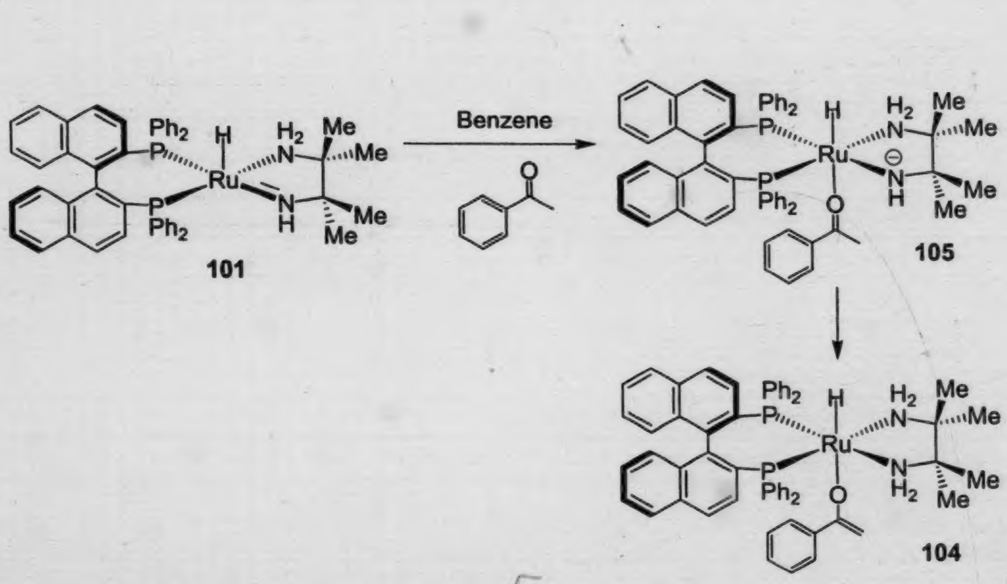

Figure 3.4: Reaction between acetophenone and a model amide.

the ketone. Although the amide-ketone adduct was proposed, there was no spectral evidence provided for its existence.

Morris *et al.* showed that ruthenium-alkoxide compounds can be made when the amide is reacted with either 1-phenylethanol, 2-PrOH, or *t*-BuOH (Figure 3.5).[2b] It was proposed that initially an amide-alcohol adduct (**106**) is formed based on a broadening of the amide ^{1}H NMR signals. The alcohol adduct ligand is proposed to be bound to ruthenium by either oxygen with a hydrogen bond to the amide nitrogen, or *via* a C-H agostic interaction with deprotonation of the OH hydrogen (**107**). The amide-alcohol adducts are in slow equilibrium with the ruthenium-alkoxide species (**108**). Only the amide **102**, however, containing PPh_3 ligands was studied and not the amide **101** which contains the (*R*)-BINAP ligand.[2b] Further, only hydride ^{1}H and ^{31}P NMR data were used to characterize **108**.

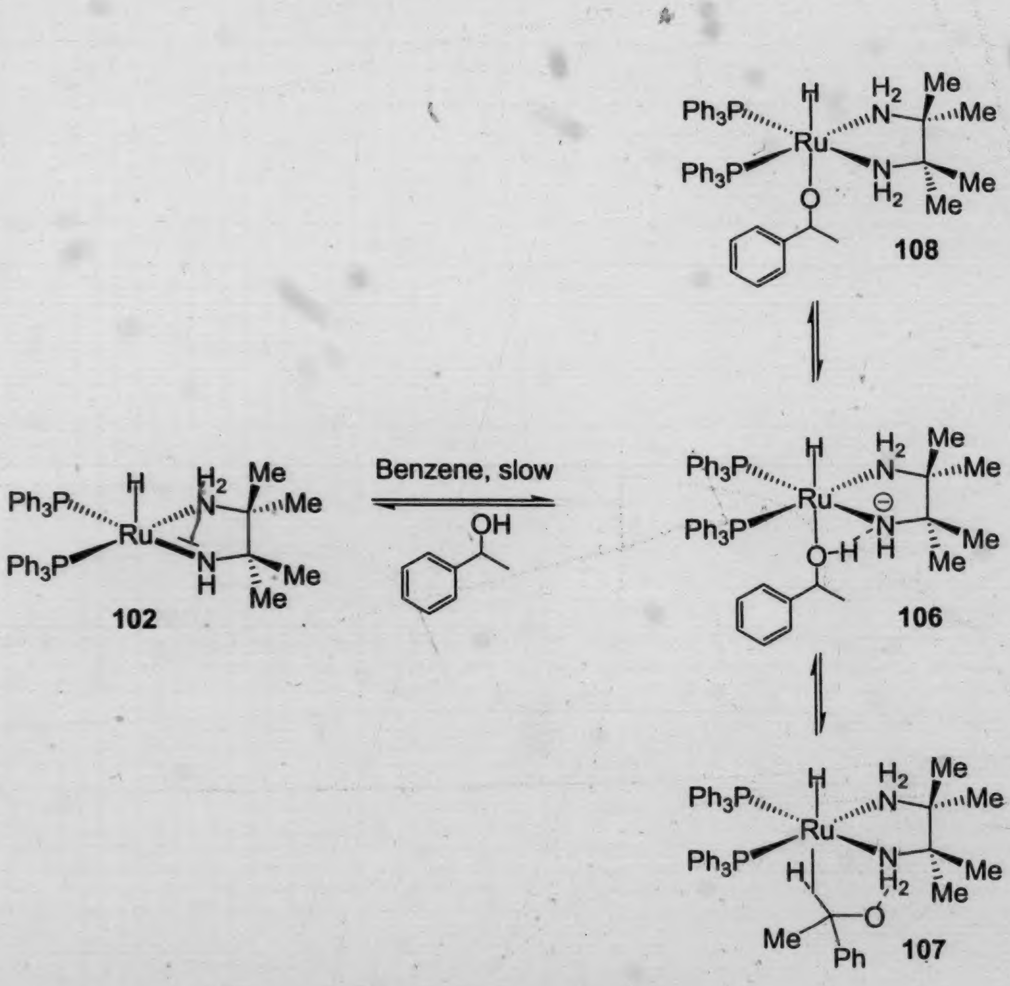

Figure 3.5: Reaction of 1-phenylethanol and a model amide.

Morris *et al.* showed that ruthenium-alkoxides can also be made when the dihydride **99** is reacted with either 1-phenylethanol or 2-PrOH (Figure 3.6).[2b] It was proposed that the alcohol protonates one of the hydride ligands to form an undetected cationinc η^2-H_2 compound ion paired to the alkoxide anion (**109**). The alkoxide anion then displaces the η^2-H_2 ligand to form the corresponding alkoxide complex (**110**). The alkoxides are proposed to be in rapid equilibrium with the dihydride as suggested by the broadening of the hydride resonance.

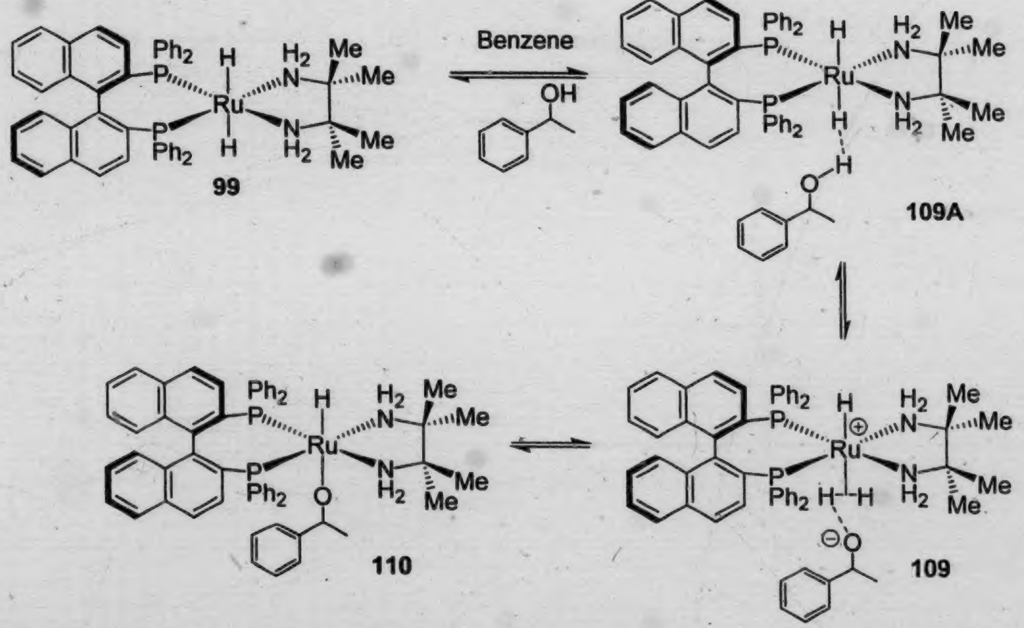

Figure 3.6: Proposed mechanism of akoxide formation.

The equilibrium shifts towards the alkoxide if more alcohol is added, and the dihydride can be regenerated if *t*-BuOK is added.[2b] As is the case for **108**, only hydride ^{1}H and ^{31}P NMR were used to characterize **110**.

Morris *et al.*'s reactivity study on the model compounds of the metal-ligand bifunctional mechanism outlined what reactivity may be expected with the actual intermediates. Although model compounds for the metal-ligand bifunctional mechanism have been made and studied, the difficulties encountered when studying these systems (*vide supra*) made the synthesis and reactivity study of the actual intermediates impossible at the time. In fact virtually none of the proposed intermediates in the metal-ligand bifunctional mechanism have been prepared.

Results and Discussion

Chapter 2 discussed a high yielding, low-temperature synthesis of the BINAP-containing cationic η^2-H_2 intermediate *trans*-[Ru((*R*)-BINAP)(H)(η^2-H_2)((*R*,*R*)-dpen)]$^+$ (**1**) in 2-PrOH-d_8 containing CD_2Cl_2.[6] Reactivity studies showed that the η^2-H_2 group in **1** is extremely labile. The η^2-H_2 is readily displaced by D_2 to form the η^2-D_2 isotopomer or by BH_4^- to form **82'**. The downfield chemical shift of the η^2-H_2 resonance, along with the relatively large $^1J_{H\text{-}D}$ coupling constant of the η^2-H-D isotopomer, shows that it retains a high degree of free H_2 character. Flushing the H_2 from 2-PrOH solutions of **1** with Ar results in decomposition, presumably by loss of H_2 and β-H elimination from the dpen ligand. Most significantly, **1** is inactive towards the hydrogenation of acetophenone at 4 atm of H_2, 30°C, and using 2000 equiv of ketone unless 1 equiv of *t*-BuOK or BH_4^- is added as base. Compound **1**, therefore, does not generate **6** without added base under these conditions.[6] Chapter 3 discusses the study of the key reaction of **1** with base under various conditions.

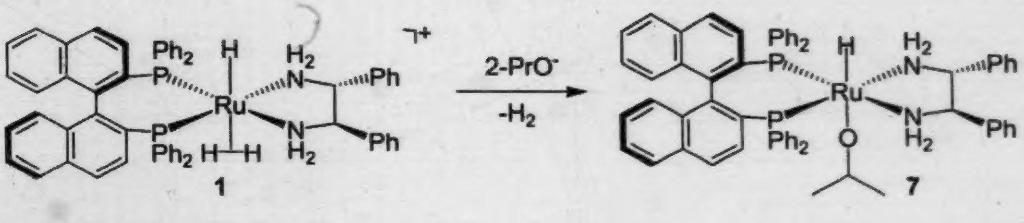

Equation 3.2

Reaction of **1** with 1 equiv of *t*-BuOK under H_2 (~2 atm H_2, 2-PrOH, -80 °C) resulted in immediate[7] formation of the 2-propoxide compound *trans*-Ru((*R*)-BINAP)(H)(2-PrO)((*R*,*R*)-dpen) (**7**) (Equation 3.2). Morris *et al.* proposed that conversion of the model dihydride **99** to the 2-propoxide compound involved an intermediate in which η^2-H_2 ligand is ion paired to 2-propoxide. The rapid formation of **7** suggests that it is more likely that any 2-propoxide formed by the reaction of base and 2-PrOH solvent would simply displace the labile η^2-H_2 group. Compound **7** can also be precipitated from CH_2Cl_2/2-PrOH solutions by the addition of hexanes and studied independently, demonstrating an unexpected stability. The results from Morris' studies (*vide supra*) infer that **6** may be in equilibrium with either the amide [Ru((*R*)-BINAP)(H)((*R*,*R*)-NH(CH(Ph))$_2$NH$_2$))] (**11**),[2b] or with the cationic solvento compound *trans*-[Ru((*R*)-BINAP)(H)(2-PrOH)((*R*,*R*)-dpen)]$^+$ (**8**).[1b] Unexpectedly, I found no evidence for the amide **11** or the solvento compound **8**. Compound **7** also displays remarkable stability towards dissolved H_2. There was no evidence for the formation of the *trans* dihydride **6** after prolonged exposures of 2-PrOH solutions of **7** to H_2 gas (~ 10 h, ~2 atm, 22 °C) in the absence of base.

Baratta *et al.* recently reported that the reaction of benzephenone with

[Ru(H)(CNN)(dppb)] (**111**, HCNN = 6-(4'-methylphenyl)-2-pyridylmethylamine, dppb=1,4-bis(diphenylphosphino)-butane) in benzene at 20 °C results in the formation of a ruthenium alkoxide (**112**, Equation 3.3).[5] The hydride catalyst contains the Ru-H/N-H motif that is proposed to be essential for the high activity of these catalysts. One of the N-H resonances in the alkoxide has a relatively downfield chemical shift of 5.3 ppm. It was proposed that the downfield shift was caused by an intramolecular hydrogen bond between the alkoxide oxygen and the N-H.[5] This interaction would also result in increased stability of the alkoxide. The unexpected stability of **7** may result from similar intramolecular H-bonding between the 2-PrO$^-$ ligand and an N-H group (Figure 3.7). Bergman *et al.* observed a similar intermolecular hydrogen bond when phenols were added

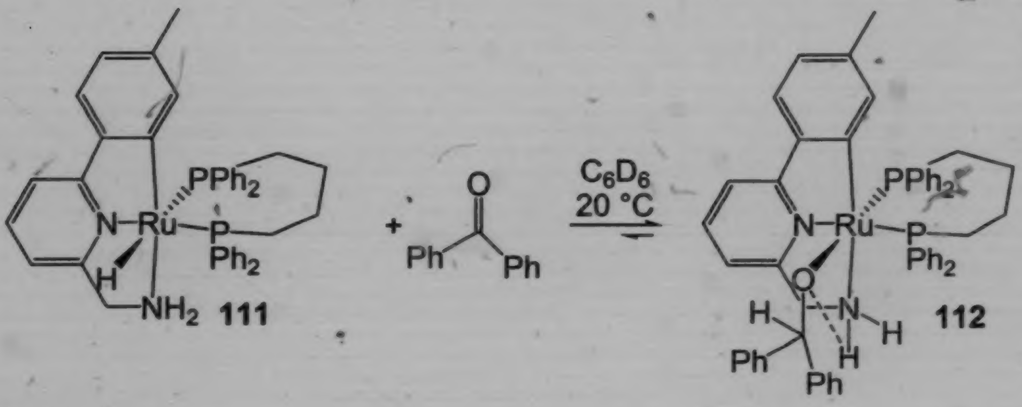

Equation 3.3

to rhodium-aryloxides.[8] The hydrogen bonded compounds were stable in the solid state, and only underwent ligand exchange upon increasing the temperature to 45 °C.

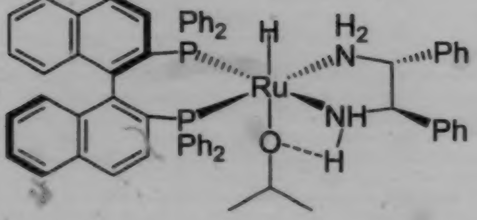

Figure 3.7: Proposed intramolecular hydrogen bonding in the 2-propoxide.

The N-H groups in the dihydrogen compound **1** undergo H-D exchange with 2-PrOH-d_8 upon mixing at -80 °C. The hydride and η^2-H_2 ligands begin to exchange with 2-PrOH-d_8 and free H_2 upon warming to ~ -60 °C. The N-H groups are therefore kinetically, at least, the most acidic protons in **1**. To prevent both H-D exchange and formation of the 2-propoxide **7**, compound **1** was prepared in THF-d_8. The compound [Ru((*R*)-BINAP(H)(2-PrOH)$_3$](BF$_4$) (**87**) decomposes at temperatures above -40 °C whereas [Ru((*R*)-BINAP(H)(THF)$_3$](BF$_4$) (**113**) is stable up to 0 °C.[9] This stability demonstrates that THF is a stronger ligand for these type of compounds than 2-PrOH. Unlike in 2-PrOH, warming THF-d_8 solutions of the η^2-H_2 compound **1** under ~2 atm H_2 reveals an equilibrium that shifts from ~84% **1** at -80 °C, to a ~ 2:1 mixture of **1** and the solvento compound *trans*-[Ru((*R*)-BINAP)(H)(THF-d_8)((*R*,*R*)-dpen)]$^+$ (**9**) at -50 °C (Equation 3.4). This change may be caused by the decreased solubility of H_2 gas in liquids upon raising the temperature. Compound **9** is the THF-d_8 analogue of the 2-PrOH adduct **8**, a catalytic intermediate that Noyori *et al.* proposes to react with H_2 and form **1**.[1d,1e] Compound **9** behaved similarly to Noyori *et al.*'s proposed reactivity for **8**. The equilibrium in THF-d_8 shifts back to the η^2-H_2 compound when cooled to -80 °C, and it shifts to **9** when the H_2 is replaced with Ar. Also, the THF-d_8 adduct **9** does not decompose *via* β-elimination, even at ~22 °C.

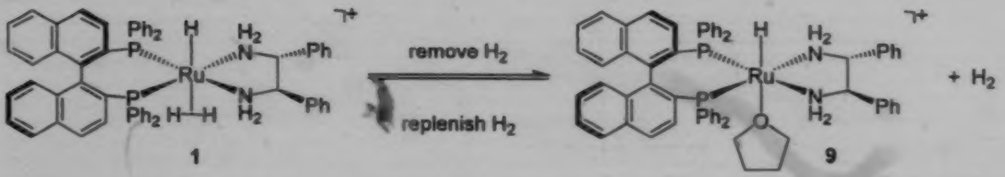

Equation 3.4

To study the reaction with base, **1** was reacted with ~1 equiv of *t*-BuOK in THF-d_8 at -60 °C. It is extremely difficult to remove all traces of water from THF-d_8. There was approximately one equiv of water present in solution, even if the THF-d_8 was freshly distilled over potassium. As such, the reaction with base resulted in the immediate formation of the hydroxide analogue of **7**, *trans*-Ru((*R*)-BINAP)(H)(OH)((*R*,*R*)-dpen) (**10**, Figure 3.8 and Equation 3.5). This result is analogous to the reaction in 2-PrOH (*vide supra*) except there is facile replacement of η^2-H_2 in **1** by a hydroxide ion to form **10**. Like the 2-propoxide compound **7**, the hydroxide compound **10** can be precipitated from solution by the addition of hexanes at –80 °C. Additionally, compound **10** did not react with

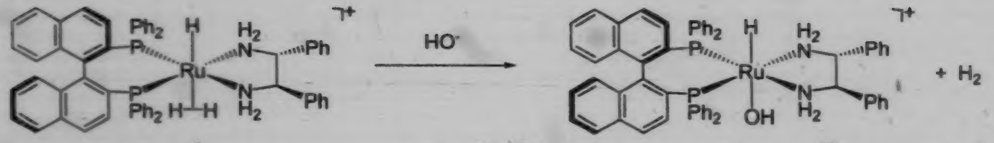

Equation 3.5

H_2 gas (~2 atm, ~22 °C) to generate the dihydride **6**. This result demonstrates that compound **10** has similar unexpected stability as compound **7**, perhaps due to the presence of similar intramolecular hydrogen bonds. Compound **10** has two downfield (5.29 and 5.41) ^{1}H NMR resonances assigned to N-H protons which may be an indication of these hydrogen bonds. The ^{1}H NMR resonance for the hydroxide proton is a sharp singlet at ~ -1 ppm which is typical for ruthenium-hydroxide compounds. Since the hydroxide ^{1}H NMR resonance is sharp, it may be an indication that it is not undergoing a rapid exchange process.

Reaction of the hydroxide **10** with ~ 1 further equiv of *t*-BuOK in THF-d_8 at -60 °C quickly produced a new compound that I formulate as the

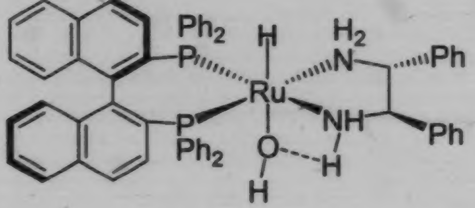

Figure 3.8: Proposed intramolecular hydrogen bonding in the hydroxide compound.

$N\cdots H_{equatorial}\cdots {}^{-}O$-*t*-Bu hydrogen-bonded species **13**. Bergman *et al.* observed similar intermolecular hydrogen bonds between ruthenium-amine complexes and alkoxide anions (Equation 3.6).[10] The signals in the NMR spectra of **13** and **10** are similar. The ^{1}H NMR resonance for the hydroxide proton shifts upfield to

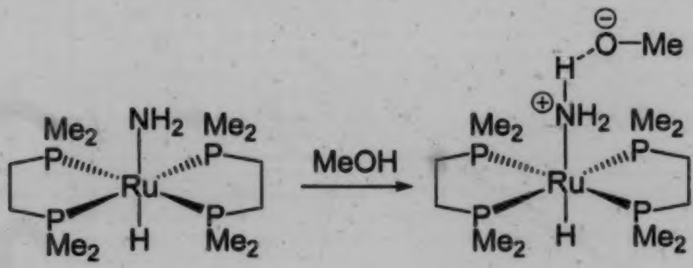

Equation 3.6

~1.5 along with significant broadening which may be an indication that the hydroxide is undergoing an exchange process. Additionally, the ^{1}H NMR resonances for the N-H protons in **13** shift upfield in comparison to **10** which may be an indication that the hydrogen bonds stabilizing **10** are disrupted. The largest shift was ~ 1.6ppm upfield by a $N\text{-}H_{equatorial}$. The analogous compound **12** forms when the 2-propoxide **7** reacts with ~ 1 equiv of *t*-BuOK in THF-d_8

(Equation 3.7). The ^{1}H NMR resonances for some the N-H protons in **12** also shift upfield in comparison to **7**. Significant to the catalytic hydrogenation, both

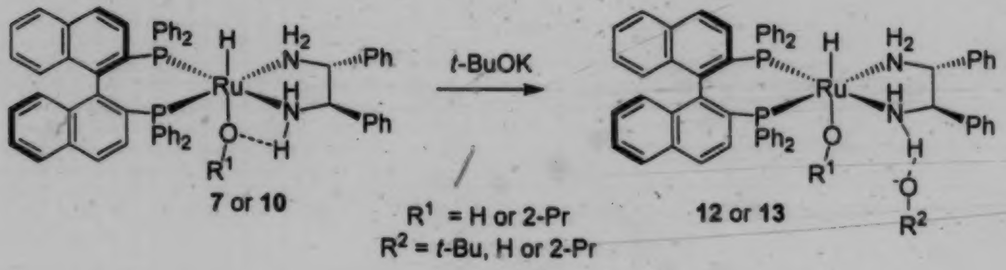

7 or **10**

R^1 = H or 2-Pr
R^2 = t-Bu, H or 2-Pr

12 or **13**

Equation 3.7

compounds **13** and **12** quickly react with H_2 gas (~2 atm H_2, -80 °C, <10 min) to generate the key catalytic intermediate, *trans*-dihydride **6**, which is stable at low temperature in THF-d_8 and therefore could be fully characterized by NMR. Morris *et al.*'s model dihydride **99** has nearly identical Ru-H ^{1}H NMR resonances, as well as the ^{31}P NMR, chemical shifts to **6** (-4.81 and 89.9 ppm versus -5.07 and 89.22 ppm, respectively).[2a] Further, Morris *et al.* reported a tentative observation of **6** in benzene based upon P and Ru-H NMR signals.[2a] A reasonable hypothesis is that these hydrogen additions proceed *via* deprotonation of the hydrogen bonded -N···H···$^-$OR group in **13** and **12** to effect an intramolecular elimination of the hydroxide- or alkoxide ligand, respectively, to form the amide **11** (Equation 3.8). The amide **11** then reacts with H_2 to produce **6**. Although a pathway involving β-hydride elimination is not ruled out, this hypothesis is supported by the reaction of the hydroxide **10** with ~ 1 equiv of the stronger, hindered base $((CH_3)_3Si)_2NK$ in the absence of H_2 gas in THF-

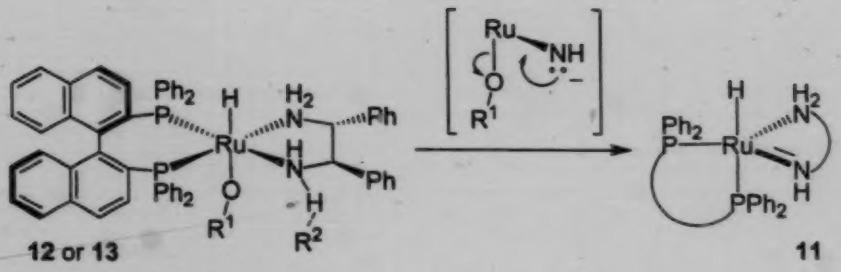

R^1 = H or 2-Pr
R^2 = *t*-BuO$^-$, 2-PrO$^-$ or (Si(CH$_3$)$_3$)$_2$N$^-$

Equation 3.8

d$_8$ at ~ -60 °C to immediately form the amide **11**, another intermediate in these catalytic hydrogenations. The amide **11** was stable at low temperature in THF-*d*$_8$, but decomposed at room temperature, presumably *via* β-hydride elimination.[2f]

The identification of **11** is in part based upon comparisons to Morris *et al.*'s characterization of the model amide Ru((R)-BINAP)(H)(NH(C(CH$_3$)$_2$)$_2$NH$_2$) (**101**) in benzene.[2a] The ^{1}H NMR resonances of the N-H's in **11** are similar to those of the model compound **101**. Most notable is the upfield shift the amide N-H being 1.39 ppm for **11** and 1.22 ppm for **101**. Compound **11** is present as two different diastereomers in an 8:2 ratio depending on which N-H is deprotonated whereas **101** is present as a single isomer. The Ru-H signal ^{1}H NMR spectrum appears as a doublet of doublets (major $^2J_{P\text{-}H}$ = 40.4, 24.4 Hz; minor $^2J_{P\text{-}H}$ = 47.5, 21.8 Hz) for both diasteromers **11**. The larger $^2J_{P\text{-}H}$ coupling constants for the Ru-H indicate that one of the phosphorus atoms is out of the equatorial plane. The $^2J_{P\text{-}H}$ coupling constant for the model compound **101** (33

Hz) is roughly an average of the $^2J_{P\text{-}H}$ coupling constants in **11** which would seem to indicate that **101** is actually present as two diastereomers as in **11**, but in rapid equilibrium with each other due to the elevated temperature. Additionally, the ^{31}P NMR resonances for the BINAP ligand in **11** and **101** are at similar chemical shifts.

Consistent with the results I obtained in wet THF, the amide **11** in dry THF-d_8 reacts immediately at -60 °C with H_2O or 2-PrOH (~5 equiv) to completely form the hydroxide **10**, or the 2-propoxide compound **7**, respectively (Equation 3.9).[11] In contrast, Morris *et al.* proposed, on the basis of preliminary product identification (P and Ru-H NMR signals), that the corresponding reaction between the amide $Ru(PPh_3)_2(H)(NH(C(CH_3)_2)_2NH_2)$ **102** and $Ph(CH_3)CHOH$ is slow, reversible, and does not go to completion. They suggested for this type of equilibrium in 2-PrOH that added base shifts the reaction towards the free amide by decreasing the net acidity of the solvent.[2b]

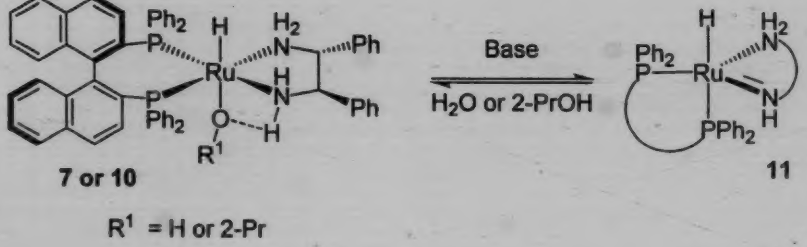

Equation 3.9

As has been proposed for these and related catalytic hydrogenations, I found that the amide **11** reacts quickly with H_2 (~2 atm H_2, -80 °C, <5 min) to generate the *trans*-dihydride **6** (Scheme 3.2).[1b,2a,3a] Reaction of the dihydride **6**

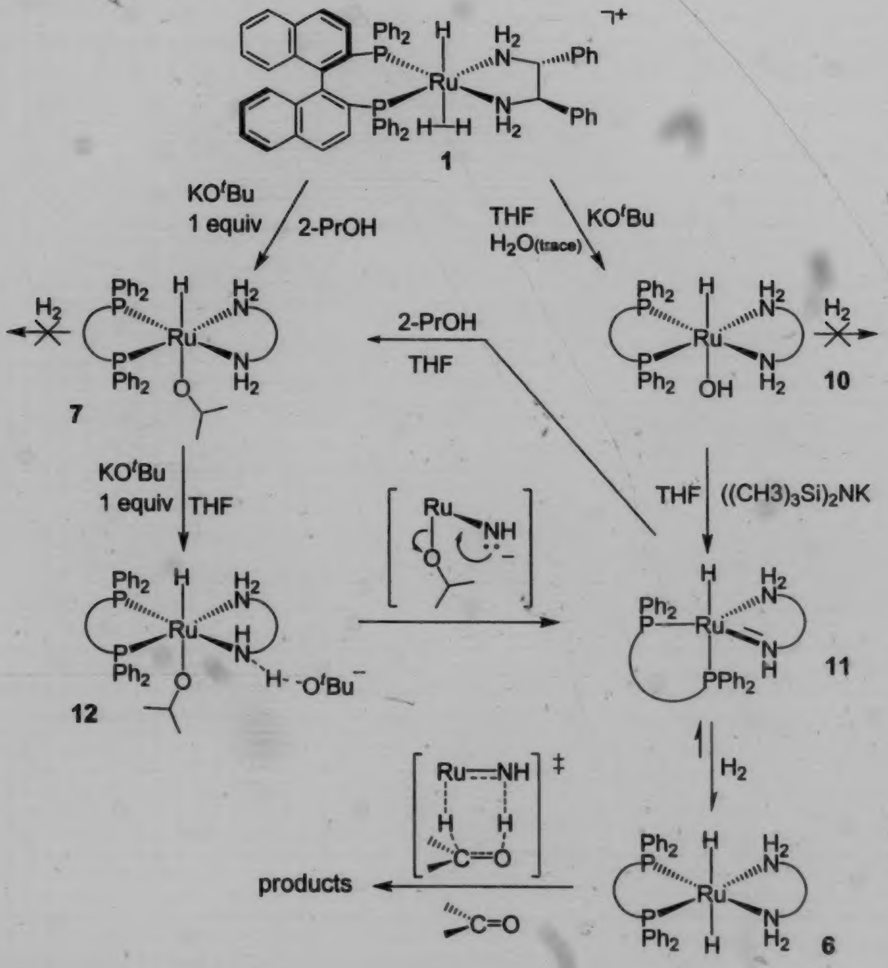

1
KO^{t}Bu
1 equiv
2-PrOH
THF
$H_2O_{(trace)}$
KO^{t}Bu
7
H_2
2-PrOH
THF
10
H_2
KO^{t}Bu
1 equiv
THF
THF
$((CH3)_3Si)_2NK$
12
H- -O^{t}Bu$^-$
11
H_2
‡
products
6

Scheme 3.2: Summary of the putative intermediates reactivity.

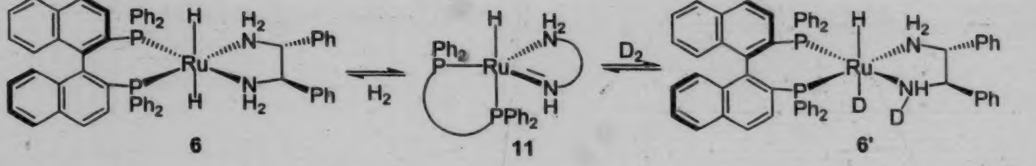

Equation 3.10

with D_2 in THF-d_8 caused H-D exchange at the Ru-H and the N-H_{axial} groups (Equation 3.10). Addition of H_2 to the amide **11** is reversible,[2b] and it is the axial N-H's that participate in this exchange. I also found that the dihydride **6** can also

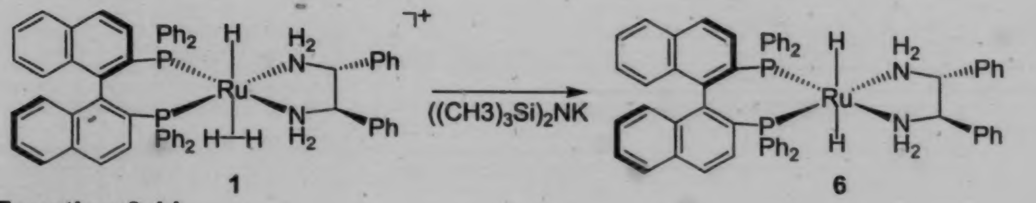

Equation 3.11

be prepared by reacting the η^2-H_2 compound **1** with $((CH_3)_3Si)_2NK$ under H_2 in dry THF-d_8 (Equation 3.11).

Conclusions

This chapter details the first low-temperature syntheses and conclusive characterizations of the illusive intermediates **9**, **11**, **6**, and a new intermediate, **12**. The results show that any amide **11** formed during a catalytic hydrogenation will quickly react with the 2-PrOH solvent to form the 2-propoxide **7** (Scheme 3.2). This observation, along with both the facile displacement of the η^2-H_2 ligand in **1** by 2-propoxide and the reversibility of H_2 addition to **6**, confirm

Morris *et al.*'s suggestion,[2b] from model studies, that the formation of **7** is in strong competition with H_2 for the amide **11** during these catalytic hydrogenations. Unlike the suggestion of Morris *et al.*, the formation of **7** was found to be fast, complete, and not kinetically reversible in the absence of base. A reasonable proposal is that adding base increases the rate of these hydrogenations by promoting the base-assisted elimination of 2-propoxide from **7** to form the amide **11**. It has been proposed that addition of H_2 to the amide **11** to produce **6** is the turnover limiting step of these hydrogenations carried out in the presence of excess base.[1b,2b] Observations show that H_2 addition to the amide **11** occurs at high rates at -80 °C. Therefore the hydrogen addition is turnover limiting in the presence of excess base because the steady-state concentration of **11** is low during the catalytic hydrogenation. Chapter 4 will discuss the key reaction between the dihydride **6** and the common ketone test substrate, acetophenone.

Materials and Methods

All operations were carried out in NMR tubes fitted with a rubber septum under an atmosphere of argon or hydrogen using standard Schlenk and glovebox techniques unless stated otherwise. The inside walls of the NMR tubes were silanized by reaction with chlorotrimethylsilane followed by removal of the excess chlorotrimethylsilane by heating under vacuum. All solvents were dried and distilled under a dinitrogen atmosphere using standard drying agents unless stated otherwise. All solvents were degassed by three freeze-pump-thaw cycles before use. Deuterated isopropanol was not dried. The deuterated solvents were obtained from Cambridge Isotope Laboratories. Common solvents were obtained from Fisher Scientific. Common chemicals were obtained from Aldrich. (*R*,*R*)-dpen and (*R*)-BINAP were obtained from Strem. Potassium tert-butoxide was sublimed immediately before use. The reactions were monitored using low-temperature NMR spectroscopy. The reaction times are approximate. If an immediate color change occurred when the reactants were mixed at low temperatures, and if the first NMR spectrum, recorded within 5 min of mixing, showed the reaction was complete, I report the reaction time as immediate at the temperature the NMR spectrum was recorded. If no visible color change occurred upon mixing, and if the first NMR spectrum showed the reaction was complete, I report the reaction time as less than the time period between mixing and when the first NMR spectrum was recorded.

^{1}H, ^{13}C, and ^{31}P NMR spectra were measured using Varian-Inova (400 or 500 MHz) spectrometers. ^{1}H and ^{13}C NMR chemical shifts are reported in parts per million (δ) relative to TMS with the solvent as the internal reference. ^{31}P chemical shifts are reported in parts per million (δ) relative to an 85% H_3PO_4 external reference. NMR peak assignments were made using COSY and ^{13}C–^{1}H HMQC 2D NMR experiments. Some axial and equatorial N-H assignments for **1** and **7** were made using NOESY NMR experiments. The N-H_{axial} adjacent to Ru-H was ~ 2 ppm upfield from the other N-H's in **1** and **7**. The same observation was reported for N-H_{axial} adjacent to Ru-H in a series of compounds studied by Noyori, *et al.*[12] This observation is used to assign the N-H_{axial} adjacent to Ru-H in compounds **9**, **10**, **13**, **11**, and **6**. Mass spectrometric analyses of organometallic compounds were performed by positive-mode electrospray ionization (ESI-MS (pos)) on a Micromass ZabSpec Hybrid Sector-TOF spectrometer. Calculated *m*/*z* values refer to the isotopes ^{12}C, ^{1}H, ^{14}N, ^{16}O, ^{31}P, and ^{102}Ru.

Reaction of 1 with *t*-BuOK to form *trans*-[Ru((*R*)-BINAP)(H)(2-PrO)((*R*,*R*)-dpen)] (7). Using a procedure described previously,[6] a solution of complex **1** (7.95 × 10^{-3} mmol) in 2-PrOH-d_8/CH_2Cl_2-d_2 (~ 0.4 and 0.2 mL, respectively) under ~2 atm H_2 was prepared at –80 °C in a 5mm NMR tube fitted with a rubber septum. A solution of *t*-BuOK (0.8mg, 7.13 × 10^{-3} mmol) in 2-PrOH-d_8 (~0.2mL) was prepared under nitrogen in a 5 mm NMR tube fitted with a rubber septum, cooled to –80 °C, and quickly transferred through a short cannula under hydrogen pressure into the solution of **1** at –80 °C. The pressure of H_2 in the reaction tube was replenished after the transfer by injecting 5 mL of H_2 with a gas-tight syringe. The contents of the tube were then thoroughly mixed by quickly shaking the tube for 2 sec outside the –80 °C bath, returning it to the bath, and repeating the process 4 more times. The color changed from dark orange to dark yellow-orange immediately during the first shake to mix the contents of the tube. An NMR spectrum recorded at –80 °C after ~ 5 min showed that the reaction was complete and formed **7-2PrO-d_7** as sole detectable product. ^1H NMR (399.79 MHz, 2-PrOH-d_8/CH_2Cl_2-d_2, –80 °C): δ –17.81 (1H, t, $^2J_{P\text{-}H}$ = 26.6 Hz, Ru–H), 3.95-4.1 (2H, om, C_aHNDD and C_bHNDD), 6-8.5 (42H, om, aromatic). $^{13}C\{^1H\}$ NMR (100.6 MHz, 2-PrOH-d_8/CH_2Cl_2-d_2, –80

°C): δ Coordinated 2-PrO-d_7 signals are obscured by 2-PrOH-d_8 solvent, 63.9 (C_aHNHH), 69.7 (C_bHNHH), 123-141 (aromatic). $^{31}P\{^1H\}$ NMR (161.9 MHz, 2-PrOH-d_8/CH_2Cl_2-d_2, –80 °C): δ 64.7 (d, $^2J_{P-P}$ = 41.5 Hz), 73.0 (d, $^2J_{P-P}$ = 41.5 Hz). The reaction mixture was reduced to dryness under vacuum at 0 °C, the residue was treated with one drop of 2-PrOH to exchange the 2-PrO-d_7 with 2-PrO, and to convert the N-D into N-H groups, the mixture was again reduced to dryness under vacuum at 0 °C, and the resulting perprotio-**7** was dissolved in dry THF-d_8. ^1H NMR (399.85 MHz, THF-d_8, –80 °C): δ –17.15 (1H, t, $^2J_{P-H}$ = 24.7 Hz, Ru–H), 1.04 (Ru–OCH(CH_3)$_2$, obscured by residual 2-PrOH solvent), 2.02 (1H, br, C_aHNH_{axial}H), 3.9-4.5 (4H, broad overlapping, partially obscured by 2-PrOH signal, C_b*H*NHH, C_a*H*NHH, C_bHNH*H*, C_bHN*H*H), 4.06 (1H, septet, $^3J_{H-H}$ = 3.9 Hz, Ru–OC*H*(CH_3)$_2$), 4.62 (1H, br, C_aHNH$H_{equatorial}$), 6-9.2(om, aromatic). $^{13}C\{^1H\}$ NMR (100.6 MHz, THF-d_8, –80 °C): δ 62.3 (C_aHNHH), 68.4 (C_bHNHH), 123-141 (aromatic). $^{31}P\{^1H\}$ NMR (161.9 MHz, THF-d_8, –80 °C): δ 64.9 (d, $^2J_{P-P}$ = 40.8 Hz), 71.6 (d, $^2J_{P-P}$ = 39.7 Hz). LRMS (ESI): *m/z* calcd for $C_{61}H_{56}N_2OP_2{}^{102}Ru$ ($[M]^+$), 996.3; found, 996.3. It is known that $[M]^+$ can result from electrochemical oxidation of organometallic compounds during ESI MS.[13]

Preparation of *trans*-[Ru((*R*)-BINAP)(H)(η^2-H_2)((*R*,*R*)-dpen)]BF_4 (1) in THF-*d_8*. A solution of *fac*-[Ru((*R*)-BINAP(H)(sol)$_3$]BF_4 (9.0 mg, 8.56×10^{-3} mmol, sol = solvent) in THF-d_8 (0.5 mL) was prepared under H_2 (~2 atm) as described previously[9] and then cooled to –80 °C. A –80 °C solution of (*R*,*R*)-dpen (1 equiv, 1.8 mg) in THF-d_8 (0.1 mL) was then quickly canulated using H_2 pressure into the tube containing *fac*-[Ru((*R*)-BINAP(H)(sol)$_3$]BF$_4$. The pressure of H_2 was replenished after the transfer by injecting 5 mL of H_2 into the tube using a gas-tight syringe. The contents of the tube were then thoroughly mixed by quickly shaking the tube for 5 sec outside the –80 °C bath, returning it to the bath, and then repeating the process four times. NMR Spectra recorded at –80 °C after ~5 min showed that the reaction was complete and formed **1** as sole detectable product. ^{1}H NMR (399.91 MHz, THF-*d*$_8$, –80 °C): δ –8.54 (1H, t, $^2J_{P\text{-}H}$ = 22.5 Hz, Ru–H), –0.48 (2H, br, Ru–η^2-H_2), 1.99 (1H, br t, $^3J_{H\text{-}H}$ = 12 Hz, C$_a$HN*H*$_{axial}$H), 3.67 (1H, br t, $^3J_{H\text{-}H}$ = 12 Hz, C$_b$HNH*H*), 3.93 (1H, app t, $^3J_{H\text{-}H}$ = 12 Hz, C$_b$*H*NHH), 4.05 (1H, br t, $^3J_{H\text{-}H}$ = 12 Hz, C$_a$*H*NHH), 4.66 (1H, br d, $^3J_{H\text{-}H}$ = 12 Hz, C$_b$HNH*H*), 5.15 (1H, br, C$_a$HNH*H*$_{equatorial}$), 6-8.8 (42H, om, aromatic). ^{13}C{^{1}H} NMR (100.6 MHz, THF-*d*$_8$, –80 °C): δ 63.9 (*C*$_a$HNHH), 69.7 (*C*$_b$HNHH), 123-141 (aromatic). ^{31}P{^{1}H} NMR (161.9 MHz, THF-*d*$_8$, –80 °C): δ 70.92 (d, $^2J_{P\text{–}P}$ = 33 Hz), 72.14 (d, $^2J_{P\text{–}P}$ = 33 Hz). Note that adding 2-PrOH-*d*$_8$ at -80 °C caused immediate H-D exchange at the N-H groups.

Preparation of *trans*-[Ru((*R*)-BINAP)(H)(THF-*d*$_8$)((*R*,*R*)-dpen)]BF$_4$ (9). Complex **1** was prepared in THF-*d*$_8$ at –80 °C as described above. Argon gas (1 atm) was bubbled through the solution for 10 min to generate **9**. Adding H_2 gas regenerated **1**. As described in the main text of the paper, relative concentrations of **1** and **9** in the mixture depended on the temperature and the amount of H_2 gas added. ^{1}H NMR (399.89 MHz, THF-*d*$_8$, –40 °C): δ –23.11 (1H, br, Ru–H), 2.30 (1H, br t, $^3J_{H\text{-}H}$ = 12 Hz, C$_a$HN*H*$_{axial}$H), 2.97 (1H, br t, $^3J_{H\text{-}H}$ = 12

Hz, C_bHNHH), 4.0 (1H, om, C_bHNHH, overlapping with C_aHNHH), 4.02 (1H, om, C_aHNHH, overlapping with C_bHNHH), 4.39 (1H, br d, $^3J_{H\text{-}H}$ = 8 Hz, C_bHNHH), 4.68 (1H, br d, $^3J_{H\text{-}H}$ = 8 Hz, $C_aHNHH_{equatorial}$), 6-8.5 (42H, om, aromatic). $^{13}C\{^1H\}$ NMR (100.6 MHz, THF-d_8, –40 °C): δ 62.8 (C_aHNHH), 69.09 (C_bHNHH), 123-141 (aromatic). $^{31}P\{^1H\}$ NMR (161.88 MHz, THF-d_8, –40 °C). δ 65.37 (d, $^2J_{P\text{–}P}$ = 35.5 Hz), 70.41 (d, $^2J_{P\text{–}P}$ = 35.5 Hz).

Reaction of Complex 1 with *t*-BuOK in wet THF-d_8 to produce *trans*-[Ru((*R*)-BINAP)(H)(OH)((*R,R*)-dpen)] (10). It was extremely difficult to maintain the THF-d_8 rigorously dry during the steps required to prepare **1**. A solution of **1** (7.2×10^{-3} mmol) in THF-d_8 (~ 0.6 mL) at –80 °C under H_2 (~ 2 atm) was prepared as described above. A solution of *t*-BuOK (0.8 mg, 7.13×10^{-3} mmol) in THF-d_8 (~0.1 mL) was prepared under nitrogen –80 °C and then quickly transferred through a short cannula under hydrogen pressure into the solution of **1** at –80 °C. The pressure of H_2 was replenished after the transfer by injecting 5mL of H_2 into the tube using a gas-tight syringe. The contents of the tube were shaken for 2 sec and returned to the cooling bath 5 times. A colour change from orange to yellow-orange occurred during the first shake. NMR spectra recorded after 5 min at –60 °C showed the reaction was complete. ^1H NMR (399.87 MHz, THF-d_8, –60 °C): δ –16.24 (1H, t, $^2J_{P\text{-}H}$ = 23.9 Hz, Ru–H), –1.08 (1H, s, Ru–OH), 2.48 (1H, br t, $^3J_{H\text{-}H}$ = 12 Hz, $C_aHNH_{axial}H$), 3.75 (1H, br, C_bHNHH), 4.32 (1H, br t, $^3J_{H\text{-}H}$ = 12 Hz, C_bHNHH), 4.63 (1H, br q, $^3J_{H\text{-}H}$ = 12 Hz, C_aHNHH), 5.29 (1H, br t, $^3J_{H\text{-}H}$ = 12 Hz, C_bHNHH), 5.41 (1H, br t, $^3J_{H\text{-}H}$ = 12 Hz,

$C_aHNHH_{equatorial}$), 6-10.1 (42H, om, aromatic). $^{13}C\{^1H\}$ NMR (100.6 MHz, THF-d_8, –60 °C): δ ~64.0 (C_aHNHH), 70.8 (C_bHNHH), 123-141 (aromatic). $^{31}P\{^1H\}$ NMR (161.88 MHz, THF-d_8, –60 °C): δ 75.7 (d, $^2J_{P–P}$ = 38.0 Hz), 69.0 (d, $^2J_{P–P}$ = 38.0 Hz). The ^{1}H NMR of **10** contains the hydroxide signal at ~–1.1 ppm, which is similar to reported ruthenium-hydroxide compounds.[13] HRMS (ESI): *m/z* calcd for $C_{58}H_{47}N_2OP_2{}^{102}Ru$ ([M-3]$^+$), 951.22016; found, 951.22011. The fragmentation of **10** during ESI MS needs to be investigated. Prolonged exposure of **10** to H_2 (~ 2 atm, room temp.) did not result in the formation of *trans*-[Ru((*R*)-BINAP)(H)$_2$((*R*,*R*)-dpen)] (**6**).

Reaction of *trans*-[Ru((*R*)-BINAP)(H)(OH)((*R*,*R*)-dpen)] (10) with *t*-BuOK in THF to produce *trans*-[Ru((*R*)-BINAP)(H)(OH)((*R*,*R*)-(NH$_2$(CH(Ph))$_2$NH···H···$^-$O-*t*-Bu)] (13). The product [Ru((*R*)-BINAP)(H)(OH)((*R*,*R*)-(NH$_2$(CH(Ph))$_2$NH···H···$^-$O-*t*-Bu)] (**13**) can be prepared by two consecutive additions of 1 equiv of *t*-BuOK to **9** in THF. The first addition will generate *trans*-[Ru((*R*)-BINAP)(H)(OH)((*R*,*R*)-dpen)] (**10**) by replacement of the labile THF ligand in **9** by OH$^-$, and the second addition will generate **13**. I found it more convenient to add *t*-BuOK to **9** in one addition. Specifically, a solution of complex **9** (1.07 × 10^{-2} mmol) in THF-d_8 (0.7) at –80 °C was prepared as described above. A –80 °C solution of *t*-BuOK (2.4 mg, 2 equiv) in THF-d_8 (0.1 mL) was quickly canulated into the solution of **9** at –80 °C. The tube was then shaken for 10 sec and returned to the bath five times in order to maintain the temperature near –80 °C. NMR spectra recorded after 5 min showed the

reaction was complete. ^{1}H NMR (399.87 MHz, THF-d_8, –60 °C): δ –16.23 (1H, t, $^2J_{P\text{-}H}$ = 24.4 Hz, Ru–H), –1.5 (1H, br, Ru–OH), 2.19 (1H, br t, $^3J_{H\text{-}H}$ = ~8 Hz, $C_aHNH_{axial}H$), 3.32 (1H, br t, $^3J_{H\text{-}H}$ = 12 Hz, C_bHNHH), 4.01 (1H, app t, $^3J_{H\text{-}H}$ = 12 Hz, C_bHNHH), 4.12 (1H, br d, $^3J_{H\text{-}H}$ = ~10 Hz, C_bHNHH), 4.38 (1H, om, C_aHNHH, overlapping with $C_aHNHH_{equatorial}$), 4.42 (1H, om, $C_aHNHH_{equatorial}$, overlapping with C_aHNHH), 6-9.5 (42H, om, aromatic). $^{13}C\{^1H\}$ NMR (100.6 MHz, THF-d_8, –60 °C): δ ~64.9 (C_aHNHH), 69.9 (C_bHNHH), 123-141 (aromatic). $^{31}P\{^1H\}$ NMR (161.88 MHz, THF-d_8, –60 °C): δ 69.0 (d, $^2J_{P\text{-}P}$ = 40.0 Hz), 74.0 (d, $^2J_{P\text{-}P}$ = 40.0 Hz).

Reaction of *trans*-[Ru((*R*)-BINAP)(H)(2-PrO)((*R,R*)-dpen)] (7) with *t*-BuOK in THF to prepare *trans*-[Ru((*R*)-BINAP)(H)(2-PrO)((*R,R*)-NH$_2$(CH(Ph))$_2$NH···H···$^-$O-*t*-Bu)] (12). A solution of complex **7** (1.03×10^{-2} mmol) in THF-d_8 (0.7 mL) at –80 °C was prepared as described above. A –80 °C solution of *t*-BuOK (1.1 mg, 0.95 equiv) in THF-d_8 (0.1 mL) was quickly canulated under argon pressure into the solution of **7** at –80 °C. The tube was then shaken for 5 sec and returned to the bath five times in order to maintain the temperature near –80 °C. NMR spectra recorded after 5 min showed the reaction was complete. ^{1}H NMR (399.85 MHz, THF-d_8, –60 °C): δ –17.50 (1H, t, $^2J_{P\text{-}H}$ = 25.4 Hz, Ru–H), 1.06 (br, Ru–OCH(CH_3)$_2$, partially obscured by residual 2-PrOH solvent), 1.95 (1H, app. t, $^3J_{H\text{-}H}$ = 12 Hz, $C_aHNH_{axial}H$), 3.50 (1H, app. t, $^3J_{H\text{-}H}$ = 12 Hz, C_bHNHH, partially obscured by THF-d_8 solvent signal), 3.91 (br, Ru–OCH(CH$_3$)$_2$, partially obscured by residual 2-PrOH solvent), 4.0 (C_bHNHH, partially obscured by 2-PrOH signal), 4.12 (C_aHNHH, overlapping with C_bHNHH), 4.14 (C_bHNHH, overlapping with C_aHNHH), 4.7 (1H, app br t, $^3J_{H\text{-}H}$ = 12 Hz, C_aHNH$H_{equatorial}$), 6-8.8 (42H, om, aromatic). $^{13}C\{^1H\}$ NMR (100.6 MHz, THF-d_8, –80 °C): δ coordinated 2-PrO- signals are obscured by residual 2-PrOH solvent, 63.8 (C_aHNHH), 69.7 (C_bHNHH), 123-141 (aromatic). $^{31}P\{^1H\}$ NMR (161.9 MHz, THF-d_8, –60 °C): δ 64.7 (d, $^2J_{P\text{–}P}$ = 40.8 Hz), 72.8 (d, $^2J_{P\text{–}P}$ = 40.8 Hz).

Reaction of *trans*-[Ru((*R*)-BINAP)(H)(OH)((*R,R*)-NH$_2$(CH(Ph))$_2$NH···H···O-*t*-Bu)] (13) with H$_2$ to prepare *trans*-[Ru((*R*)-BINAP)(H)$_2$((*R,R*)-dpen)] (6). A solution of complex **13** (7.2 × 10^{-3} mmol) in THF-d_8 (0.7 mL) was prepared as described above under an atmosphere of argon and kept at –80 °C. H_2 gas (5 mL, ~ 2 atm) was injected into the tube using a gas tight syringe, and the tube was shaken for 10 sec outside the cooling bath, and returned 5 times in order to mix the contents of the tube and to maintain the temperature at –80 °C. NMR spectra recorded at –60 °C and 10 min after mixing showed the formation of **6** was complete. ^1H NMR (499.83 MHz, THF-d_8, –60 °C): δ –5.07 (2H, t, $^2J_{P\text{-}H}$ = 15.7 Hz, Ru–H), 2.62 (2H, br. t, $^3J_{H\text{-}H}$ = 9 Hz, CHNH_{axial}H), 3.84 (2H, br d, $^3J_{H\text{-}H}$ = 9 Hz, CHNHH), 3.95 (2H, br d, $^3J_{H\text{-}H}$ = 9 Hz, CHNH$H_{equatorial}$), 6-9.2 (om, aromatic). $^{13}C\{^1H\}$ NMR (125.7 MHz, THF-d_8, –60 °C): δ 66.5 (CHNHH, overlapping with solvent signal), 123-141 (aromatic). $^{31}P\{^1H\}$ NMR (202.34 MHz, THF-d_8, –60 °C): δ 89.22 (s).

Reaction of *trans*-[Ru((*R*)-BINAP)(H)(2-PrO)((*R,R*)-$NH_2(CH(Ph))_2NH\cdots H\cdots O$-*t*-Bu)] (12) with H_2 to prepare *trans*-[Ru((*R*)-BINAP)$(H)_2$((*R,R*)-dpen)] (6). A solution of **12** (1.03×10^{-2} mmol) in THF-d_8 (0.7 mL) was prepared as described above under an atmosphere of argon and kept at –80 °C. H_2 gas (5 mL, ~ 2 atm) was injected into the tube using a gas tight syringe, and the tube was shaken for 1 sec outside the cooling bath, and returned 5 times in order to mix the contents of the tube and to maintain the temperature at –80 °C. NMR spectra recorded at –80 °C and 10 min after mixing showed the formation of **6** was complete.

Reaction of *trans*-[Ru((*R*)-BINAP)(H)(OH)((*R,R*)-dpen)] (10) with $((CH_3)_3Si)_2NK$ in THF to prepare [Ru((*R*)-BINAP)(H)((*R,R*)-$NH(CH(Ph))_2NH_2$)] (11). It was extremely difficult to prepare and maintain THF that was absolutely dry to avoid the facile reaction between the product amide **11** and trace water to regenerate the hydroxide **10**. I found it convenient to avoid this difficulty by preparing the solvento complex **9** in THF as described above, and then to dry the THF of trace H_2O by reaction with one equiv of $((CH_3)_3Si)_2NK$ to generate the hydroxide compound **10**. In my experience, the resulting solution of **10** is sufficiently dry to react with 1 further equiv $((CH_3)_3Si)_2NK$ to prepare the amide **11** in 80 to 90 % yield, the remainder being the hydroxide **10**. Specifically, a –80 °C solution of complex **9** (8.93×10^{-3} mmol) in THF-d_8 (0.6 mL) was prepared as described above. A solution of $((CH_3)_3Si)_2NK$ (3.5 mg, 1.96 equiv) in THF-d_8 (0.1 mL) at –80 °C was quickly canulated into the solution of **9** using argon pressure. The tube was quickly shaken for 1 sec outside the bath and then returned to the bath 5 times in order to mix the contents while maintaining the temperature near –80 °C. A colour change from orange to deep red occurred during the first shake. Two diasteromers of **11** in an approximately 8:2 ratio are observed in NMR spectra recorded at –60 °C ~ 5 min after mixing. Both diastereomers of **11** are distorted trigonal bipyramidal with the hydride trans to a phosphine, and with the dpen occupying two equatorial positions. I believe that they differ by which diastereotopic nitrogen of the dpen ligand exists as the amide. *Major*: ^{1}H NMR (399.84 MHz, THF-d_8, –60 °C): δ –17.17 (1H, dd, $^{2}J_{P\text{-}H}$ = 24.4 Hz, $^{2}J_{P\text{-}H}$ = 40.4 Hz, Ru–H), 1.38 (obscured, C$_a$HN*H*H), 3.3 (1H, app. t, $^{3}J_{H\text{-}H}$ = 12 Hz, C$_a$*H*NHH), 3.72 (1H, br, C$_b$HN*H*), 4.24 (1H, app t, $^{3}J_{H\text{-}H}$ = 8 Hz, C$_b$*H*NH), 5.02 (1H, br d, $^{3}J_{H\text{-}H}$ = ~8 Hz, C$_a$HNH*H*), 6-8.8 (42H, om, aromatic). ^{13}C{^{1}H} NMR (100.6 MHz, THF-d_8, –60 °C): δ ~67.2 (*C*HNHH, obscured by solvent signal), 76.1 (*C*HNH), 123-141 (aromatic). ^{31}P{^{1}H} NMR (161.86 MHz, THF-d_8, –60 °C): δ 72.14 (d, $^{2}J_{P\text{–}P}$ = 35.4 Hz), 81.58 (d, $^{2}J_{P\text{–}P}$ = 35.4 Hz). *Minor*: (observable peaks) ^{1}H NMR (399.84 MHz, THF-d_8, –60 °C): δ –18.44 (dd, $^{2}J_{P\text{-}H}$ = 21.8 Hz, $^{2}J_{P\text{-}H}$ = 47.5 Hz, Ru–H), 2.58 (1H, br d, $^{3}J_{H\text{-}H}$ = ~9 Hz, C$_a$HN*H*H), 3.3 (C$_a$*H*NHH, obscurred by *major* C$_a$*H*NHH), 4.02 (1H, br, C$_b$HN*H*), 4.41 (1H, br, C$_b$*H*NH). ^{13}C{^{1}H} NMR (100.6 MHz, THF-d_8, –60 °C): The concentration of the minor diastereomer was too dilute for detection of ^{13}C signals. ^{31}P{^{1}H} NMR (161.86 MHz, THF-d_8, –60 °C): δ 75.9 (d, $^{2}J_{P\text{–}P}$ = 26.8 Hz), 80.73 (d, $^{2}J_{P\text{–}P}$ = 26.8 Hz). Complex **11** decomposes at temperatures greater than ~–40 °C.

Reaction of [Ru((*R*)-BINAP)(H)((*R,R*)-NH(CH(Ph))$_2$NH$_2$)] (11) with ROH (R = H or 2-Pr). (a) A solution of complex **11** (1.09×10^{-2} mmol) in THF-d_8 (0.7 mL) was prepared under argon using 2 equiv of ((CH$_3$)$_3$Si)$_2$NK at –80 °C as described above. Water (0.15 μL) was injected into the tube using a gas tight syringe. The tube was shaken briefly for 1 sec and then returned to the cooling bath five times in order to mix the contents of the tube while maintaining the temperature near –80 °C. A colour change occurred from deep red to orange-red immediately during the first shake. ^{1}H and ^{31}P NMR spectra recorded 5 min after mixing at –60 °C showed the complete formation of **10**. The same procedure was used for the reaction of **11** with 5 μL of 2-PrOH to result in the immediate formation of **7**.

Reaction of [Ru((*R*)-BINAP)(H)((*R,R*)-NH(CH(Ph))$_2$NH$_2$)] (11) with H$_2$ to prepare *trans*-[Ru((*R*)-BINAP)(H)$_2$((*R,R*)-dpen)] (6). A solution of complex **11** (8.72×10^{-3} mmol) in THF-d_8 (0.7 mL) was prepared as described above and kept under argon at –80 °C. Hydrogen gas (5 mL, ~2 atm final pressure) was injected into the tube using a gastight syringe, and the tube was shaken for 10 sec and returned to the cooling bath 5 times. ^{1}H and ^{31}P NMR spectra recorded at –80 °C after 5 min showed the conversion to **6** was complete.

Reaction of Complex 6 with D$_2$. D$_2$ gas (1 atm) was cooled to –80 °C and bubbled through a THF-d_8 solution of **6** for 10 min at –80 °C. A ^{1}H NMR spectrum recorded at –80 °C after ~20 min showed a reduction (~25 %) in the axial N-H and Ru-H signal integrations concomitant with a 0.06 downfield shift of the signal for the Ru-H group *trans-* to a deuteride ligand. The integration for the equatorial N-H signal did not decrease during this period.

Reaction of Complex 1 with $((CH_3)_3Si)_2NK$. Complex **1** (8.7 × 10^{-3}) was prepared in *just distilled/dried* THF-d_8 (0.7 mL) as described above and kept at –80 °C under an atmosphere of H_2 gas (~ 2 atm). A –80 °C solution containing 0.75 equiv (1.3 mg, 6.5 × 10^{-3}) of $((CH_3)_3Si)_2NK$ in *freshly distilled/dried* THF-d_8 (0.1 mL) was canulated using H_2 pressure into the solution of **1** at –80 °C. 5 mL of H_2 gas (~ 2 atm) was injected into the tube using a gas tight syringe, and the tube was then shaken for 1 sec and returned to the cooling bath 5 times in order to mix the contents of the tube while maintaining the temperature near –80 °C. NMR spectra recorded 5 min later at –80 °C showed the product mixture contained **6** (~65%, 86 % based upon added base), **1** (~25%), and **10** (~10%). Compound **10** resulted from traces of H_2O remaining in the THF.

References

(1) (a) Ohkuma, T.; Koizumi, M.; Muniz, K.; Hilt, G.; Kabuto, C.; Noyori, R. *J. Am. Chem. Soc.* **2002**, *124*, 6508-6509. (b) Sandoval, C. A.; Ohkuma, T.; Muniz, K.; Noyori, R. *J. Am. Chem. Soc.* **2003**, *125*, 13490-13503. (c) Ohkuma, T.; Sandoval, C. A.; Srinivasan, R.; Lin, Q.; Wei, Y.; Muniz, K.; Noyori, R. *J. Am. Chem. Soc.* **2005**, 127, 8288-8289.

(2) (a) Abdur-Rashid, K.; Faatz, M.; Lough, A. J.; Morris, R. H. *J. Am. Chem. Soc.* **2001**, *123*, 7473-7474. (b) Abdur-Rashid, K.; Clapham, S. E.; Hadzovic, A.; Harvey, J. N.; Lough, A. J.; Morris, R. H. *J. Am. Chem. Soc.* **2002**, *124*, 15104-15118. (c) Rautenstrauch, V.; Hoang-Cong, X.; Churlaud, R.; Abdur-Rashid, K.; Morris, R. H. *Chem. Eur. J.* **2003**, *9*, 4954-4967. (d) Clapham, S. E.; Hadzovic, A.; Morris, R. H. *Coord. Chem. Rev.* **2004**, 248, 2201-2237. (e) Li, T.; Churlaud, R.; Lough, A. J.; Abdur-Rashid, K.; Morris, R. H. *Organometallics* **2004**, 23, 6239-6247. (f) Abbel, R.; Abdur-Rashid, K.; Faatz, M.; Hadzovic, A.; Lough, A. J.; Morris, R. H. *J. Am. Chem. Soc.* **2005**, 127, 1870-1882.

(3) (a) Casey, C. P.; Singer, S. W.; Powell, D. R.; Hayashi, R. K.; Kavana, M. *J. Am. Chem. Soc.* **2001**, *123*, 1090-1100. (b) Casey, C. P.; Johnson, J. B.; Singer, S. W.; Cui, Q. *J. Am. Chem. Soc.* **2005**, 127, 3100-3109. (c) Casey, C. P.; Johnson, J. B.; *Can. J. Chem.* **2005**, 83, 1339-1346.

(4) Hedberg, C.; Kallstrom, K.; Arvidsson, P. I.; Brandt, P.; Andersson, P. G. *J. Am. Chem. Soc.* **2005**, 127, 15083-15090.

(5) Baratta, W.; Chelucci, G.; Gladiali, S.; Siega, K.; Toniutti, M.; Zanette, M.; Zangrando, E.; Rigo, P. *Angew. Chem. Int. Ed.* **2005**, 44, 6214-6219.

(6) Hamilton, R. J.; Leong, C. G.; Bigam, G.; Miskolzie, M.; Bergens, S. H. *J. Am. Chem. Soc.* **2005**, 127, 4152-4153.

(7) All reaction times are approximate. See Method and Materials.

(8) Fulton, J. R.; Holland, A. W.; Fox, D. J.; Bergman, R. G. *Acc. Chem. Res.* **2002**, 35, 44-56.

(9) Wiles, J. A.; Daley, C. J. A.; Hamilton, R. J.; Leong, C. G.; Bergens, S. H. *Organometallics* **2004**, *23*, 4564-4568.

(10) For a similar example of H-bonding: Fulton, J. R.; Sklenak, S.; Bouwkamp, M. W.; Bergman, R. G. *J. Am. Chem. Soc.* **2002**, 124, 4722-4737.

(11) For a similar addition: Koike, T.; Ikariya, T. *Organometallics* **2005**, 24, 724-730.

(12) Sandoval, C. A.; Yamaguchi, Y.; Ohkuma, T.; Kato, K.; Noyori, R. Mag. Res. Chem. **2006**, 44, 66-75.

(13) Henderson, W.; McIndoe, J. S. In *Mass Spectrometry of Inorganic and Organometallic Compounds Tools – Techniques – Tips*; Woollins, D.; Crabtree, B.; Atwood, D.; Meyer, G.; Eds.; John Wiley & Sons, Ltd.: The Atrium, Southern Gate, Chichester, West Sussex PO19 8SQ, England, 2005.

(13) Kaplan, A. W.; Bergman, R. G. *Organometallics* **1998**, 17, 5072-5085.

Chapter 4: Direct Observations of the Bifunctional Ligand-Assisted Addition Step in an Enantioselective Ketone Hydrogenation.[§]

Introduction

The accepted mechanism using the Noyori-type catalysts, Ru(diphosphine)H_2(diamine), for ketone hydrogenation has largely been determined from the study of model compounds, isotope labeling, kinetics, product distributions, and from theoretical studies.[1-9] Mechanistic information on the enantioselective step is particular important since it describes the origins of selectivity. The best fit with the currently available data is that the enantioselective step is a metal-ligand bifunctional addition involving the dihydride intermediate **6**. It is proposed that a nucleophilic hydride on Ru and a protic hydrogen on nitrogen add to the carbon and oxygen atoms of the ketone, respectively (Equation 4.1). This concerted addition proceeds through a pericyclic, 6-membered transition state to form the alcohol product and the amide **11**.[2a] The amide **11** then undergoes a turnover-limiting addition of dihydrogen to regenerate **6**. This chapter will discuss the key hydrogen transfer step in metal-ligand bifunctional catalysts.

There are relatively few direct, stoichiometric studies investigating the

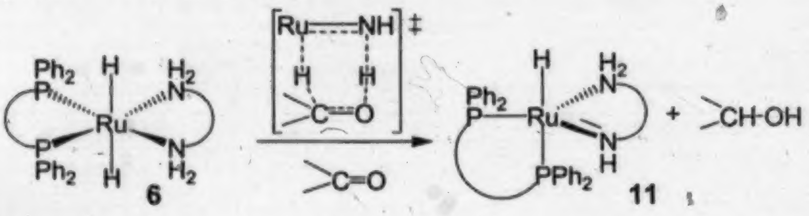

Equation 4.1

[§] A version of this chapter has been accepted for publication. *J. Am. Chem. Soc.* Available online August 2008.

hydrogen transfer step in metal-ligand bifunctional catalysts. This shortage of direct experimental information is most likely due to the difficulties in the preparation and study of the catalytic intermediates. Most information on this step comes by extrapolation from related systems. For example, Baratta *et al.* studied the hydrogenation of benzophenone using the transfer hydrogenation catalyst, [Ru(H)(CNN)(dppb)] (**111**, HCNN = 6-(4'-methylphenyl)-2-pyridylmethylamine, dppb = 1,4-bis(diphenylphosphino)butane).[6a] They reported that the hydride **111** reacts with benzophenone in benzene (~ 1:1, 20 °C) to produce the corresponding Ru-diphenylmethoxide species **112**, not the expected Ru-amide that would result from the metal-ligand bifunctional mechanism (Figure 4.1).[6a] They proposed that the alkoxide forms directly, rather than by an addition reaction between the corresponding amide and diphenylmethanol. In the proposed mechanism, the N-H moieties form hydrogen bond with the oxygen of the ketone to activate the carbonyl carbon towards nucleophilic attack by the hydride. Hydride transfer then forms an alkoxide anion that then migrates to the ruthenium center to form product alkoxide (**114**, Figure 4.1, top). Baratta *et al.*, however, could not rule out the possibility that ruthenium-diphenylmethoxide formation occurs *via* dissociation of the NH_2 functionality to create a vacant coordination cite *cis* to the hydride followed by a conventional hydride transfer step (**115**, Figure 4.1, bottom pathway).[6a]

The groups of Casey and Bäckvall have investigated the hydrogenation of polar bonds using Shvo's catalysts, $[(2,5\text{-}Ph_2\text{-}3,4\text{-}Tol_2(\eta^5\text{-}C_4COH))Ru(CO)_2H]$

(**37**) and [(2,3,4,5-$Ph_4(\eta^5\text{-}C_4COH))Ru(CO)_2H$] (**37'**) respectively.[4,8] Deuterium labeling rate studies by both Casey and Bäckvall indicate that the reduction of aldehydes by **37** and **37'** proceed through a pathway with simultaneous transfer of the hydride on ruthenium and the proton on oxygen to the carbon, and oxygen, of the ketone respectively. Casey *et al.* determined the kinetic isotope

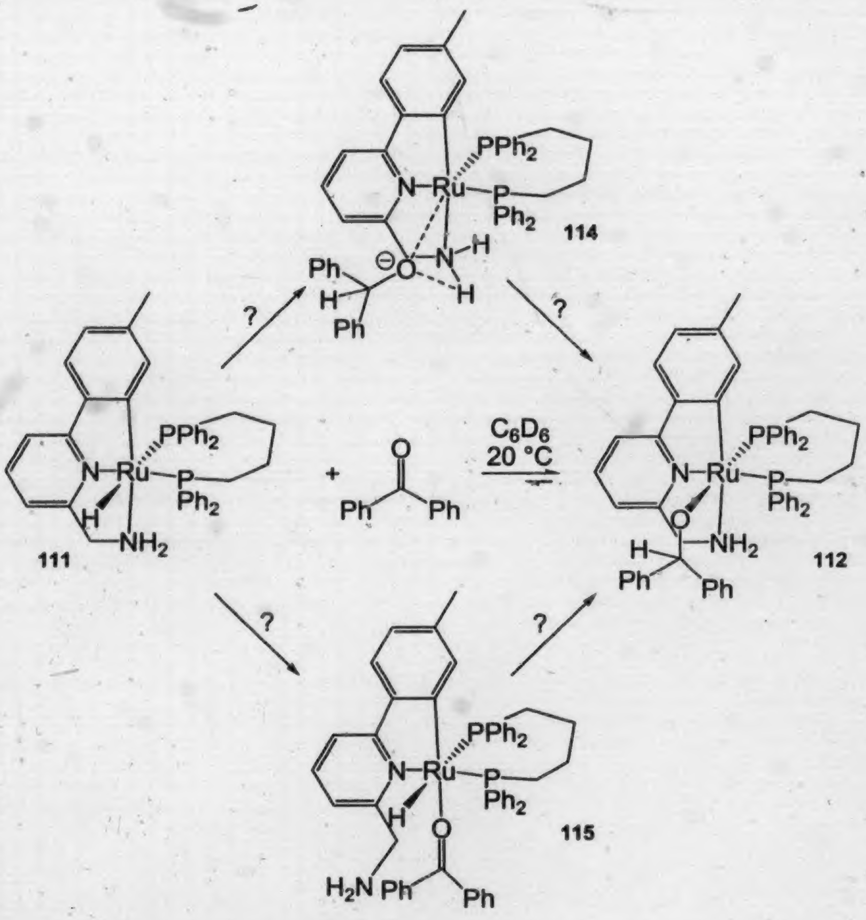

Figure 4.1: Formation of Ru-diphenylmethoxide.

effect (KIE) for the reduction of benzaldehyde by **37** (Figure 4.2).[4a] In a concerted reaction, with simultaneous transfer of both hydrogens, the product of

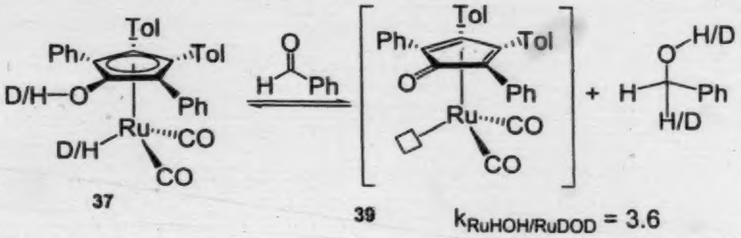
Tol
Ph
Tol
D/H—O
Ph
Ru
CO
D/H
CO
37
O
H
Ph
Tol
Ph
Tol
O
Ph
Ru
CO
CO
39
+
H/D
O
H
Ph
H/D

$k_{RuHOH/RuDOD} = 3.6$
$k_{RuHOH/RuHOD} = 2.2$
$k_{RuHOH/RuDOH} = 1.5$
$(k_{RuHOH/RuDOH})(k_{RuHOH/RuHOD}) = 3.3$

Figure 4.3: KIE for the reduction of benzaldehyde by Shvo's catalyst.

the individual KIE should be roughly equal to measured KIE when both the hydride and hydroxyl proton are replaced by deuterium. Indeed Casey *et al.* found that the product of the individual KIE was close to the measured KIE. Bäckvall *et al.* corroborated Casey *et al.*'s findings by investigating the oxidation of 1-(4-fluorophenyl)ethanol, *i.e.* the microscopic reverse of the reduction.

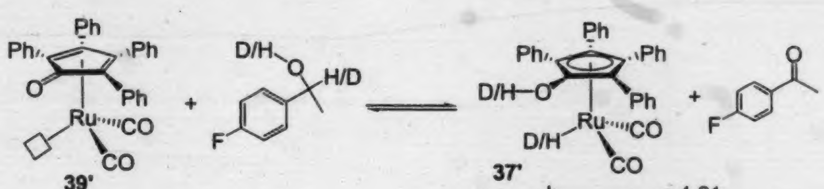
Ph
Ph
Ph
O
Ph
Ru
CO
CO
39'
+
D/H
O
H/D
F
Ph
Ph
Ph
D/H—O
Ph
Ru
CO
D/H
CO
37'
+
O
F

$k_{CHOH/CDOD} = 4.61$
$k_{CHOH/CHOD} = 1.87$
$k_{CHOH/CDOH} = 2.57$
$(k_{CHOH/RuDOH})(k_{CHOH/CHOD}) = 4.81$

Figure 4.2: KIE for the oxidation of 1-(4-fluorophenyl)ethanol.

Bäckvall *et al.* found that the product of the individual KIE was close to the measured KIE (Figure 4.3)[8a]. Although Casey and Bäckvall agree that Shvo's catalyst reduces aldehydes by a simultaneous transfer of a hydride on ruthenium and a protic hydrogen on oxygen to the substrate, they disagree on the mechanism of the hydrogen transfer step. Bäckvall contends that there is initial coordination of the ketone through the oxygen concurrent with η^5 to η^3 ring slippage of the hydroxycyclopentadienyl ligand to allow for coordination of the ketone to ruthenium (Scheme 4.1). Ketone coordination is then followed by simultaneous transfer of the hydride and hydroxyl proton to the carbon and oxygen atoms of the ketone, respectively. Casey *et al.* propose that hydrogenation occurs *via* the metal-ligand bifunctional mechanism (Scheme 4.2).

Casey and Bäckvall have also studied the hydrogenation of imines using Shvo's catalyst to further investigate the mechanism of hydrogenation.[4a-c,f,8c-d] Interestingly, both observed that a ruthenium-amine species formed as the product at low temperatures.[4b,8c] Decomplexation of the amine occurs once the temperature is raised to give the product amine and regenerate the catalyst. Bäckvall *et al.* proposed that the ruthenium-amine species results from an inner-sphere mechanism *via* an initial η^5 to η^3 ring slippage of the hydroxycyclopentadienyl ligand followed by coordination of the imine through the nitrogen. Subsequent hydrogen transfer would result in the amine coordinated to the ruthenium (**116**). Casey *et al.* contend that hydrogenation occurs *via* the metal-ligand bifunctional mechanism. The product amine remains hydrogen bonded to the oxygen on the cyclopentadienone ligand before coordinating to ruthenium to give the observed ruthenium-amine species (**117**).

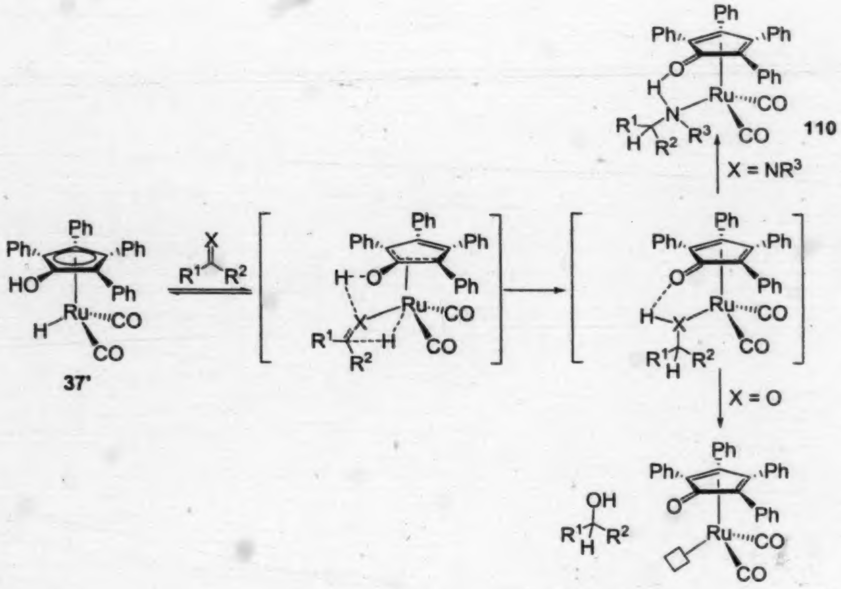
37'
110
X = NR^3
X = O
Ru
CO
Ph
HO
OH
R^1
R^2
R^3

Scheme 4.1: Bäckvall *et al.*'s proposed mechanism for imine and ketone reduction.

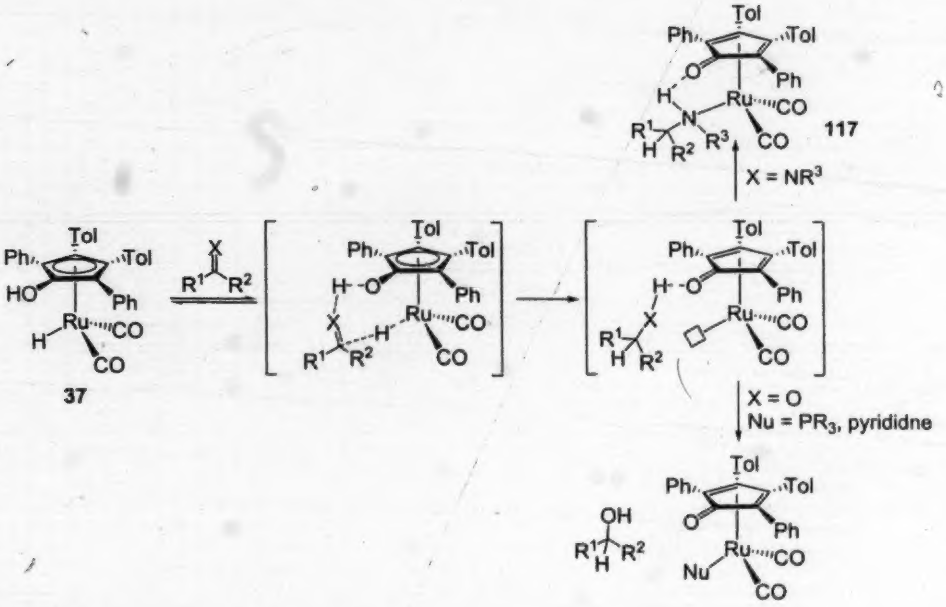
Tol
Ph
Tol
HO
Ph
Ru
CO
H
CO
37
X
R1
R2
H
O
X
H
Ru
R1
R2
X = NR3
117
X = O
Nu = PR3, pyrididne
OH
Nu

Scheme 4.2: Casey *et al.*'s proposed mechanism for imine and ketone reduction.

Intra- and intermolecular trapping experiments were investigated to distinguish between the proposed inner- and outer-sphere mechanisms.[4b,d,f,8c] The outer-sphere mechanism predicts that the unsaturated intermediate could be trapped by added amine. The inner-sphere mechanism, however, should not result in trapping products. Casey *et al.* observed that the reduction of imines by Shvo's catalyst in the presence of added amine (H_2N-Ph) led only to the ruthenium-amine complex that would be derived from the reduced imine (**118**, Equation 4.2).[4d] This result suggests that hydrogenation occurs *via* the inner-sphere mechanism. The observed ruthenium-amine complex may also, however, be explained by the formation of the hydrogen bonded intermediate within a solvent cage that collapses to the ruthenium-amine complex faster than the amine can break its hydrogen bond to the cyclopentadienone carbonyl,

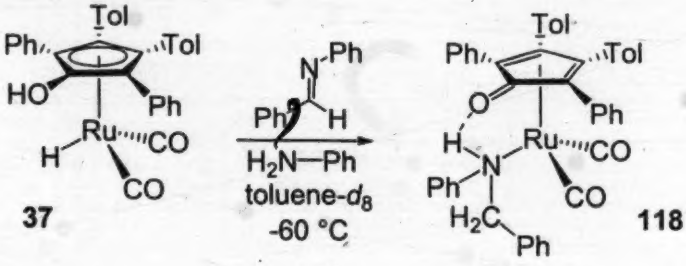

Equation 4.2

escape the solvent cage, and then be trapped by the added amine. For example, hydrogenation of the imine forms an amine that is hydrogen bonded to the cyclopentadienone oxygen (Scheme 4.3, Step A). This hydrogen bonded species can either collapse to form a ruthenium-amine species (Scheme 4.3, Step B), or the hydrogen bond can break to form free amine and a coordinatively unsaturated ruthenium species (Scheme 4.3, Step C). If the amine added to trap the coordinatively unsaturated ruthenium species cannot penetrate the solvent cage before the reformation of the hydrogen bond (Scheme 4.3, reverse of Step C), then the only Ruthenium-amine species observed would be derived from the hydrogenated imine. Alternatively, if the formation of the ruthenium-amine species is very much faster than hydrogen bond breaking, then the same result would be observed (Scheme 4.3, Step B much faster than Step C). These results would suggest that the hydrogenation proceeds *via* inner-sphere mechanism. Casey *et al.* therefore performed intramolecular trapping experiments to distinguish between these mechanistic interpretations. They

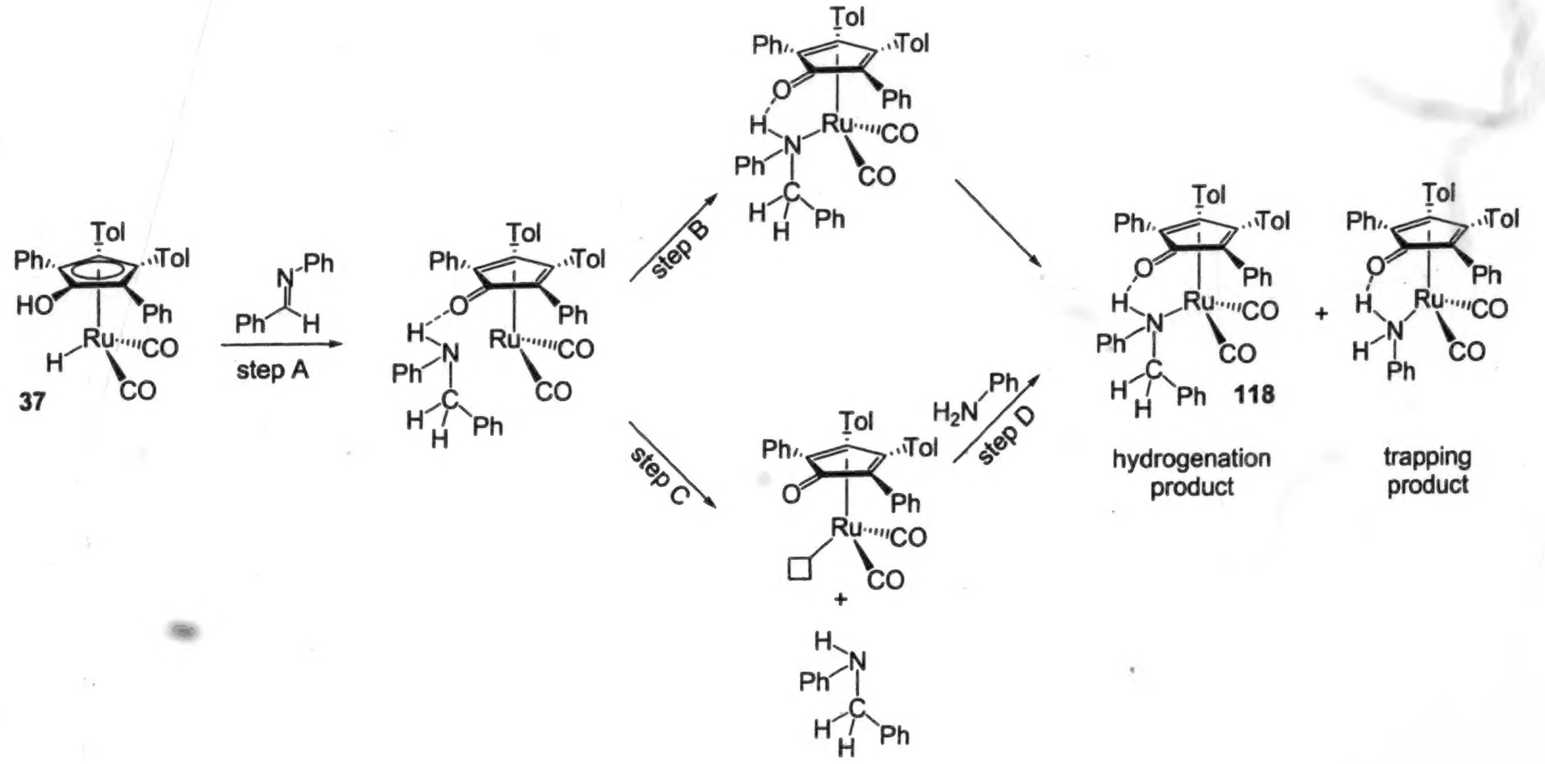
37
step A
step B
step C
step D
118
hydrogenation product
trapping product

Scheme 4.3: Proposed pathway for the formation of intermolecular trapping products.

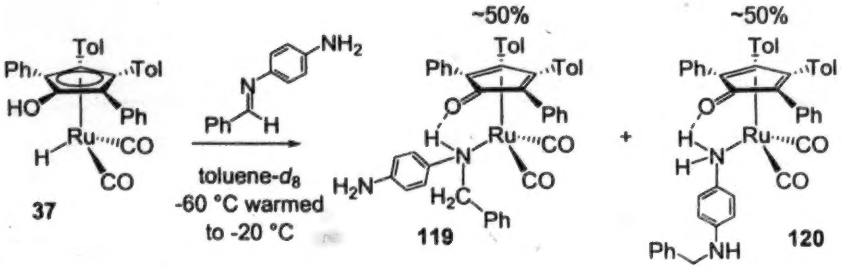
~50%
~50%
Tol
Ph
Tol
HO
Ph
Ru
CO
H
CO
37
NH$_2$
N
Ph
H
toluene-d_8
-60 °C warmed
to -20 °C
Tol
Ph
Tol
O
Ph
H
N
Ru
CO
H$_2$N
CO
H$_2$C
Ph
119
+
Tol
Ph
Tol
O
Ph
H
N
Ru
CO
H
CO
Ph
NH
120

Equation 4.3

found that reduction of the imine $\mathrm{H_2N}$-p-$\mathrm{C_6H_4N{=}CHPh}$ at temperatures below -20 °C in toluene resulted in a 1:1 mixture of the ruthenium-amine complexes (**119** and **120**, Equation 4.3).[4d] This result is consistent with an outer-sphere reduction followed by competitive coordination of the newly formed and preexisting amines. The 1:1 mixture indicates that the breaking of the hydrogen bond is faster than the rate of amine complexation (Figure 4.4, top reaction). Bäckvall *et al.*, however, observed that intramolecular trapping experiments using the imine 1,4-$\mathrm{NH(CH_2Ph)}$(c-$\mathrm{C_6H_{10}}$)=NPh resulted in only the ruthenium-amine complex **121** derived from the newly formed amine

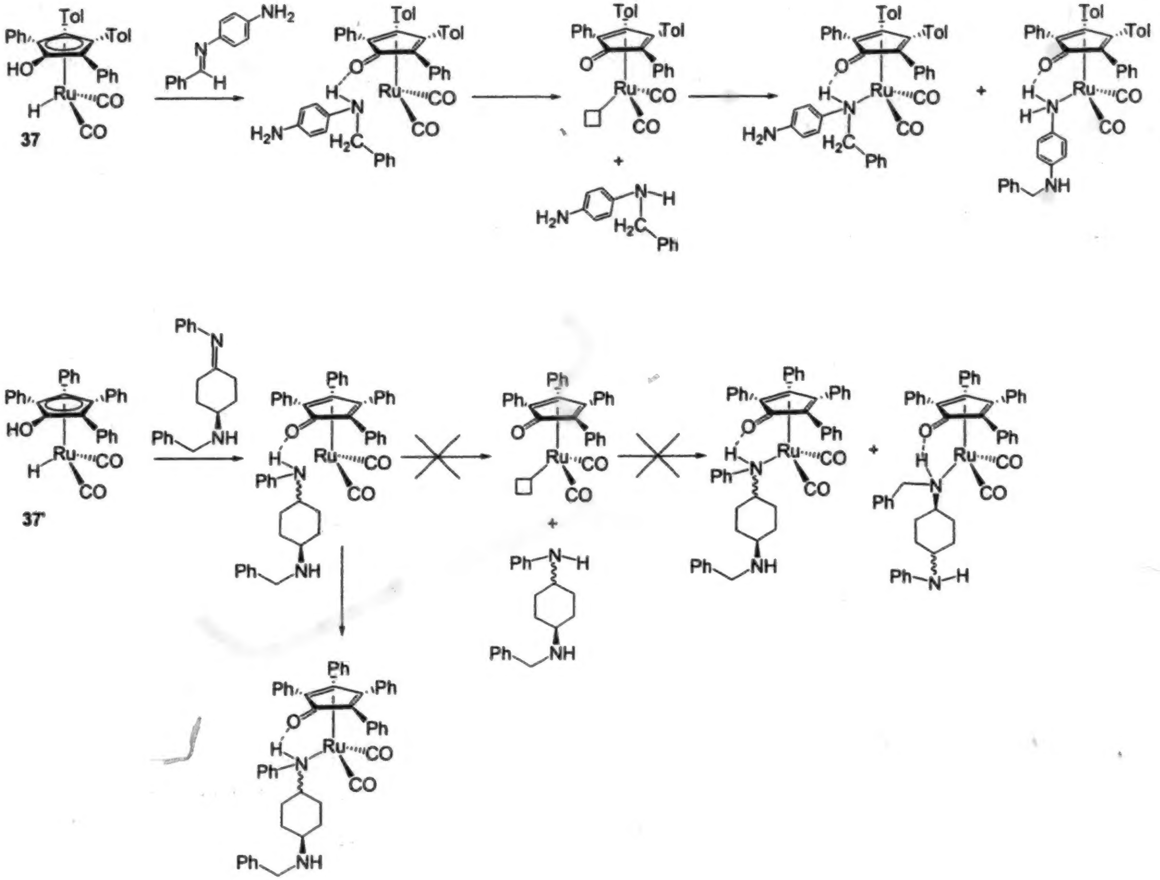
37
37'
Tol
Ph
HO
Ru
CO
H
NH2
H2N
H2C
NH
N-H
+

Figure 4.4: Comparison of Bäckvall's (bottom) and Casey's (top) intramolecular trapping experiments.

(Equation 4.4).[8c] Bäckvall suggested that Casey *et al.*'s intramolecular trapping experiments resulted from ruthenium migration from one nitrogen to the other in a η^5-cyclopentadienone complex. Casey *et al.* maintains that the reduction proceeds *via* the outer-sphere mechanism, and that the discrepancies in trapping experiments are a result of the relative ability of the amine to hydrogen bond to the cyclopentadienone carbonyl. Specifically, benzyl amines will form a stronger hydrogen bond to the cyclopentadienone carbonyl than alkyl amines. This strong hydrogen bonding prevents the formation of trapping products, which gives the impression of an inner-sphere mechanism (Figure 4.4, bottom reaction). To investigate this possibility Casey *et al.* performed intramolecular

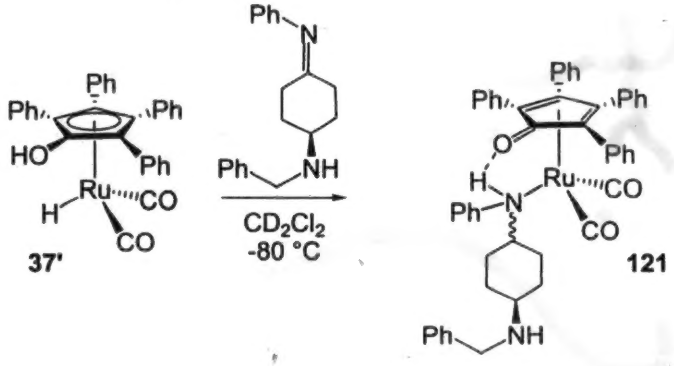

Equation 4.4

trapping experiments using the pseudo-symmetric imine 1,4-(PhCH$_2$)N=(*c*-C$_6$H$_{10}$)^{15}NH(CH$_2$Ph).[4f] This imine should result in a symmetrical diamine upon reduction (Figure 4.5), and therefore does not have a thermodynamic preference for amine complexation, *i.e.* the strength of the hydrogen bond formed between the amines and the cyclopentadienone carbonyl should be the same. Casey *et al.* found that the reduction of 1,4-(PhCH$_2$)N=(*c*-C$_6$H$_{10}$)^{15}NH(CH$_2$Ph) at -45 °C in toluene forms a mixture of the Ru-N:Ru^{15}N amine complexes. ^{15}N NMR showed that there was an 85:15 mixture of the Ru-N:Ru^{15}N amine complexes, respectively (**122** and **123**, Equation 4.5).[4f] The product ratios did not change when the temperature was raised to 24 °C, and only isomerized to a 50:50 mixture when heated at 50 °C for 4 hours. Casey

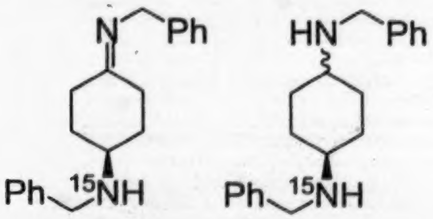

Figure 4.5: Pseudo-symmetric imine and the symmetrical diamine produced upon hydrogenation used in intramolecular trapping experiments.

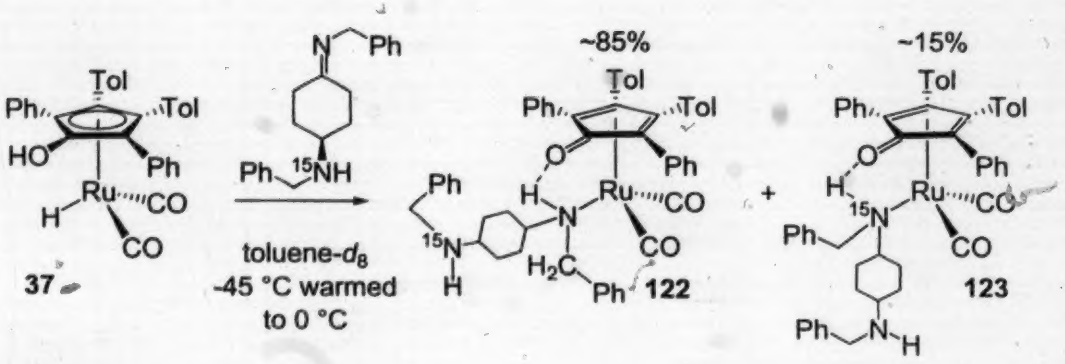

Tol
Ph
Tol
HO
Ph
Ru
CO
H
CO
37
N
Ph
Ph
^{15}NH
toluene-d_8
-45 °C warmed
to 0 °C
~85%
Tol
Ph
Tol
O
Ph
Ph
H
Ru
CO
^{15}N
H
N
H$_2$C
CO
Ph
122
+
~15%
Tol
Ph
Tol
O
Ph
H
^{15}N
Ru
CO
Ph
CO
123
Ph
N
H

Equation 4.5

therefore suggests that kinetic products are obtained and that the discrepancies in the intramolecular trapping experiments are a result of the relative rates of amine complexation and hydrogen bond breaking. In order for trapping products to form there must be decomplexation of the amine, breaking of the hydrogen bond, and finally coordination of the trapping amine. If the hydrogen bond breaks faster than recoordination of the amine, then a 50:50 mixture of Ru-amine complexes is expected (Figure 4.6, step C much faster than step B). If the rate of recomplexation is very much faster than the rate of hydrogen bond breaking, then the Ru-amine complex resulting from reduction of the imine should be the only product observed (Figure 4.6, step B much faster than step C). If the rate of recomplexation is only moderately faster than the rate of hydrogen bond breaking, then product ratios in between 50:50 and 100:0 are expected (Figure 4.6, step B ~ equal to step C). Casey *et al.* therefore suggest that Bäckvall's intramolecular trapping results are due to the formation of strong hydrogen bonds, and not due to the inner-sphere mechanism. It is also possible, however, that hydrogen transfer is proceeding through both the inner-

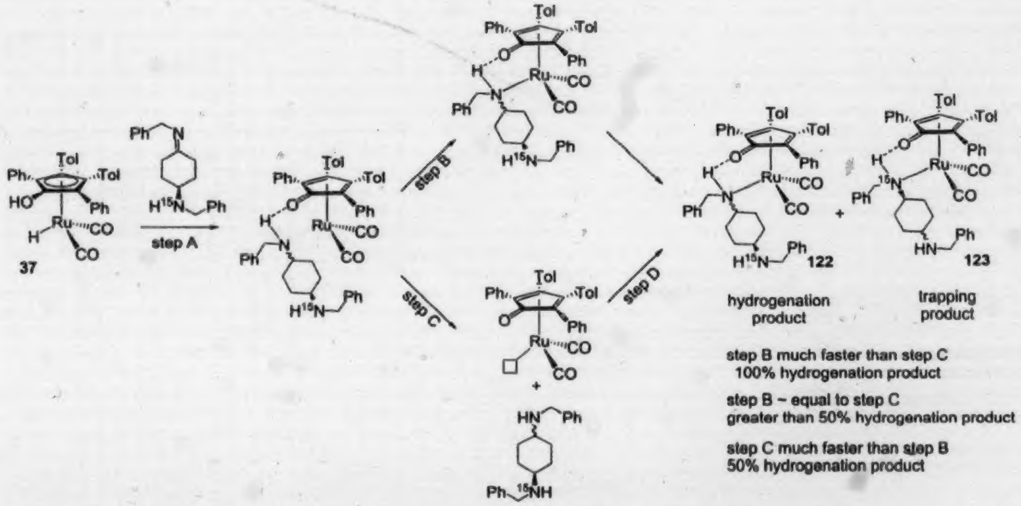

step B much faster than step C
100% hydrogenation product

step B ~ equal to step C
greater than 50% hydrogenation product

step C much faster than step B
50% hydrogenation product

Figure 4.6: Potential trapping products and their expected ratios.

and outer-sphere pathways. The inner-sphere pathway would not result in trapping products, while the outer-sphere pathway will have trapping products as described above. The amount of trapping products would then depend on the relative rates of the inner- and outer-sphere hydrogen transfer steps. Therefore Casey *et al.*'s observation of 15% trapping products in toluene (7% in CH_2Cl_2) does not definitively prove an exclusively outer-sphere hydrogenation mechanism.

To the best of my knowledge, there are no *low temperature* studies investigating the stoichiometric reduction of ketones using Ru(diphosphine)H_2(diamine) catalysts. Morris *et al.* reported that either *trans*-[Ru((*R*)-BINAP)$(H)_2$(tmen)] (**99**) or *trans*-[Ru$(PPh_3)_2(H)_2$(tmen)] (**96**) reacts at *room temperature* in the absence of hydrogen in benzene with one equiv of acetophenone to form the corresponding amides (**101** and **102**, respectively) and 1-phenylethanol (Figure 4.7).[3b] Further, Morris *et al.* propose that the 1-phenylethanol weakly and reversibly binds to the amide species, which causes a broadening of the amido NMR signals. Morris *et al.* also reported that the addition of excess acetophenone to **99** at room temperature resulted in 1-phenylethanol and an equilibrium mixture of amide and the enolate complex [Ru((*R*)-BINAP)(H)(OC(Ph)=CH_2)(tmen)] (**104**).[3b] Morris *et al.* found that the equilibrium favoured the enolate complex upon the addition of more acetophenone. The only methods used to study these equilibria, however, were ^{31}P and hydride ^{1}H NMR, without complete spectroscopic characterization of amide-alcohol and amide-ketone adducts.

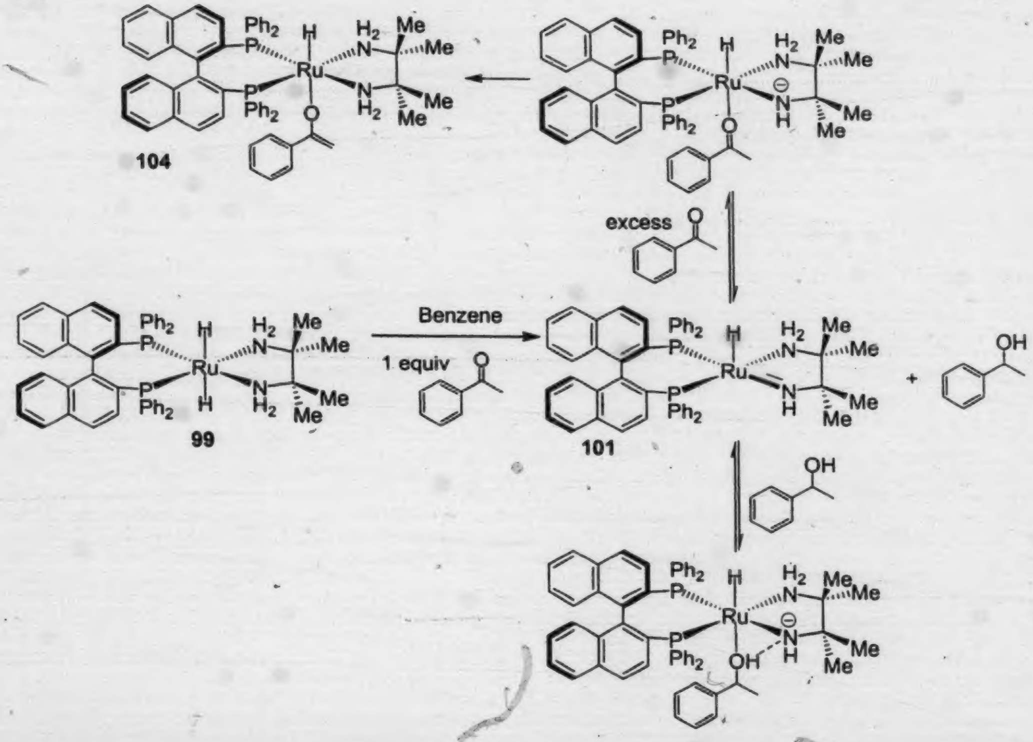

Figure 4.7: Reduction of acetophenone by model compounds in the absence of hydrogen at room temperature.

Theoretical studies provide insight into mechanisms that cannot be studied experimentally due to the short lifetime of reactive intermediates.[3b,e,5,9] Noyori *et al.* used theoretical studies to investigate the hydrogenation of ketones using the transfer hydrogenation catalyst [Ru(H)(η^6-mesitylene)((*S*,*S*)-Ts-dpen)] (**67**, (*S*,*S*)-Ts-dpen = (1*S*,2*S*)-N-(*p*-toluenesulfony1)-1,2-diphenylethylenediamine).[9a] In this study, benzene and either ethylenediamine or ethanolamine were used as ligands to model the reduction of formaldehyde to methanol. In the proposed mechanism, the ketone hydrogen bonds to N-H of the amine ligand, which activates the carbonyl carbon towards nucleophilic attack (Figure 4.8). Hydrogen transfer then proceeds through the metal-ligand bifunctional mechanism to form the ruthenium-amide species hydrogen bonded *via* the amide nitrogen to the newly formed methanol. This species then reacts to form a ruthenium-methoxide species. Noyori *et al.* found that the ruthenium-methoxide compound was the most stable and should therefore be the catalyst resting state.[9a]

In recent theoretical studies using a similar simplified model, Meijer *et al.* found that the metal-ligand bifunctional mechanism is preferred over migratory insertion of the ketone into the Ru-hydride bond, *i.e* an inner-sphere mechanism.[9b] The proposed transition state for hydride transfer, however, does not include a hydrogen bond between the ketone oxygen and the amine N-H's. This hydrogen bonding would activate the carbonyl carbon towards nucleophilic attack and lower the activation barrier for hydride transfer. As such, the activation barrier for migratory insertion is likely lower than originally calculated. Meijer *et al.* similarly found that the most stable compound is the ruthenium-methoxide species.[9b]

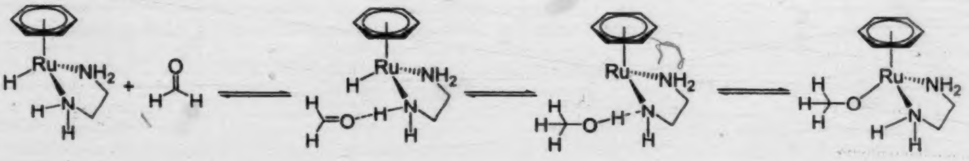

Figure 4.8: Noyori *et al.*'s proposed mechanism for Ru-methoxide formation.

The Noyori and Meijer modeling studies are conducted in the gas phase, and do not take into account the effect of solvent molecules. Meijer *et al.* recently reported more realistic modeling studies incorporating the effect that MeOH solvent molecules have on the reaction mechanism.[9c] They reported that hydrogen transfer may proceed through an indirect metal-ligand bifunctional mechanism. In the presence of methanol solvent, the hydride is transfered to the formaldehyde to form a methoxide product that is strongly hydrogen bonded with the solvent (Figure 4.9). This methanol solvent molecule also hydrogen-bonded to the ligand N-H. There is then simultaneous shortening of the newly formed C-H bond, and proton transfer from the solvent to the methoxide oxygen to convert the solvent molecule into a new methoxide anion and the substrate into methanol.[9c] There is then a series of proton transfers between the

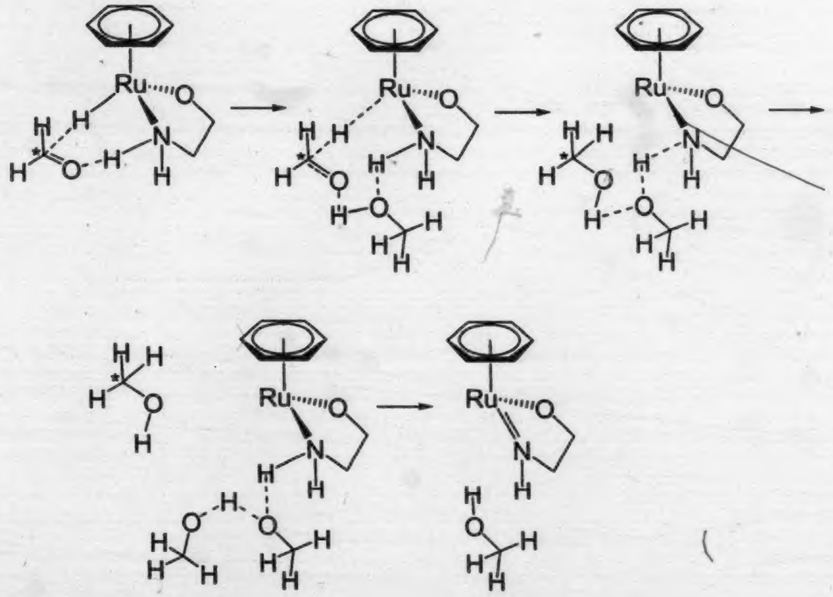

Figure 4.9: Meijer *et al.*'s proposed solvent assisted mechanism.

methoxide and the solvent to result in the eventual deprotonation of the ligand N-H group to form the Ru-amide complex and methanol.

Morris *et al.* recently reported theoretical studies on the model amido system [$Ru(H)(PH_3)_2(2\text{-}NHCH_2\text{-}(C_5H_4N))$] (**124**) in the presence of 2-PrOH solvent.[3e] They found that 2-PrOH assists the heterolytic cleavage of H_2 to form *trans,cis*-[$Ru(H)_2(PH_3)_2(2\text{-}NH_2CH_2\text{-}(C_5H_4N))$] (**125**). Further, they found that ketone hydrogenation under these conditions may proceed through two pathways. One pathway is similar to the metal-ligand bifunctional mechanism. In this pathway, the ketone oxygen hydrogen bonds to the amine N-H which activates the carbonyl carbon towards nucleophilic attack. The ketone oxygen also hydrogen bonds to the hydroxyl proton of a 2-PrOH solvent molecule. The proton on nitrogen and the hydride on ruthenium then transfer simultaneously to the oxygen and carbon of the ketone, respectively, to form Ru-amide compound and the product alcohol that is hydrogen bonded to a 2-PrOH solvent molecule (Figure 4.10, top).[3e] In the alternate pathway, 2-PrOH solvent hydrogen bonds simultaneously to the amine N-H and the oxygen of the ketone, acting as a proton shuttle. The hydride on ruthenium transfers to the carbonyl carbon, without protonation of the ketone oxygen by the amine N-H (Figure 4.10, bottom). Morris *et al.* expected that the hydride on ruthenium would transfer to the carbonyl carbon concomitant with proton transfer through 2-PrOH-amine the hydrogen bonding network. The product would be alcohol and amide with a hydrogen bond between the amide nitrogen and the 2-PrOH solvent. They reported, however, that all attempts to optimize this structure failed. Instead,

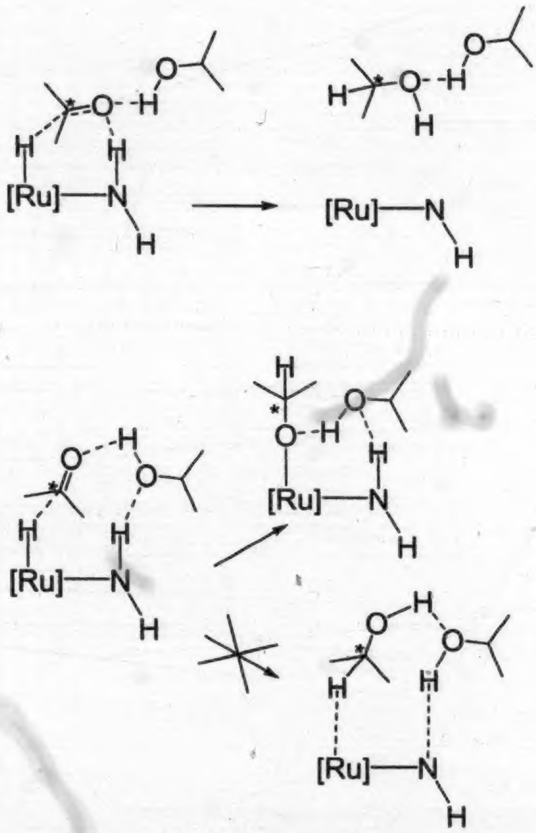

Figure 4.10: Morris *et al.*'s proposed alcohol assisted mechanisms.

calculations indicated that a ruthenium-alkoxide species formed, with both the alkoxide oxygen and the amine N-H hydrogen bonding to a 2-PrOH solvent molecule.[3e] Further, calculations indicated that this Ru-alkoxide compound is the most stable species in solution.

Theoretical studies on the Ru(diphosphine)$(H)_2$(diamine) catalyst system have mostly focused on the proposed bifunctional addition. Morris *et al.* used the model system *trans*-Ru$(PPh_3)_2(H)_2$(ethylendiamine) (**126**) for the hydrogenation of acetone to study the mechanism theoretically.[3b] Figure 4.11 summarizes the proposed mechanism. The mechanism begins with the formation of the 6-membered pericyclic transition state for the bifunctional addition (**127**). Complete hydrogen transfer would result in the amide species and 2-PrOH. Morris *et al.*'s theoretical studies show that the most stable product is the amide, stabilized by hydrogen bonding between the amide N and the hydroxyl proton of the product alcohol (**128**).[3b] The regeneration of the dihydride catalyst involves heterolytic cleavage of H_2 by the amide. It is proposed that this reaction is the turnover limiting step in the reaction. Morris *et al.* found that the transition state energy for H_2 cleavage (**129**) is a high barrier process (13.4 kcal/mol higher than amide + H_2) and agrees with the hypothesis that the turnover limiting step is the regeneration of the dihydride catalyst. The calculated activation energy, 13.4 kcal/mol, is higher, however, than the experimentally determined value of ~8 kcal/mol determined by kinetic experiments. Morris *et al.* attributed this difference to inaccuracies of the computational method such as neglecting solvent effects and using a small model system rather than the real compounds.[3b] Brandt *et al.* reported that the

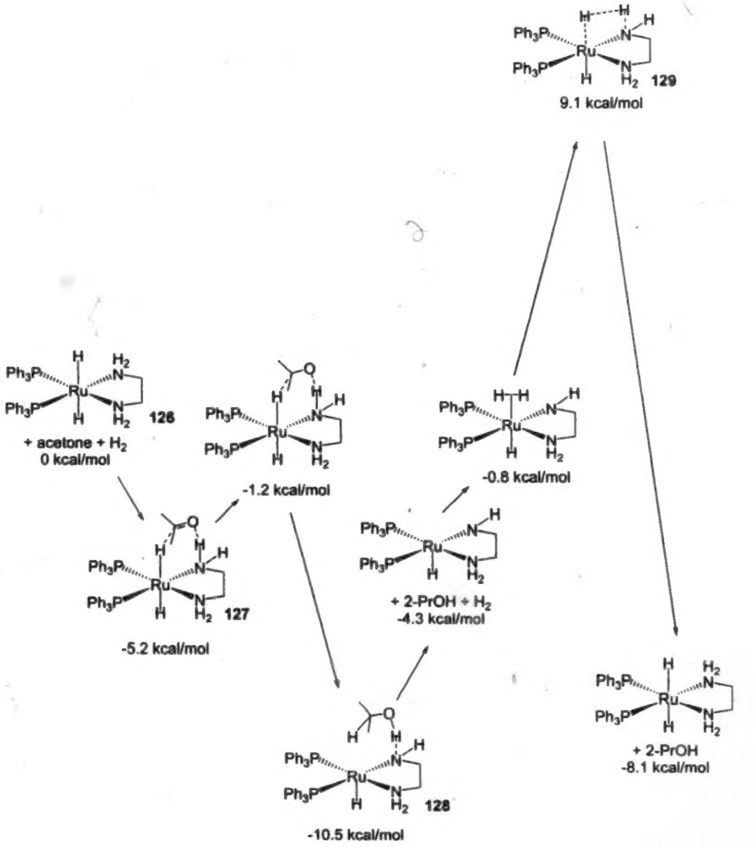
Ph₃P
Ru
9.1 kcal/mol
126
+ acetone + H₂
0 kcal/mol
-1.2 kcal/mol
-0.8 kcal/mol
127
-5.2 kcal/mol
+ 2-PrOH + H₂
-4.3 kcal/mol
+ 2-PrOH
-8.1 kcal/mol
128
-10.5 kcal/mol
129

Figure 4.11: Morris *et al.*'s theoretical study on the metal-ligand bifunctional mechanism.

transition state for H_2 cleavage is ~ 18kcal/mol higher than amide $+H_2$.[5] They note, however, that alcohol can mediate the H_2 cleavage, lowering the energy to ~5.3 kcal/mol (Figure 4.12). Specifically, the hydroxyl proton of methanol forms a hydrogen bond to the amide nitrogen (**130**). Upon H_2 coordination, the amide deprotonates the methanol to form a methoxide that is hydrogen bonded to both the N-H and the dihydrogen ligand (**131**). The methoxide then deprotonates the η^2-H_2 ligand to give the dihydride that is stabilized by hydrogen bonding to methanol (**132**).[5] Di Tommaso *et al.* have recently used different density functionals to investigate the metal-ligand bifunctional hydrogenation step and the heterolytic cleavage of H_2 by the amide to form the dihydride catalyst.[9d,f] They reported similar energy barriers (~ 4 kcal/mol) to Morris *et al.* for the hydrogen transfer step. Heterolytic cleavage of H_2 to regenerate the dihydride catalyst has a calculated activation barrier of ~9 kcal/mol, which is in closer agreement to Morris *et al.*'s experimentally determined value (*vide supra*).

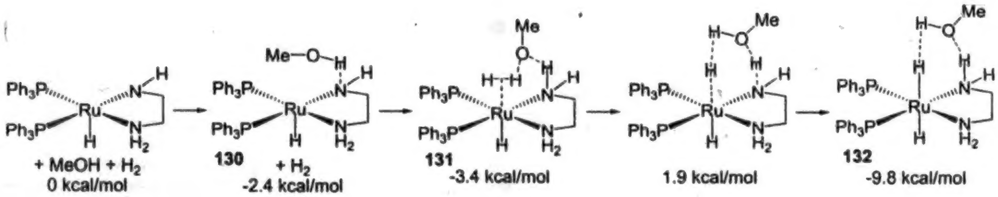

Figure 4.12: Brandt *et al.*'s theoretical energies in the alcohol-assisted heterolytic cleavage of H_2.

This brief literature review shows that although a great deal of study has been carried out with model compounds and calculations, the steps have never been directly observed with the proposed catalytic intermediates as reactants.

Chapter 3 discussed high yielding, low temperature preparations with full NMR characterizations of the putative intermediates in the metal-ligand bifunctional mechanism.[7b] An unexpected pathway whereby base increases the rate of hydrogenation was also identified. This chapter will discuss the direct study of H_2 addition to acetophenone using **6** as a catalyst in the metal-ligand bifunctional mechansim.

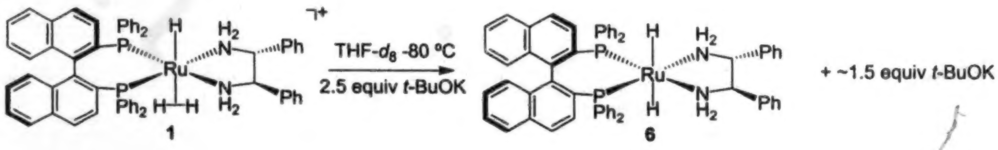

Equation 4.6

Results and Discussion

Unless stated otherwise, the dihydride **6** was prepared for this study in THF-d_8 by reacting the dihydrogen complex *trans*-[Ru((*R*)-BINAP)(H)(η^2-H_2)((*R,R*)-dpen)](BF_4) (**1**) with *t*-BuOK (~2.5 equiv) under H_2 (~2 atm) at -80 °C.[10] As in Chapter 2, this reaction yields the dihydride in good yield in the presence of ~1.5 equiv of *t*-BuOK (Equation 4.6).[10] If water is present in solution, either from residual water in the THF-d_8 even after distillation or introduced during the preparation of the compounds, then a ruthenium-hydroxide compound *trans*-Ru((*R*)-BINAP)(H)(OH)((*R,R*)-dpen) (**10**) is formed. I found that the ruthenium-hydroxide compound does not react with hydrogen unless there is excess base present. The use of 2-PrOH-d_8 as solvent was avoided because of rapid and quantitative formation of the 2-propoxide *trans*-Ru((*R*)-BINAP)(H)(2-PrO)((*R,R*)-dpen) (**7**).[7b] The addition of 1 equiv of acetophenone to **6** was carried out at -80 °C under ~2 atm H_2, and monitored by NMR spectroscopy.

The addition was complete within 60 s (first spectrum), demonstrating the high activity of **6** as a reducing agent. Contrary to previous mechanistic propositions, the addition did not form the expected amide **11** and 1-phenylethanol.[3b] Instead, the product is the 1-phenylethoxide **14**, the net result of ketone-hydride insertion (Equation 4.7). The alkoxide **14** was too unstable to allow a solid-state structure determination by X-ray diffraction. Compound **14** underwent alkoxide elimination in the presence of 1.5 equiv of excess base at elevated temperatures (~ -40 °C) to give 1-phenylethanol and the dihydride **6** without any indication of the formation of the amide **11** (Equation 4.7). This result confirms that the reaction between H_2 and amide in solution is fast under these conditions. The phenylethoxide **14** was stable, however, in solution at -80°C

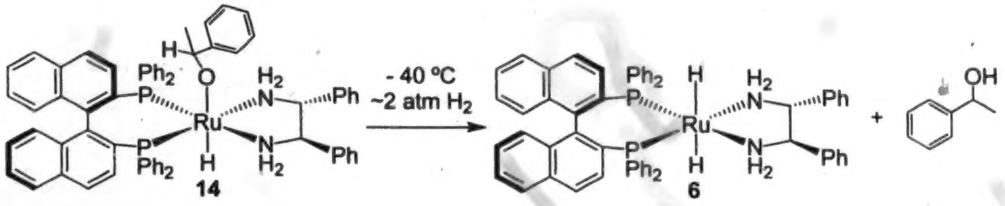

Equation 4.7

under ~2 atm H_2. Compound **14** could thereby be identified using ^{1}H, ^{13}C, ^{31}P, HSQC, NOE, and COSY NMR experiments, as well as ESI-mass spectrometry. Noyori *et al.* found that irradiating the Ru-H will have a large NOE on the N-H_{axial} in compounds containing the Ru-H/N-H_{axial} motif.[11] I found similar results for the putative intermediates discussed in Chapter 3.[7b] Compound **14** also exhibits this large NOE on the α-C-N-H_{axial} ^{1}H NMR signal upon irradiation of the Ru-H resonance. Further, the α-C-N-H_{axial} ^{1}H NMR signal is shifted upfield in comparison to the other ligand N-H resonances. Morris *et al.* observed a similar upfield shift for the model dihydride **99**.[3a] This provided a useful starting point

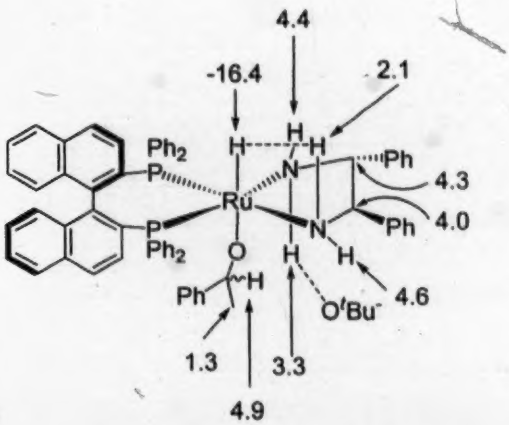

Figure 4.13: ^{1}H NMR assignments for 1-phenylethoxide **14**.

for the full characterization of **14**. COSY and HSQC NMR experiments could therefore be used to assign the dpen and 1-phenylethoxide ^{1}H (Figure 4.13) and ^{13}C NMR signals. COSY NMR experiments indicated that the α-C-N-H_{axial} was coupled to protons at 4.6 and 4.3 ppm. These signals can be assigned to either the α-C-N-$H_{equatorial}$ or the α-C-H protons. HSQC NMR experiments, however, showed that the signal at 4.3 can be assigned to the α-C-H proton.

The signal at 4.6 ppm can, therefore, be assigned to the α-C-N-$H_{equatorial}$ proton. Additionally, COSY showed that the α-C-H proton is coupled to a proton at 4.0 ppm, which in turn is coupled to protons at 4.4 and 3.3 ppm. HSQC showed that the signal at 4.0 ppm can be assigned to the β-C-H proton. The signals at 4.4 and 3.3 ppm can, therefore, be assigned to either the β-C-N-H_{axial} or β-C-N-$H_{equatorial}$ protons. Additional NOE experiments determined which of the β-C-N-H's were axial and equatorial (Figure 4.14). The β-C-N-H ^{1}H NMR resonance at 4.4 ppm overlapped with the α-C-H signal at 4.3 ppm and therefore could not be irradiated to observe NOE's without observing NOE's associated with the α-C-H proton. The β-C-N-H resonance at 3.3 ppm is, however, far removed from other signals and could be used in NOE experiments. There was a NOE interaction between the β-C-N-H resonance at

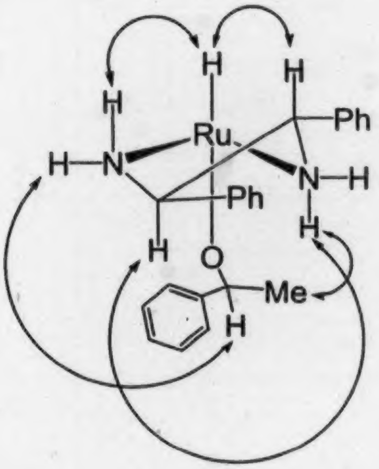

Figure 4.14: Observed NOE intereactions in the 1-phenylethoxide **14**.

3.3 ppm and the α-C-H signal at 4.3 ppm. The β-C-N-H resonance at 3.3 ppm and the α-C-H signal at 4.3 ppm would only be close enough to each other to observe NOE's if the dpen ligand is in the λ orientation, and the β-C-N-H was in the axial position. The signals at 4.4, and 3.3, could therefore be assigned to the β-C-N-$H_{equatorial}$, and β-C-N-H_{axial}, respectively. There were also weak NOE's between the O-C-H and O-C-CH_3 protons of the 1-phenylelthoxide ligand and some of the dpen protons. Additionally, the β-C-N-H_{axial}, the O-C-H, and O-C-CH_3 protons all had a NOE interaction with a common aromatic proton. These NOEs would only occur if the 1-phenylelthoxide were coordinated to Ru.

Morris *et al.* reported preliminary hydride ^1H and ^{31}P NMR data for the proposed model product *trans*-[Ru((*R*)-BINAP)(H)(PhCH(CH_3)O)(tmen)] (**110**) prepared from the addition of 90 % (*S*)-1-phenylethanol to the dihydride *trans*-[Ru((R)-BINAP)$(H)_2$(tmen)] (**99**).[3b] Approximately 30 % of the dihydride was converted to the alkoxide under these conditions (Figure 4.15). Additionally, based on the hydride signal in the ^1H NMR, two diastereomers of the alkoxide were present in a 9:1 ratio. The *ee* of the catalytic hydrogenation of acetophenone using **1** plus base in 2-PrOH is ~ 80%. The expected ratio of the two diastereomers for the stoichiometric addition of acetophenone to the dihydride **6** should therefore be ~ 9:1. In my case, using the actual catalytic intermediates, I found that when the alkoxide was prepared by the addition of acetophenone to the dihydride **6**, only one set of NMR signals was obtained. A comparison of the ^1H NMR spectra shows that the hydride chemical shift of **14** is downfield by ~ 0.6 ppm with respect to Morris' model compound **110** (-16.4

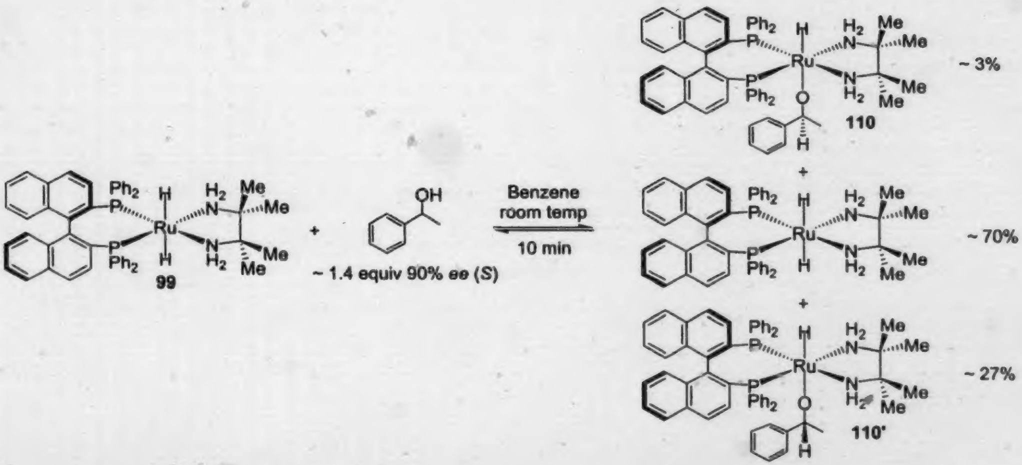

Figure 4.15: Morris *et al.*'s preparation of the model 1-phenylethoxide.

versus -17.0 ppm). There is, however, excess 1-phenylethanol in solution with **110**. When excess 1-phenylethanol is added to **14**, the hydride signal shifts upfield from approximately -16.4 to -16.7 ppm. Thus there are some discrepancies between Morris' model alkoxide and the actual alkoxide prepared in this study. The ^{31}P chemical shifts for the major diastereomer of the model compound **110** (67.8, 73.8 ppm) were nearly identical to those of **14** (68.44, 73.68 ppm).[3b] Morris *et al.*'s preliminary characterization of the model alkoxide does not contain ^{1}H or ^{13}C NMR data for the tmen and phenylethoxide ligands, therefore no comparisons between the actual and model product alkoxides could not be made.

The assignments of the alkoxy- and methyl-^{13}C signals in the 1-phenylethoxide ligand were confirmed using acetophenone labeled with ^{13}C at C1 and C2. I found that the alkoxy- and methyl-^{13}C signals of the phenylethoxide ligand were broad in comparison to free alcohol and to the carbonyl- and methyl-^{13}C of the ketone. The typical $^{3}J_{P\text{-}C}$ coupling constant for these types of compounds is ~ 4 Hz. Although this $^{3}J_{P\text{-}C}$ coupling could not be measured, the alkoxy-^{13}C signals sharpened slightly when phosphorus decoupled experiments were performed. This is further proof that the 1-phenylethoxide is coordinated to the ruthenium.

Morris *et al.* proposed that reacting 1-phenylethanol with the model amide $Ru(PPh_3)_2(H)(NH(C(CH_3)_2)_2NH_2)$ (**102**) results in a 1:1 equilibrium mixture between free alcohol/amide, and the alkoxide species through an unobserved amide-alcohol adduct (Figure 4.16).[3b] I found that the 1-phenylethoxide **14** can be prepared independently by reacting **11** with 1-phenylethanol at -80°C in THF. Unlike the results proposed by Morris, the product **14** formed on mixing, and it was identical to that from the addition of acetophenone to the dihydride **6**. I found no evidence for the presence of

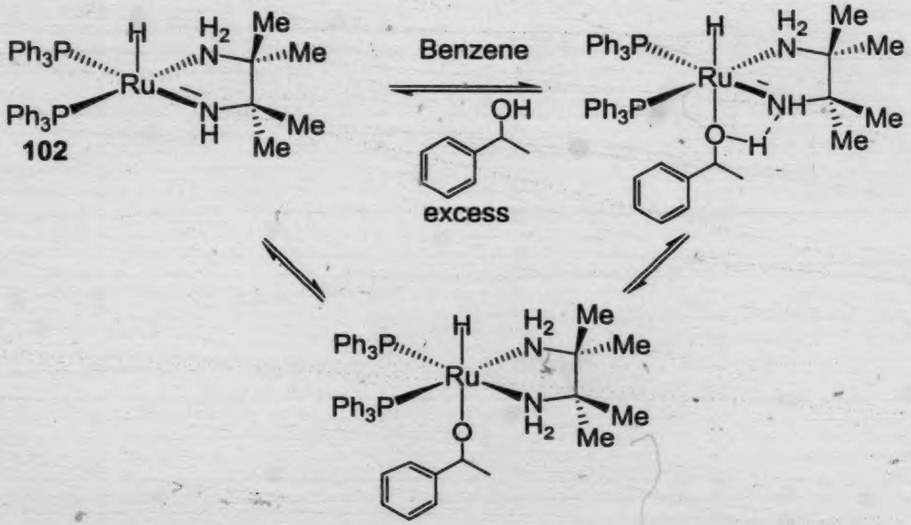
Ph3P
H
H2
Me
N
Me
Ru
Ph3P
N
H
Me
Me
102
Benzene
OH
excess
Ph3P
H
H2
Me
N
Me
Ru
Ph3P
NH
O
H
Me
Me
Ph3P
H
H2
Me
N
Me
Ru
Ph3P
N
H2
Me
Me
O

Figure 4.16: Reaction of a model amide with 1-phenylethanol.

unreacted amide. Although its origins were not investigated further, this difference in activity and reactivity underscores how seemingly minor changes in structure can cause significant changes in the activity of catalytic intermediates, and that caution is warranted when extrapolating the results from model compounds to catalytic cycles. As I reported previously for **7** (see chapter 3), the ~1.5 equiv of excess *t*-BuOK formed weak hydrogen bonds with the N-H groups in **14**. When prepared without excess *t*-BuOK, the dihydride **6** reacted quickly at -80°C with acetophenone to form **14** without these hydrogen bonds. As is the case with the 2-propoxide, some of the 1-phenylethoxide N-H ^{1}H NMR signals shift in the absence of base. The most significant shift is observed for β-C-N-H_{axial} proton (~ 0.3 ppm downfield shift). The shift is most likely due to the N-H hydrogen bonding to the oxygen of the 1-phenylethoxide ligand rather than to the added base. Additionally, the ^{1}H NMR for the alkoxide C-H is slightly shifted downfield in the absence of base.

The net result of the addition of acetophenone to the dihydride is the 1-phenylethoxide **14**. This can arise from three different reactivity pathways. The addition step may proceed by the metal-ligand bifunctional mechanism to yield

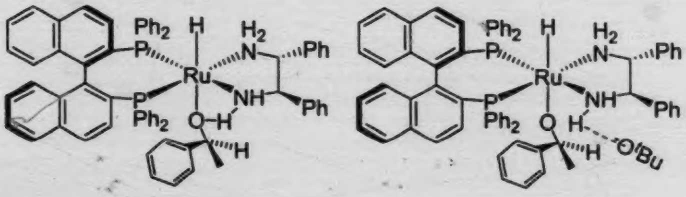

Figure 4.17: Intra- and intermolecular hydrogen bonding of the 1-phenylethoxide **14**.

the amide **11** plus product alcohol (Figure 4.18, pathway A). I showed that subsequent reaction between the amide and free alcohol would yield the observed alkoxide. A related possibility is that the addition step proceeds to form the amide but with the product alcohol hydrogen bonded to the amide nitrogen (**133**). The amide-alcohol adduct then converts into the alkoxide **14** without the formation of distinct amide and alcohol species (Figure 4.18, pathway B). A third possibility involves an addition step in which the carbonyl oxygen is hydrogen bonded to amine N-H, activating it towards nucleophilic attack. Alkoxide formation occurs *via* a concerted process in which the hydride is transferred to the carbon with simultaneous formation of a ruthenium-oxygen bond without the transfer of the N-H to the oxygen (**134**, Figure 4.18, pathway C). This process would remove electron density from Ru through the hydride to the carbonyl carbon. This loss of electron density may allow access to the Ru center by the ketone to undergo hydride insertion to form **14**, perhaps with hydrogen bonding between the alkoxide ligand and the adjacent, axial N-H group (*vide supra*).

To investigate these possibilites, H_2 and alcohol were used as trapping agents. Specifically, the amide **11** reacts rapidly with alcohols or hydrogen in solution to form alkoxide or dihydride respectively (Chapter 3). [7b] Therefore, if the alkoxide **14** formed after the bifunctional addition *via* the rapid reaction

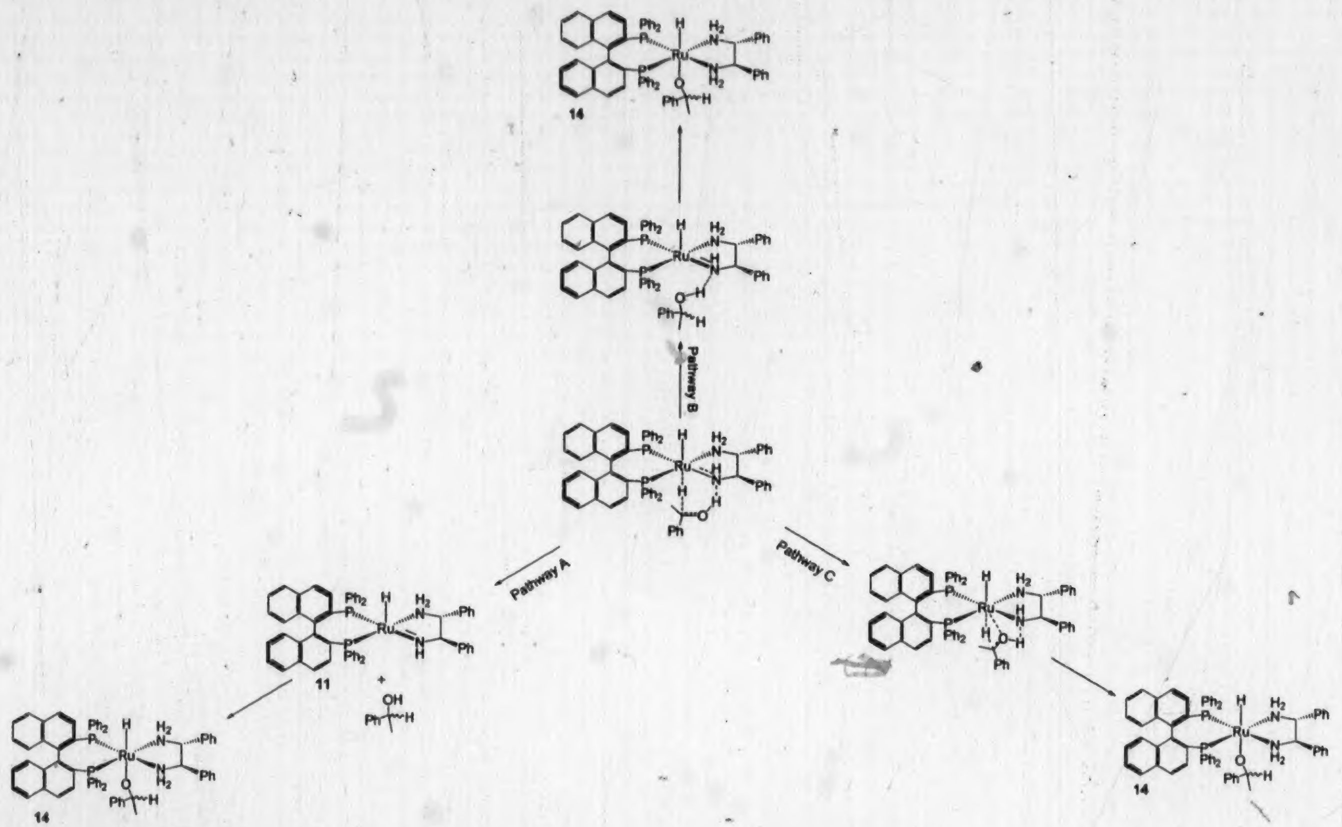
Pathway A
Pathway B
Pathway C
11
14
14
14
Ph2
H2
Ru
Ph
OH

Figure 4.18: Different pathways for the formation of 1-phenylethoxide 14.

between 1-phenylethanol and the amide **11** (Scheme 4.4) then the presence of H_2 or another alcohol will act as a trapping agent. If this is the case, then either the dihydride or the alkoxide produced from the reaction between amide and the trapping alcohol should be present along with the product alkoxide **14**. Excess H_2 (~2 atm) is present during the addition of acetophenone to **6**. The only species observed in solution, however, was the alkoxide **14** indicating that if the amide formed, H_2 did not serve as a trapping agent. As the excess H_2 did not trap the amide **11**, I also carried out the addition in the presence of 2-PrOH as trap. 2-PrOH is the typical solvent used in these hydrogenations, and

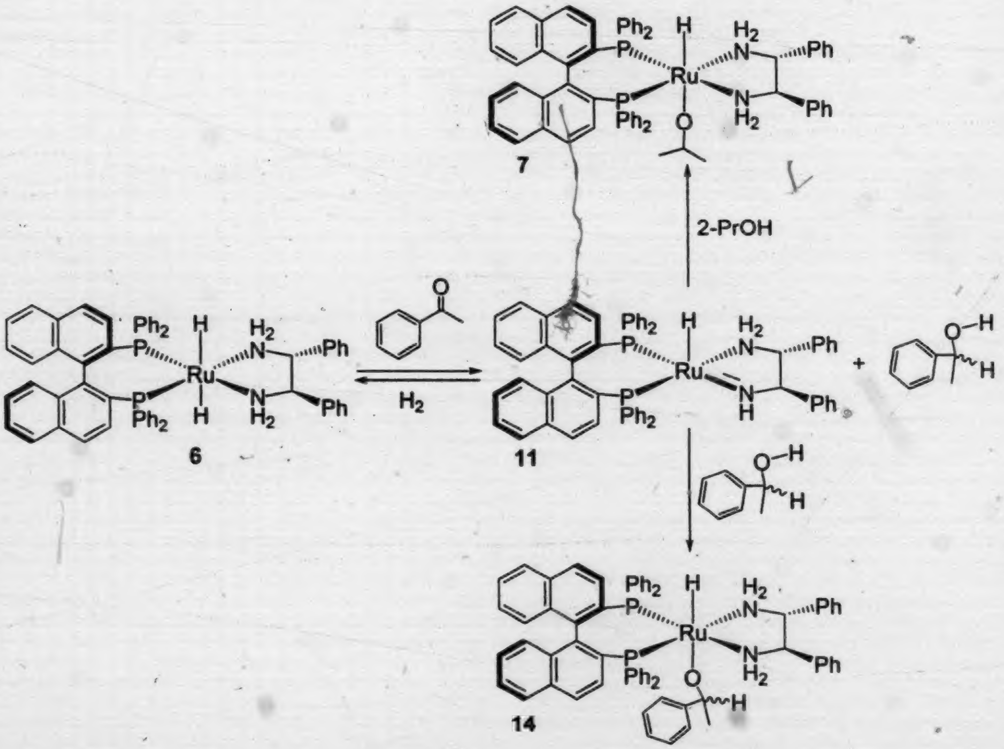

Scheme 4.4: Proposed trapping experiments for the interception of the amide.

therefore its use of a trap is relevant to the mechanism. A difficulty with this experiment is the rapid, base-enhanced exchange between the 1-phenylethoxide **14** and 2-PrOH in solution (Equation 4.9). For example, **14** reacts with 10 equiv 2-PrOH to rapidly form the 2-propoxide **7** at -80°C in THF-d_8. Such exchanges likely proceed *via* a base-assisted intramolecular elimination of the 1-phenyethoxide ligand, followed by addition of 2-PrOH to **11** (see Chapter 3).[7b] This complication was accommodated by preparing frozen THF layers that contained **6** in the lower layer, and a mixture of acetophenone, 2 equiv and 2-PrOH, ~150 equiv, in the upper layer. The sample was placed in a -80 °C NMR probe, and spectra were recorded when the layers thawed. The addition was complete within 60s, with the 1-phenylethoxide **14** as the sole product. ^{1}H NMR indicated that ~ 5 equiv 2-PrOH had diffused into the product layer during this time. A -80 °C reaction between a pre-formed mixture of the dihydride **6** and 2-PrOH (5 equiv) in THF-d_8 with acetophenone (1 equiv) also gave the 1-phenylethoxide **14** as sole product (Equation 4.10).[12] It is possible that the amide simply reacts faster with 1-phenylethanol than with 2-PrOH. In a competition experiment, the amide **11** was prepared in THF-d_8 and reacted with a mixture of 2-PrOH, 5 equiv, and 1-phenylethanol, 1 equiv, at -80 °C. The result was a mixture of the alkoxides **7** and **14** in a ~1:1 ratio (Equation 4.11). Thus a kinetic preference exists for the reaction of 2 with 1-phenylethanol over 2-PrOH, but this preference is insufficient to account for the exclusive formation of **14** by the addition of acetophenone to **6**. I therefore conclude that this addition does not proceed with the formation of amide and alcohol as distinct species in solution.

The enantioselectivity of the addition reaction was investigated by reacting the dihydride **6** with 1 equiv acetophenone in THF at -80 °C, followed by addition of excess 2-PrOH. The 2-PrOH was added to liberate the 1-phenylethanol product *via* the displacement reaction shown in Equation 4.8. This procedure was adopted because **14** could not be isolated for structure determination, and NMR spectroscopy did not allow us to determine the ratio of diastereomers. The *ee* of the liberated 1-phenylethanol was 83% (*S*). Thus, the absolute configuration of the 1-phenylethoxide ligand in the major diastereomer of **14** is *S*, and the minor diastereomer of **14** was present in ~8.5 % abundance.

The initial *ee* of the catalytic hydrogenation in THF, recorded after 6 turnovers, was 69 % (*S*) (1000 equiv ketone, 2.5 equiv *t*-BuOK, 30 °C, 4 atm H_2). The *ee* of the hydrogenation in 2-PrOH was ~80% (*S*). Thus, the intrinsic

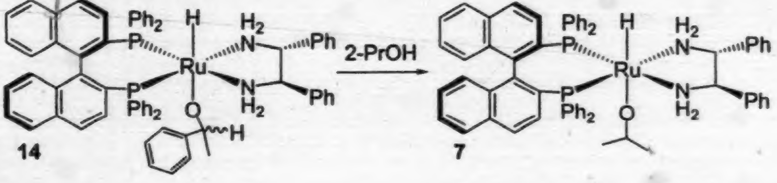

Equation 4.8

enantioselectivity of the catalytic hydrogenation in THF is less than it is in 2-PrOH. Further, the *ee* of the catalytic hydrogenation in THF decreased to 59 %

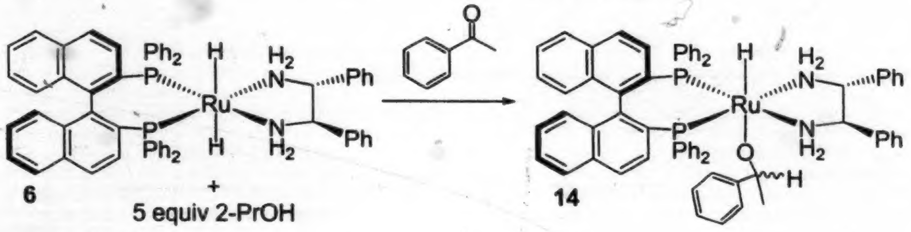

Equation 4.9

(*S*) after 94 turnovers. To investigate whether the addition reaction is reversible in THF, 10 equiv of the minor product enantiomer, (*R*)-$CH_3(Ph)CHOH$ (*ee* ~ 99%), was reacted with the dihydride catalyst **6** in THF at 30°C under ~2 atm H_2 in the presence of ~1.5 equiv *t*-BuOK, conditions similar to those used for the catalytic hydrogenation. The *ee* was 35 % (*R*) after 5 min, 10 % (*R*) after 10 min, the alcohol was racemized after 15 min, and it was still racemic after 30 min. The racemization was somewhat faster with the amide **11** in the absence of H_2. I showed previously that addition reaction of H_2 to the amide **11** to form the dihydride **6** is reversible, it proceeds *via* elimination of the Ru-H and N-H hydrogen atoms in **6**, and the reaction strongly favors **6** in THF (Scheme 4.5, top).[7b] Isotope exchange studies with D_2 also showed that the reversible addition proceeds *via* exchange between D_2 and the Ru-H and N-H_{axial} at -80°C.[7b] Morris has also reported that the addition reaction of H_2 to *trans*-[Ru((*R*)-BINAP)$(H)_2$(tmen)] is reversible and that this compound also reacts with excess 1-phenylethanol to generate *trans*-[Ru((*R*)-BINAP)(H)((Ph)(Me)CHO)(tmen)].[3b] I thereby propose that the racemization of

$CH_3(Ph)CHOH$ occurs by the sequence shown in Scheme 4.5. Specifically, loss of H_2 from **6** to form **11**, followed by rapid reaction with (*R*)-$CH_3(Ph)CHOH$ to form the alkoxide **14** and then a net β-hydride elimination to from **6** and acetophenone. The net β-hydride elimination is the reverse of the addition reaction (Equation 4.10). As discussed below, all of these steps are rapid in the reverse direction in the presence of base. The sequence in Scheme 4.5 thereby provides a kinetically competent route for the racemization with the net β-hydride elimination being the slow step in the process.

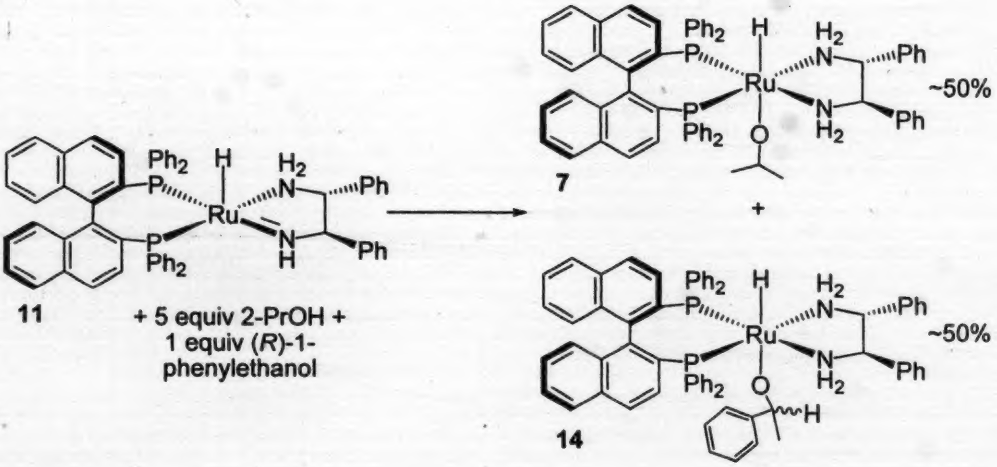

Equation 4.10

The sequence of steps in Scheme 4.5 predicts that a large excess of 2-PrOH would inhibit the racemization reaction by intercepting the amide **11** before it reacts with (*R*)-$CH_3(Ph)CHOH$. Indeed, carrying out the reaction between 10 equiv of (*R*)-$CH_3(Ph)CHOH$ and **6** in a 1:1 mixture of THF and 2-PrOH at 30°C dramatically slowed the rate of racemization. The *ee* dropped to

84% (*R*) after 10 min, but remained at this value for several hours afterwards. The initial drop in *ee* likely resulted from racemization occurred before complete mixing of the THF and 2-PrOH, or perhaps from local warming by the heat of mixing. These experiments show that one role of 2-PrOH during catalytic hydrogenations carried out in 2-PrOH is to inhibit racemization of the alcohol product by intercepting the amide **11** to form the 2-propoxide **7**, thereby preventing reaction between the product 1-phenylethanol and **11**.

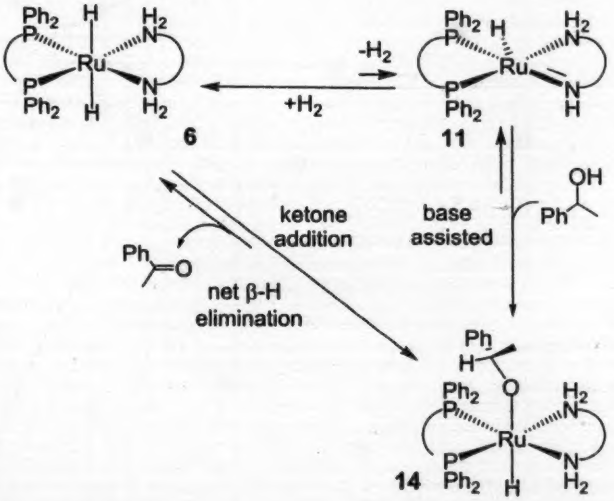

Scheme 4.5: Observed reactivity of the key intermediates in the catalytic cycle.

Conclusion

This research is a stoichiometric study of the proposed catalytic intermediates and steps in these catalytic hydrogenations. The sum of the results from this investigation leads to the proposed pathway for the catalytic hydrogenation shown in Scheme 4.6. The first step is a rapid addition reaction of acetophenone to the dihydride **6** to generate the alkoxide **14** as the net product (Scheme 4.6, and Equation 4.10). This addition reaction is slowly

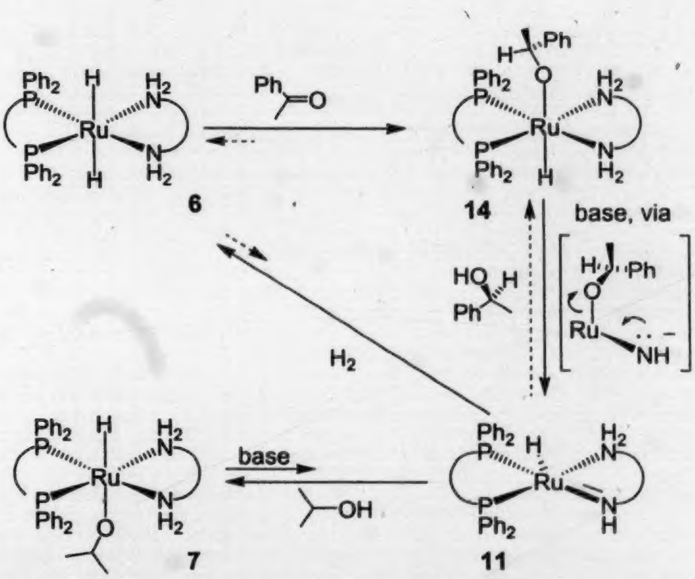

Scheme 4.6: Observed reactivity of the putative intermediates.

reversible in THF solution, presumably by a mechanism that is the microscopic reverse of the addition reaction. In THF, the alkoxide **14** eliminates the product alcohol and reforms **6** under dihydrogen (Scheme 4.6 right, and Equation 4.7). Based upon the reactivity I established previously for the related 2-propoxide **7**,[7b] and the observation of the hydrogen-bond between the β-N-H_{axial} group and $^-O^tBu$ in **14**, I propose that this elimination is promoted by base in THF *via* deprotonation of an N-H group in the dpen ligand, followed by displacement of the alkoxide ligand by the resulting lone pair on nitrogen to form the product alkoxide and the amide **11** (Scheme 4.6, 2nd step). The product alkoxide either reacts with the acid form of the base to generate the product alcohol, or a small of amount of the product exists as the alkoxide during the catalytic hydrogenation to act as base promoter. In THF, this elimination is reversible, and the amide **11** reacts with product alcohol to regenerate **14** (Scheme 4.6, 2nd step reverse). The amide **11** also reacts reversibly with H_2 to generate **6** to thereby complete the catalytic cycle.

As demonstrated by Equation 4.8, the alkoxide intermediate **14** will undergo rapid exchange with 2-PrOH to generate the 2-propoxide **7** and the product $CH_3(Ph)CHOH$ during hydrogenations carried out in 2-PrOH solvent. As discussed previously, **7** is not a catalyst for the hydrogenation in the absence of base under the conditions of my experiments (30°C, 4 atm H_2),[7a] but it will react quickly, even at -80 °C, *via* the base-promoted elimination reaction to form the amide **11** and 2-propoxide. The amide **11** then reacts with H_2 to form **6** and complete the catalytic cycle (Scheme 4.6). The experiments do not rule out the possibility that **7** or related alkoxides eliminate alcohol and generate the amide **11** under more forcing conditions in the absence of base.

This research provides the most direct experimental insight into the mechanisms of these hydrogenations to date. All of the steps in the proposed catalytic cycle, except the net β-hydride elimination within **14**, are rapid in the presence of base at -80 °C, and thereby cannot be ruled out on the basis that they are too slow to account for the reported rates for these catalytic hydrogenations.[2a,3b]

The net product of the addition reaction of acetophenone to **6** is the 1-phenylethoxide **14**, without formation of free amide **11**. The addition reaction is rapid even at -80°C. While it is possible that **11** formed trapped in a solvent cage and/or hydrogen bonded to the $CH_3(Ph)CHOH$ product,[3e,4d] or that ligand arm dissociation generates a vacant site on ruthenium during the addition reaction, my experiments present the possibility that the direct product of the addition reaction is the alkoxide **14**. A possible route for the direct addition reaction **14** begins with formation of the pericyclic 6-membered species proposed for the bifunctional addition (Equation 4.1). This process would remove electron density from Ru through the hydride to the carbonyl carbon. This loss of electron density may allow access to the Ru center by the ketone to undergo hydride insertion to form **14**, perhaps with hydrogen bonding between the alkoxide ligand and the adjacent, axial N-H group (*vide supra*). Further kinetic, isotopic, and computational studies are required to obtain more information about the detailed workings of this step, the other steps in the proposed cycle, and their relevance to the catalytic hydrogenation.

Materials and Methods

All operations were carried out in NMR tubes fitted with a rubber septum under an atmosphere of argon or hydrogen using standard Schlenk and glovebox techniques unless stated otherwise. All solvents were dried and distilled under a dinitrogen atmosphere using standard drying agents unless stated otherwise. Deuterated 2-PrOH was not dried. The deuterated solvents were obtained from Cambridge Isotope Laboratories. Common solvents were obtained from Fisher Scientific. Common chemicals were obtained from Aldrich. (*R,R*)-dpen and (*R*)-BINAP (dpen = 1,2-diphenylethylenediamine, BINAP = 2,2′-bis(diphenylphosphino)-1,1′-binaphthyl) were obtained from Strem. Potassium *tert*-butoxide was sublimed immediately before use. The acetophenone was distilled, washed with 0.1 M $KOH_{(aq)}$, and distilled again before use. All solids were recrystallized before use. The 1-phenylethanol (Fluka) and acetophenone-α,β-$^{13}C_2$ (Aldrich) were used without further purification. The hydrogen gas was ultra high purity grade purchased from Praxair. The reactions were monitored using low temperature NMR spectroscopy. The reaction times are approximate. If an immediate color change occurred when the reactants were mixed at low temperatures, and if the first NMR spectrum was recorded within 5 min of mixing showed the reaction was complete, I report the reaction time as immediate at the temperature the NMR spectrum was recorded. If no visible color change occurred upon mixing, and if the first NMR spectrum showed the reaction was complete, I report the reaction time as less than the time period between mixing and when the first NMR spectrum was recorded. ^{1}H, ^{13}C, and ^{31}P NMR spectra were measured using Varian-Inova (400 MHz) spectrometers. ^{1}H and ^{13}C NMR chemical shifts are reported in parts per million (δ) relative to TMS with the solvent as the internal reference. ^{31}P chemical shifts are reported in parts per million (δ) relative to an 85% H_3PO_4 external reference. NMR peak assignments were made using COSY and ^{13}C–^{1}H HSQC 2D NMR experiments. Some axial and equatorial N-H assignments were made using NOESY NMR experiments. The N-H_{axial} adjacent to Ru-H was ~ 2 ppm upfield from the other N-H's. The same observation was reported for N-H_{axial} adjacent to Ru-H in a series of compounds studied by Noyori *et al.*[11] This observation is used to assign the N-H_{axial} adjacent to Ru-H in compounds. Masses reported for compounds prepared *in situ* are relative to the initial starting material. Masses for compounds that could be weighed were measured with either a Mettler

AE260 DelataRange® or AND ER-60A analytical balance. The masses were allowed to stabilize for 5 min before a reading was taken. Air and moisture sensitive compounds were weighed in the glove box. Liquid reagents were added *via* microlitre syringe, or 1 mL and 5 mL gas tight syringe when appropriate. Stoichiometric amounts of cyclooctane, cycloctene, KBF_4, HO^tBu and $((CH_3)_3Si)_2NH$ may be present in solution from the *in situ* preparation of the compounds. Mass spectrometric analyses of organometallic compounds were performed by positive-mode electrospray ionization (ESI-MS (pos)) on a Micromass ZabSpec Hybrid Sector-TOF spectrometer. Calculated *m/z* values refer to the isotopes ^{12}C, ^{1}H, ^{14}N, ^{16}O, ^{31}P, and ^{102}Ru. Gas chromatography was performed using a Hewlett Packard 5890 chromatograph equipped with a flame ionization detector, a 3392A integrator, and a Beta Dex™ 120 fused silica capillary column (30m × 0.25mm × 0.25μm thickness, Supelco) using 20.5 psi He as carrier gas. The standard conditions used to determine enatiomeric excess (*ee*) of 1-phenylethanol were: initial oven temperature 70 °C increased at 1 °C/min to 120 °C; held at 120 °C for 10 min. The retention times were (*R*)–(+)–1–Phenylethanol, $t_R(R)$ = 43.5 min; (*S*)–(-)–1–Phenylethanol, $t_R(S)$ = 45.6 min; acetophenone, t_R = 29.9 min. The *ee* measurements were confirmed against (±)–1–Phenylethanol.

Typical preparation of *trans*-[Ru((*R*)-BINAP)(H)$_2$((*R*,*R*)-dpen)] (6) in THF-d_8. A solution of *trans*-[Ru((*R*)-BINAP)(H)(η^2-H_2)((*R*,*R*)-dpen)]BF_4 (9.2 mg, 8.72×10^{-3} mmol) in THF-d_8 (0.7 mL) was prepared under H_2 (~2 atm) as described previously[7a] and kept at –80 °C. The *trans*-[Ru((*R*)-BINAP)(H)(η^2-H_2)((*R*,*R*)-dpen)]BF_4 solution was then quickly canulated using H_2 pressure into a tube containing potassium *tert*-butoxide (2.45 equiv, 2.4 mg, 2.14 × 10^{-2} mmol) and kept at –80 °C. The pressure of H_2 was replenished after the transfer by injecting 10 mL of H_2 into the tube using a gas-tight syringe. The contents of the tube were then thoroughly mixed by shaking the tube for 10 sec outside the –80 °C bath and then returned to the bath. The process was repeated four times in order to mix the contents while maintaining the temperature near –80 °C. A colour change from orange to red occurred during the first shake. NMR Spectra recorded at –80 °C after ~5 min showed that the reaction was complete and formed **6** as sole detectable product.

Typical preparation of [Ru((*R*)-BINAP)(H)((*R*,*R*)-NH(CH(Ph))$_2$NH$_2$)] (11). A solution of *trans*-[Ru((*R*)-BINAP)(H)(THF-*d*$_8$)((*R*,*R*)-dpen)]BF_4 (9.7 mg, 8.72 × 10^{-3} mmol) in THF-*d*$_8$ (0.7 mL) was prepared as described previously[7b] and kept at –80 °C. The *trans*-[Ru((*R*)-BINAP)(H)(THF-*d*$_8$)((*R*,*R*)-dpen)]BF_4 solution was quickly canulated using argon pressure into a tube containing $((CH_3)_3Si)_2NK$ (2.47 equiv, 4.3 mg, 2.16 × 10^{-2} mmol) and kept at –80. The tube was shaken for 1 sec and then returned to the bath. The process was repeated four times in order to mix the contents while maintaining the temperature near –80 °C. A colour change from orange to deep red occurred during the first shake. NMR spectra recorded at –80 °C after ~5 min showed that the reaction was complete and formed two diasteromers of **11** in an approximately 8:2 ratio.

Reaction of *trans*-[Ru((*R*)-BINAP)$(H)_2$((*R*,*R*)-dpen)] (6) with acetophenone in the presence of ~1.5 equiv of excess potassium *tert*-butoxide. A solution **6** (7.6 mg, 7.97× 10^{-3} mmol) was prepared in THF-d_8 (0.7 mL) as described above using potassium *tert*-butoxide (2.46 equiv, 2.2 mg, 1.96 × 10^{-2} mmol) as added base and kept at –80 °C. Acetophenone (1 μL, 1.1 equiv, 1 mg, 8.5 × 10^{-3} mmol) was injected into the tube containing **6**. The tube was shaken for 1 sec and then returned to the bath to mix the contents while maintaining the temperature near –80 °C. NMR spectra recorded at –80 °C after ~1 min showed that the reaction was complete and formed *trans*-[Ru((*R*)-BINAP)(H)(PhCH(CH_3)O)((*R*,*R*)-(NH_2(CH(Ph))$_2$NH···H···$^-$O-*t*-Bu)] (**14**) as sole detectable product. ^{1}H NMR (399.95 MHz, THF-d_8, –80 °C): δ –16.4 (1H, t, $^2J_{P\text{-}H}$ = 24.0 Hz, Ru–H), 1.3 1H, PhCH(C*H*$_3$)O– Ru, partially obscured), 2.12 (1H, br, C_aHN*H*$_{axial}$H), 3.3 (1H, br, C_bHN*H*H), 4.0 (1H, br, C_b*H*NHH), 4.3 (1H, multiplet, C_a*H*NHH, overlapping with C_bHNH*H*), 4.4 (1H, multiplet, C_bHNH*H*, overlapping with C_a*H*NHH), 4.6 (1H, br, C_aHNH*H*$_{equatorial}$), 4.96 (1H, br, PhC*H*(CH_3)O– Ru), 6-10 (overlapping multiplets, aromatic). $^{13}C\{^1H\}$ NMR (100.6 MHz, THF-d_8, –80 °C): δ 28.0 (PhCH(*C*H$_3$)O– Ru), 63.0 (*C*$_a$HNHH), 69.0 (Ph*C*H(CH_3)O– Ru), 71.1 (*C*$_b$HNHH), 123-141 (aromatic). $^{31}P\{^1H\}$ NMR (161.88 MHz, THF-d_8, –80 °C). δ 68.44 (d, $^2J_{P\text{–}P}$ = 40.5 Hz), 73.68 (d, $^2J_{P\text{–}P}$ = 40.5 Hz). LRMS (ESI): *m/z* calcd for $C_{66}H_{57}N_2OP_2{}^{102}Ru$ ([M-1]$^+$), 1057.3 found, 1057.3

Reaction of *trans*-[Ru((*R*)-BINAP)$(H)_2$((*R*,*R*)-dpen)] (6) with acetophenone

in the absence of excess potassium *tert*-butoxide. A solution of *trans*-[Ru((*R*)-BINAP)(H)(η^2-H_2)((*R*,*R*)-dpen)]BF_4 (8.2 mg, 7.96 × 10^{-3} mmol) in THF-d_8 (0.7 mL) was prepared under H_2 (~2 atm) as described previously[7a] and kept at –80 °C. The *trans*-[Ru((*R*)-BINAP)(H)(η^2-H_2)((*R*,*R*)-dpen)]BF_4 solution was then quickly canulated using H_2 pressure into a tube containing potassium *tert*-butoxide (1.23 equiv, 1.1 mg, 9.8 × 10^{-3} mmol) and kept at –80 °C. The pressure of H_2 was replenished after the transfer by injecting 10 mL of H_2 into the tube using a gas-tight syringe. The contents of the tube were then thoroughly mixed by shaking the tube for 10 sec outside the –80 °C bath and then returned to the bath. The process was repeated four times in order to mix the contents while maintaining the temperature near –80 °C. A colour change from yellow to orange occurred during the first shake. NMR Spectra recorded at –80 °C after ~5 min showed 70 percent conversion to **6**. The remaining 30 percent was *trans*-[Ru((*R*)-BINAP)(H)(OH)((*R*,*R*)-dpen)] indicating the absence of excess base.[7b] Acetophenone (0.6 µL, ~ 1 equiv relative to **6**, 0.62 mg, 5.1 × 10^{-3} mmol) was injected into the tube containing **6**. The tube was shaken for 1 sec and then returned to the bath to mix the contents while maintaining the temperature near –80 °C. NMR spectra recorded at –80 °C after ~1 min showed that **6** reacted with acetophenone to form *trans*-[Ru((*R*)-BINAP)(H)(PhCH(CH_3)O)((*R*,*R*)-dpen)] (**14′**). ^{1}H NMR (399.95 MHz, THF-d_8, –80 °C): δ –16.43 (1H, t, $^2J_{P\text{-}H}$ = 22.0 Hz, Ru–H), 1.22 1H, PhCH(CH_3)O– Ru, partially obscured), 2.12 (1H, br, C_aHNH_{axial}H), 3.6 (1H, br, C_bHN*H*H), 4.05 (1H, br, C_b*H*NHH), 4.28 (1H, multiplet, C_a*H*NHH, overlapping with C_bHNH*H*), 4.45

(1H, multiplet, C_bHNHH, overlapping with C_aHNHH), 4.6 (1H, br, $C_aHNHH_{equatorial}$), 5.05 (1H, br, $PhCH(CH_3)O$– Ru), 6-10 (overlapping multiplets, aromatic). $^{13}C\{^1H\}$ NMR (100.6 MHz, THF-*d*$_8$, –80 °C): δ 30.1 ($PhCH(CH_3)O$–Ru), 63.1 (C_aHNHH), 70.0 ($PhCH(CH_3)O$– Ru), 70.2 (C_bHNHH), 123-141 (aromatic). $^{31}P\{^1H\}$ NMR (161.88 MHz, THF-*d*$_8$, –80 °C). δ 68.4 (d, $^2J_{P-P}$ = 38.86 Hz), 73.66 (d, $^2J_{P-P}$ = 38.86 Hz).

Reaction of *trans*-[Ru((*R*)-BINAP)(H)$_2$((*R*,*R*)-dpen)] (6) with acetophenone-α,β-$^{13}C_2$ in the presence of ~1.5 equiv of excess potassium *tert*-butoxide. A solution of **6** (7.3 mg, 7.95 × 10^{-3} mmol) was prepared in THF-*d*$_8$ (0.7 mL) as described above using potassium *tert*-butoxide (2.5 equiv, 2.2 mg, 1.96 × 10^{-2} mmol) as added base and kept at –80 °C. Acetophenone-α,β-$^{13}C_2$ (0.9 μL, 0.97 equiv, 0.94 mg, 7.7 × 10^{-3} mmol) was injected into the tube containing **6**. The tube was shaken for 1 sec and then returned to the bath to mix the contents while maintaining the temperature near –80 °C. NMR spectra recorded at –80 °C after ~1 min showed that the reaction was complete and formed *trans*-[Ru((*R*)-BINAP)(H)(Ph^{13}CH(^{13}CH$_3$)O((*R*,*R*)-(NH$_2$(CH(Ph))$_2$NH···H···$^-$O-*t*-Bu)] (**14″**) as sole detectable product. LRMS (ESI): *m/z* calcd for $C_{64}{}^{13}C_2H_{56}N_2OP_2{}^{102}Ru$ ([M-2]$^+$), 1058.3; found, 1058.3.

Reaction of [Ru((*R*)-BINAP)(H)((*R*,*R*)-NH(CH(Ph))$_2$NH$_2$)] (11) with (±)–1–Phenylethanol to form *trans*-[Ru((*R*)-BINAP)(H)(PhCH(CH$_3$)O)((*R*,*R*)-dpen)] (14). A solution of **11** (8.4 mg, 8.97 × 10^{-3} mmol) was prepared in THF-*d*$_8$ (0.7

mL) as described above using $((CH_3)_3Si)_2NK$ (2.46 equiv, 4.4 mg, 2.20 × 10^{-2} mmol) as added base and kept at –80 °C. (±)–1–Phenylethanol (1.1 μL 1.01 equiv, 1.1 mg, 9.0 × 10^{-3} mmol) was injected into the tube containg **11**. The tube was shaken for 1 sec and then returned to the bath to mix the contents while maintaining the temperature near –80 °C. NMR spectra recorded at –80 °C after ~1 min showed that the reaction was complete and formed **14** as sole detectable product.

Reaction of *trans*-[Ru((*R*)-BINAP)(H)(PhCH(CH_3)O)((*R*,*R*)-dpen)] (14) with 2-PrOH to form *trans*-[Ru((*R*)-BINAP)(H)(2-PrO)((*R*,*R*)-dpen)] (7). (a) A solution of **14** (8.5 mg, 8.0 × 10^{-3} mmol) was prepared in THF-d_8 (0.7 mL) as described above using potassium *tert*-butoxide (2.6 equiv, 2.3 mg, 2.05 × 10^{-2} mmol) as added base and kept at –80 °C. 2-Propanol (48.7 equiv, 23.5 mg, 30 μL, 0.39 mmol) was injected into the tube containing **14**. The tube was shaken for 1 sec, frozen in N_2(l), and then thawed in the NMR probe at –80 °C. The first spectra upon thawing showed complete conversion to **7**. (b) A solution of **14** (8.5 mg, 7.8 × 10^{-2} mmol) was prepared in THF-d_8 (0.7 mL) as described above and kept at –80 °C. 2-Propanol (9.75 equiv, 4.7 mg, 6 μL, 0.39 mmol) was injected into the tube containing **14**. The tube was shaken for 1 sec, frozen in N_2(l), and thawed in the NMR probe at –80 °C. The first spectra upon thawing showed complete conversion to **7**.

Reaction of *trans*-[Ru((*R*)-BINAP)$(H)_2$((*R*,*R*)-dpen)] (6) with acetophenone

in the presence of 2-PrOH-d_8. A solution of **6** (7.5 mg, 8.00 × 10^{-3} mmol) was prepared in THF-d_8 (0.7 mL) as described above using potassium *tert*-butoxide (2.6 equiv, 2.3 mg, 2.05 × 10^{-2} mmol) as added base then frozen in N_2(l). Acetophenone (2 equiv, 1.9 µL, 1.95 mg, 1.62 × 10^{-3} mmol) was dissolved in 2-PrOH (0.1mL) in a NMR tube under argon and cooled to –80 °C. The acetophenone solution was then canulated using H_2 pressure onto the frozen solution of **6** to form a frozen layer on top of the frozen layer of **6**. The sample was then thawed in the NMR probe at –80 °C. The first spectra upon thawing showed conversion to **14** and that approximately 5 equiv of 2-PrOH had diffused into the THF-d_8.

Reaction of *trans*-[Ru((*R*)-BINAP)(H)$_2$((*R*,*R*)-dpen)] (6) with acetophenone in the presence of 5 equiv of 2-PrOH. A solution of **6** (7.7 mg, 8.06 × 10^{-3} mmol) was prepared in THF-d_8 (0.7 mL) at as described above using potassium *tert*-butoxide (2.5 equiv, 2.3 mg, 2.05 × 10^{-2} mmol) as added base and kept at –80 °C. 2-PrOH (5 equiv, 3 µL, 2.4 mg, 3.99 × 10^{-2} mmol) was injected into the tube containing **6**. The mixture was shaken for 1 sec and frozen in N_2(l) to prevent the reaction of **6** with 2-PrOH to form **7**. The sample was then thawed in the NMR probe at –80 °C. NMR spectra at –80 °C did not show detectable amounts of **7**. The sample was frozen in N_2(l) immediately upon removal from the NMR to ensure that **6** remained in solution. Acetophenone (1.06 equiv, 1 µL, 1 mg, 8.5 × 10^{-3} mmol) was dissolved in THF-d_8 (0.1 mL) in a NMR tube under argon and cooled to –80 °C. The acetophenone solution was then canulated using H_2 pressure into the tube containing **6** to form a frozen layer on top of the frozen layer of **6**. The sample was then thawed in the NMR probe at –80 °C. The first spectra upon thawing showed complete conversion of acetophenone into **14**.

Reaction of *trans*-[Ru((*R*)-BINAP)(H)$_2$((*R*,*R*)-dpen)] (6) with acetophenone in the presence of 10 equiv of 2-PrOH and excess base. A solution of **6** (7.7 mg, 8.06×10^{-3} mmol) was prepared in THF-d_8 (0.7 mL) as described above using potassium *tert*-butoxide (2.5 equiv, 2.3 mg, 2.05×10^{-2} mmol) as added base and kept at –80 °C. 2-PrOH (10 equiv, 6 μL, 2.4 mg, 8.0×10^{-2} mmol) was injected into the tube containing **6**. The mixture was shaken for 1 sec and frozen in N_2(l) to prevent the reaction of **6** with 2-PrOH to form **7**. The sample was then thawed in the NMR at –80 °C. NMR spectra at –80 °C showed that approximately 10 percent of **6** had converted to **7**. The sample was frozen in N_2(l) immediately upon removal from the NMR to ensure that **6** remained in solution. Acetophenone (1.06 equiv, 1 μL, 1 mg, 8.5×10^{-3} mmol) was dissolved in THF-d_8 (0.1 mL) in a NMR tube under argon and cooled to –80 °C. The acetophenone solution was then canulated using H_2 pressure into the tube containing **6** and **7** to form a frozen layer on top of the frozen layer of **6** and **7**. The sample was then thawed in the NMR probe at –80 °C. The first spectra upon thawing showed conversion to **7** with no detectable amounts of **14**.

Reaction of *trans*-[Ru((*R*)-BINAP)(H)$_2$((*R*,*R*)-dpen)] (6) with acetophenone

in the presence of 10 equiv of 2-PrOH in the absence of excess base. A solution of *trans*-[Ru((*R*)-BINAP)(H)(η^2-H_2)((*R*,*R*)-dpen)]BF_4 (8.3 mg, 8.06 × 10^{-3} mmol) in THF-d_8 (0.7 mL) was prepared under H_2 (~2 atm) as described previously[7a] and kept at –80 °C. The *trans*-[Ru((*R*)-BINAP)(H)(η^2-H_2)((*R*,*R*)-dpen)]BF_4 solution was then quickly canulated using H_2 pressure into a tube containing potassium *tert*-butoxide (1.1 equiv, 1 mg, 8.91 × 10^{-3} mmol) and kept at –80 °C. The pressure of H_2 was replenished after the transfer by injecting 10 mL of H_2 into the tube using a gas-tight syringe. The contents of the tube were then thoroughly mixed by shaking the tube for 10 sec outside the –80 °C bath and then returned to the bath. The process was repeated four times in order to mix the contents while maintaining the temperature near –80 °C. A colour change from yellow to orange occurred during the first shake. NMR Spectra recorded at –80 °C after ~5 min showed ~50 percent conversion to **6**. The remaining 50 percent was *trans*-[Ru((*R*)-BINAP)(H)(OH)((*R*,*R*)-dpen)] indicating the absence of excess base.[7b] 2-PrOH (~10 equiv relative to **6**, 3 µL, 2.4 mg, 3.99 × 10^{-2} mmol) was injected into the tube containing **6**. The mixture was shaken for 1 sec and frozen in N_2(l) to prevent the reaction of **6** with 2-PrOH to form **7**. The sample was then thawed in the NMR probe at –80 °C. Approximately 5 percent of **6** had converted to **7**. The sample was frozen in N_2(l) immediately upon removal from the NMR to ensure that **6** remained in solution. Acetophenone (0.5 µL, ~ 1 equiv relative to **6**, 0.5 mg, 4.2 × 10^{-3} mmol) was dissolved in THF-d_8 (0.1 mL) in a NMR tube under argon and cooled to –80 °C. The acetophenone solution was then canulated using H_2 pressure into the tube containing **6** and **7** to form a frozen layer on top of the frozen layer of **6** and **7**. The sample was then thawed in the NMR probe at –80 °C. The first spectra upon thawing showed conversion to **7** with approximately 5 percent of **14.** Complex **14** reacted with 2-PrOH to form **7** within 5 min.

Competition reaction of [Ru((*R*)-BINAP)(H)((*R,R*)-NH(CH(Ph))$_2$NH$_2$)] (11) with 1 equiv (±)–1–Phenylethanol and 5 equiv of 2-PrOH. A solution of **11** (8.4 mg, 8.97 × 10^{-3} mmol) was prepared in THF-*d*$_8$ (0.7 mL) as described above using ((CH$_3$)$_3$Si)$_2$NK (2.46 equiv, 4.4 mg, 2.20 × 10^{-2} mmol) as added base and kept at –80 °C. (±)–1–Phenylethanol (0.93 equiv, 1 µL, 1.01 mg, 8.3 × 10^{-3} mmol) and 2-PrOH (4.3 equiv, 3 µL, 2.4 mg, 3.9 × 10^{-2} mmol) were injected into the tube containing **11**, shook for 1 sec outside the bath and immediately placed in the NMR probe at –80 °C. The first spectra upon thawing showed a 1:1 mixture of **14** and **7**.

Reaction of *trans*-[Ru((*R*)-BINAP)(H)$_2$((*R,R*)-dpen)] (6) with acetophenone followed by the addition of a large excess of 2-PrOH. A solution of **6** (5.7 mg, 5.99 × 10^{-3} mmol) was prepared in THF (0.7 mL) as described above using potassium *tert*-butoxide (2.5 equiv, 1.7 mg, 1.51 × 10^{-2} mmol) and kept at –80 °C. Acetophenone (1 equiv, 0.7 mg, 0.70 µL, 5.99 × 10^{-3} mmol) was injected into the tube containing **6**, shook briefly (~ 1 sec) at room temp and 2-PrOH (0.7 mL) was added to halt the reaction. The reaction mixture was then emptied into a vial containing EtOH and passed through a small column of Florosil to remove catalyst residues using EtOH as eluent. Gas chromatography showed that there was ~50 % conversion to 1–Phenylethanol with an *ee* of 83% (*S*).

Reaction of *trans*-[Ru((*R*)-BINAP)(H)$_2$((*R,R*)-dpen)] (6) with (*R*)–(+)–1–Phenylethanol. (a) A solution of **6** (5.7 mg, 5.99 × 10^{-3} mmol) was prepared in THF (0.7 mL) as described above using potassium *tert*-butoxide (2.5 equiv, 1.7 mg, 1.51 × 10^{-2} mmol) and kept at –80 °C. (*R*)–(+)–1–Phenylethanol (10 equiv, 7.0 µL, 7.2 mg, 5.99 × 10^{-2} mmol) was injected into the tube containing **6** and shook outside the bath for 5 seconds and immersed in a room temp (21 °C) bath. Aliquots (~0.05 mL) were taken into a vial containing EtOH and passed through a small column of Florosil to remove catalyst residues using EtOH as eluent. Gas chromatography showed that the *ee* had dropped to 61% (*R*) after 5 min and to 4% (*R*) after 35 min. (b) A solution of **6** (5.7 mg, 5.99 × 10^{-3} mmol) was prepared in THF (0.7 mL) as described above using potassium *tert*-butoxide (2.5 equiv, 1.7 mg, 1.51 × 10^{-2} mmol) and kept at –80 °C. (*R*)–(+)–1–Phenylethanol (10 equiv, 7.0 µL, 7.2 mg, 5.99 × 10^{-2} mmol) was injected into the tube containing **6** and shook outside the bath for 5 seconds and immersed in 30 °C bath. Aliquots (~0.05 mL) were taken into a vial containing EtOH and passed through a small column of Florosil to remove catalyst residues using EtOH as eluent. Gas chromatography showed that the *ee* had dropped to 35% (*R*) after 5 min and was racemic after 15 min. The 1–Phenylethanol was still racemic after 30 min. (c) A solution of **6** (5.7 mg, 5.99 × 10^{-3} mmol) was prepared in THF (0.35 mL) as described above using potassium *tert*-butoxide (2.5 equiv, 1.7 mg,

1.51×10^{-2} mmol) and kept at –80 °C. (*R*)–(+)–1–Phenylethanol (10 equiv, 7.0 µL, 7.2 mg, 5.99×10^{-2} mmol) was dissolved in 2-PrOH (0.35 mL), cooled to –80 °C, canulated using H_2 pressure into the tube containing **6**, shook outside the bath for 5 seconds, and then immersed in a 30 °C bath. Aliquots (~0.05 mL) were taken into a vial containing EtOH and passed through a small column of Florosil to remove catalyst residues using EtOH as eluent. Gas chromatography showed that the *ee* had dropped to 84 % (*R*) after 10 min. An aliquot taken after 230 min showed that the ee dropped to 66 % (*R*).

Reaction of [Ru((*R*)-BINAP)(H)((*R,R*)-NH(CH(Ph))$_2$NH$_2$)] (11) with (*R*)–(+)–1–Phenylethanol. A solution of **11** (5.7 mg, 5.99×10^{-3} mmol) was prepared in THF (0.7 mL) as described above using $((CH_3)_3Si)_2NK$ (2.5 equiv, 3.0 mg, 1.50 $\times 10^{-2}$ mmol) as added base and kept at –80 °C. (*R*)–(+)–1–Phenylethanol (10 equiv, 7.0 µL, 7.2 mg, 5.99×10^{-2} mmol.) was added to the tube containing **11** and shook outside the bath for 5 seconds, and then immersed in a 30 °C bath. Aliquots (~0.05 mL) were taken into a vial containing EtOH and passed through a small column of Florosil to remove catalyst residues using EtOH as eluent. Gas chromatography showed that the *ee* had dropped to 14% (*R*) after 5 min, and was racemic after 10 min.

Hydrogenation of Acetophenone using *trans*-[Ru((*R*)-BINAP)(H)$_2$((*R,R*)-dpen)] (6) as catalyst. A solution of **6** (11.4 mg, 1.19×10^{-2} mmol) was prepared in THF (0.7 mL) as described above using potassium *tert*-butoxide

(~2.5 equiv, 3.4 mg, 3.0 × 10^{-2} mmol) as added base, diluted to 2 mL with THF, and kept at –80 °C. A glass pressure reactor equipped with a magnetic stir bar was fitted with a rubber septum, charged with acetophenone (1.44 g, 1.2 ×10^{-2} mol, 1000 equiv) in dry, distilled THF (4.8 mL), and then flushed with H_2. Hydrogen gas was bubbled through the solution with stirring for 1 min, and then the solution of **6** was canulated using H_2 pressure into the glass pressure reactor (total THF 6.8 mL). The septum was replaced with a high pressure fitting, and the reactor was pressurized to 44 psi (gauge). The mixture was rapidly stirred at 30 °C. Aliquots were taken by first depressurizing the reactor to ~1.5 atm, removing an aliquot (~ 0.1 mL) into a vial containing EtOH, and then repressurizing the reactor to 44 psi. All aliquots were passed through a small column of Florosil to remove catalyst residues using EtOH as eluent. Gas chromatography showed that there was ~ 6 turnovers with 69 % *ee* (*S*) after 18 min, ~ 22 turnovers with 66% *ee* (*S*) after 49 min, and ~94 turnovers with 59 % *ee* (*S*) after 97 min. An aliquot taken at 1198 min indicated that the reaction was complete with 53 % *ee* (*S*). The *ee* dropped to 47 % (*S*) after an additional 428 min under H_2 pressure (44 psi gauge).

References

(1) For reviews see (a) Noyori, R.; Yamakawa, M.; Hashiguchi, S. *J. Org. Chem* **2001**, *66*, 7931-7944. (b) Noyori, R.; Kitamura, M.; Ohkuma, T. *Proc. Natl. Acad. Sci U.S.A* **2004**, *101*, 5356-5362. (c) Noyori, R.; Sandoval, C. A.; Muñiz, K.; Ohkuma, T. *Phil. Trans. R. Soc. A.* **2005**, *363*, 901-912. (d) Muñiz, K. *Angew. Chem. Int. Ed.* **2005**, *44*, 6622-6627. (e) Gladiali, S.; Alberico, E. *Chem. Soc. Rev.* **2006**, *35*, 226-236. (f) Samec, J. S. M.; Bäckvall, J.-E.; Andersson, P. G.; Brandt, P. *Chem. Soc. Rev.* **2006**, *35*, 237-248. (g) Ikariya, I.; Blacker, A. J. *Acc. Chem. Res.* **2007**, *44*, 1300-1308. (h) Ito, M.; Ikariya, T. *Chem. Commun.* **2007**, *48*, 5134-5142. (i) Morris, R. H. In *Handbook of Homogeneous Hydrogenation*; de Vries, J. G., Elsevier, C. J., Eds.; Wiley-VCH: Weinheim, 2007; Vol. 1, p 45. (j) Ohkuma, T.; Noyori, R. In *Handbook of Homogeneous Hydrogenation*; de Vries, J. G., Elsevier, C. J., Eds.; Wiley-VCH: Weinheim, 2007; Vol. 3, p 1105.

(2) (a) Sandoval, C. A.; Ohkuma, T.; Muniz, K.; Noyori, R. *J. Am. Chem. Soc.* **2003**, *125*, 13490-13503. (b) Ohkuma, T.; Sandoval, C. A.; Srinivasan, R.; Lin, Q.; Wei, Y.; Muniz, K.; Noyori, R. *J. Am. Chem. Soc.* **2005**, *127*, 8288-8289.

(3) (a) Abdur-Rashid, K.; Faatz, M.; Lough, A. J.; Morris, R. H. *J. Am. Chem. Soc.* **2001**, *123*, 7473-7474. (b) Abdur-Rashid, K.; Clapham, S. E.; Hadzovic, A.; Harvey, J. N.; Lough, A. J.; Morris, R. H. *J. Am. Chem. Soc.* **2002**, *124*, 15104-15118. (c) Clapham, S. E.; Hadzovic, A.; Morris, R. H. *Coord. Chem. Rev.* **2004**, *248*, 2201-2237. (d) Abbel, R.; Abdur-Rashid, K.; Faatz, M.;

Hadzovic, A.; Lough, A. J.; Morris, R. H. *J. Am. Chem. Soc.* **2005**, *127*, 1870-1882. (e) Hadzovic, A.; Song, D.; MacLaughlin, C. M.; Morris, R. H. *Organomettalics* **2007**, *26*, 5987-5999.

(4) (a) Casey, C. P.; Singer, S. W.; Powell, D. R.; Hayashi, R. K.; Kavana, M. *J. Am. Chem. Soc.* **2001**, *123*, 1090-1100. (b) Casey, C. P.; Johnson, J. B. *J. Am. Chem. Soc.* **2005**, *127*, 1883-1894. (c) Casey, C. P.; Johnson, J. B.; Singer, S. W.; Cui, Q. *J. Am. Chem. Soc.* **2005**, *127*, 3100-3109. (d) Casey, C. P.; Bikzhanova, G. A.; Cui, Q.; Guzei, I. A. *J Am. Chem. Soc.* **2005**, *127*, 14062-14071. (e) Casey, C. P.; Bikzhanova, G. A.; Guzei, I. A. *J Am. Chem. Soc.* **2006**, *128*, 2286-2293.(f) Casey, C. P.; Clark, T. B.; Guzei, L. A. *J. Am. Chem. Soc* **2007**, *129*, 11821-11827. (g) Casey, C. P.; Beetner, S. E.; Johnson, J. B. *J. Am. Chem. Soc.* **2008**, *130*, 2285-2295.

(5) Hedberg, C.; Kallstrom, K.; Arvidsson, P. I.; Brandt, P.; Andersson, P. G. *J. Am. Chem. Soc.* **2005**, *127*, 15083-15090.

(6) (a) Baratta, W.; Chelucci, G.; Gladiali, S.; Siega, K.; Toniutti, M. Z.; Zangrando, E.; Rigo, P. *Angew. Chem. Int. Ed.* **2005**, *44*, 6214-6219. (b) Baratta, W.; Siega, K.; Rigo, P. *Chem. Ur. J.* **2007**, *13*, 7479-7486.

(7) (a) Hamilton, R. J.; Leong, C. G.; Bigam, G.; Miskolzie, M.; Bergens, S. H. *J. Am. Chem. Soc.* **2005**, *127*, 4152-4153. (b) Hamilton, R. J.; Bergens, S. H. *J. Am. Chem. Soc.* **2006**, *128*, 13700-13701.

(8) (a) Johnson, J. B.; Bäckvall, J.-E. *J. Org. Chem.* **2003**, *123*, 7681-7684. (b) Åberg, J. B.; Samec, J. S. M.; Bäckvall, J.-E. *Chem. Commun.* **2006**, 2771-2773. (c) Samec, J. S. M.; Éll, A. H.; Åberg, J. B.; Privalov, T.; Eriksson, L.;

Bäckvall, J.-E. *J. Am. Chem. Soc.* **2006**, *128*, 14293-14305. (d) Privalov, T.; Samec, J. S. M.; Bäckvall, J.-E. *Organometallics* **2007**, *26*, 2840-2848.

(9) (a) Yamakawa, M.; Ito, H.; Noyori, R. *J. Am. Chem. Soc.* **2000**, *122*, 1466-1478. (b) Handgraaf, J. –W.; Reek, J. N. H.; Meijer, E. J. *Organometallics*, **2003**, *22*, 3150-3157. (c) Handgraaf, J. –W.; Meijer, E. J. *J. Am. Chem. Soc.* **2007**, *129*, 3099-3103. (d) Tommaso, D. D.; French, S. A.; Catlow,C. R. A. *J. Mol. Struct. (THEOCHEM)* **2007**, *812*, 39-49. (e) Comas-Vives, A.; Ujaque, G.; Lledos, A. *Organometallics* **2007**, *26*, 4135-4144. (f) Tommaso, D. D.; French, S. A.; Zanotti-Gerosa, A.; Hancock, F.; Palin, E. J.; Catlow, C. R. A. *Inor. Chem.* **2008**, *47*, 2674-2687. (g) Leyssens, T.; Peeters, D.; Harvey, J. N. *Organometallics* **2008**, 27, 1514-1523.

(10) This reaction likely proceeds by loss of η^2-H_2, then deprotonation of a N-H group to form **11**, and addition of H_2 to form **6**. Ref. 7b.

(11) Sandoval, C. A.; Yamaguchi, Y.; Ohkuma, T.; Kato, K.; Noyori, R. *Magn. Reson. Chem.* **2006**, *44*, 66-75.

(12) Reaction of a mixture of **6** and 10 equiv of 2-PrOH in the absence of base with acetophenone showed a small amount of **14** in the first spectrum, that converted to **7** by the second spectrum.

Chapter 5: Summary and future work.

Summary

Noyori *et al.*'s hydrogenation catalyst system *trans*-Ru(diphosphine)Cl_2(diamine) plus base in 2-PrOH along with its base free analogue *trans*-Ru(diphosphine)(H)(η^1-BH_4)(diamine) are amongst the most successful, and influential catalysts ever developed for the hydrogenation of polar bonds. Simply by changing the phosphine and amine ligands, variants of this catalyst system can hydrogenate a wide range of ketone substrates with high enantioselectivity, chemoselectivity, turnover numbers and rates.[1]

The mechanisms of these, and related, hydrogenations are the subject of intense study.[2-9] It is difficult, however, to obtain direct information about the individual steps in the cycle because of the high reactivity of the proposed intermediates.[7] As such, direct NMR evidence for the steps in the catalytic cycle was difficult to obtain at the time. Therefore the proposed mechanism was based on intuition and indirect evidence such as kinetics, isotope labeling studies, preparation of model compounds, and theoretical calculations. Theoretical calculations indicate that the best fit for the key steps in the catalytic cycle, the enantioselective product formation step and the regeneration of the active dihydride catalyst, proceed through a metal-ligand bifunctional addition which is followed by a turnover-limiting reaction with dihydrogen to regenerate the active catalyst.[3b] It is proposed that metal-ligand bifunctional addition is a concerted process in which a nucleophilic hydride on ruthenium and a protic hydrogen on nitrogen add to the carbon and oxygen of the ketone, respectively, through a pericyclic 6-membered transition state to form product alcohol and a ruthenium-amide species (equation 5.1).[2a] The amide then heterolytically cleaves dihydrogen to regenerate the active catalyst. Indeed kinetic studies indicate a rate dependence on hydrogen which corroborates with theoretical calculations.[2a]

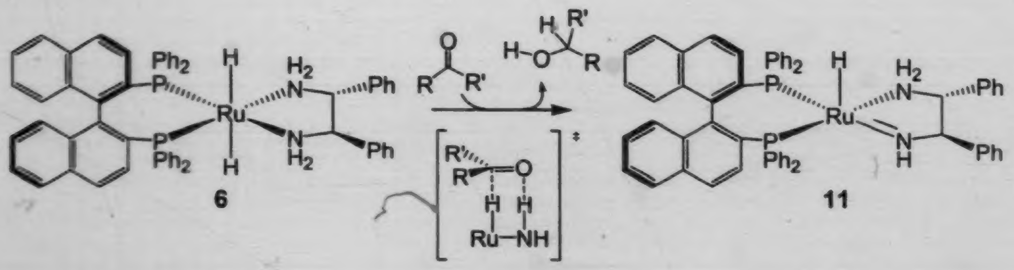

Equation 5.1

The goal of the work in this dissertation was to prepare and characterize the actual proposed intermediates in the metal-ligand bifunctional mechanism. The individual steps in the catalytic reaction were studied by carrying out each stoichiometrically at low temperatures. The results were then used to propose an alternate route for the hydrogenation.

One of the proposed interemediates in the catalytic cycle is the η^2-H_2 compound *trans*-[Ru((*R*)-BINAP)(H)(η^2-H_2)((*R*,*R*)-dpen)]$^+$ (**1**). Although 2-PrOH-d_8 is not the optimal solvent for the observation of the proposed catalytic intermediate, compound **1** can be prepared at low temperatures in 2-PrOH-d_8-rich solutions without H-D exchange of the hydride or η^2-H_2 ligands, thereby allowing its conclusive ^{1}H NMR characterization and study.[7a] The η^2-H_2 ligand in **1** is very labile and has the shortest H-H bond distance reported to date. The η^2-H_2 ligand it can be easily displaced by D_2 to make the η^2-D_2 analogue. This substitution resulted in a sharpening and down-field shift of the *trans* hydride signal due to the difference in *trans* influence of η^2-D_2 versus η^2-H_2. Additionally, **1** reacts with $NaBH_4$ to displace the η^2-H_2 ligand and make the Noyori base-free catalyst precursor *trans*-[Ru((*R*)-BINAP)(H)(η^1-BH_4)((*R*,*R*)-dpen] (**82'**).

Noyori *et al.* proposed that 2-PrOH solvent displaces the η^2-H_2 ligand to form a solvento compound,[2a] although there was no evidence for the proposed solvento species upon removal of hydrogen. Additionally, Noyori *et al.* proposed that the η^2-H_2 ligand is sufficiently acidic to be deprotonated by 2-PrOH solvent under base-free conditions. There is rapid H-D exchange with the solvent at room temperature which suggests that **1** is weakly acidic. The dihydride was not, however, detected in NMR experiments.[7a] Further, compound **1** does not generate sufficient amounts of the active catalyst for rapid ketone hydrogenations under the base-free conditions used for this study (4 atm H_2, 30 °C). Therefore, under base-free conditions the mechanism likely proceeds *via* a different pathway than originally proposed.

Noyori *et al.* proposed that **1** reacts with base in 2-PrOH solvent to form the dihydride catalyst *trans*-[Ru((*R*)-BINAP)$(H)_2$((*R*,*R*)-dpen)] (**6**).[2a] We found, however, that **1** reacts with 1 equiv of *t*-BuOK in 2-PrOH to form the 2-propoxide compound *trans*-[Ru((*R*)-BINAP)(H)(2-PrO)((*R*,*R*)-dpen)] (**7**), not the expected dihydride compound.[7b] Further, the 2-propoxide **7** is remarkably stable and can be isolated and studied in THF-d_8. Compound **7** did not react with H_2 (~2 atm, room temp) to form the dihydride. This unexpected stability of **7** may result from either intramolecular H-bonding between the 2-PrO$^-$ ligand and an

N-H group or intermolecular hydrogen bonding network between the alkoxide oxygen, the amine N-H, and the 2-PrOH solvent. Under catalytic conditions (4 atm H_2, 30 °C), stoichiometric amounts of base (either $NaBH_4$ or *t*-BuOK) converts **1** into an active species, resulting in the catalytic hydrogenation of acetophenone.[7a] This results demonstrates that under Noyori *et al.*'s "base-free" conditions, $(BH_4)^-$ is playing a key role in catalyst activation.

The catalytic cycle was studied in THF-d_8 due to the problems associated with using 2-PrOH-d_8. The dihydrogen compound **1** can be prepared cleanly at low temp in THF-d_8. Since THF is a stronger ligand than 2-PrOH, the solvento compound *trans*-[Ru((*R*)-BINAP)(H)(THF-d_8)((*R*,*R*)-dpen)]$^+$ (Scheme 5.1 top left, **9**) is formed upon the removal of H_2. Noyori *et al.* proposed that the solvento compound will react with base to form the amide **11**.[2a] We found, however, that the solvento compound **9** reacts with 1 equiv of *t*-BuOK in wet THF-d_8 at -80 °C to form the ruthenium-hydroxide compound *trans*-[Ru((*R*)-BINAP)(H)(OH)((*R*,*R*)-dpen)] (Scheme 5.1 middle right, **10**). Similarly, the η^2-H_2 compound **1** reacts with 1 equiv of *t*-BuOK in wet THF-d_8 at -80 °C to form **10**. The hydroxide compound **10** is also exceptionally stable. It does not react with H_2 to form the dihydride **6**, even at elevated temperatures. The hydroxide **10** does, however, react with a further equiv of t-BuOK to generate what we propose is a new $N\cdots H_{equatorial}\cdots{}^-O$-*t*-Bu hydrogen-bonded species **13**. Similarily the 2-propoxide **7** reacts with another equiv of *t*-BuOK to generate an analogous hydrogen-bonded species **12** (Scheme 5.1, middle left). Compounds **13** and **12** subsequently react with H_2 at -80 °C in THF-d_8 to form the dihydride

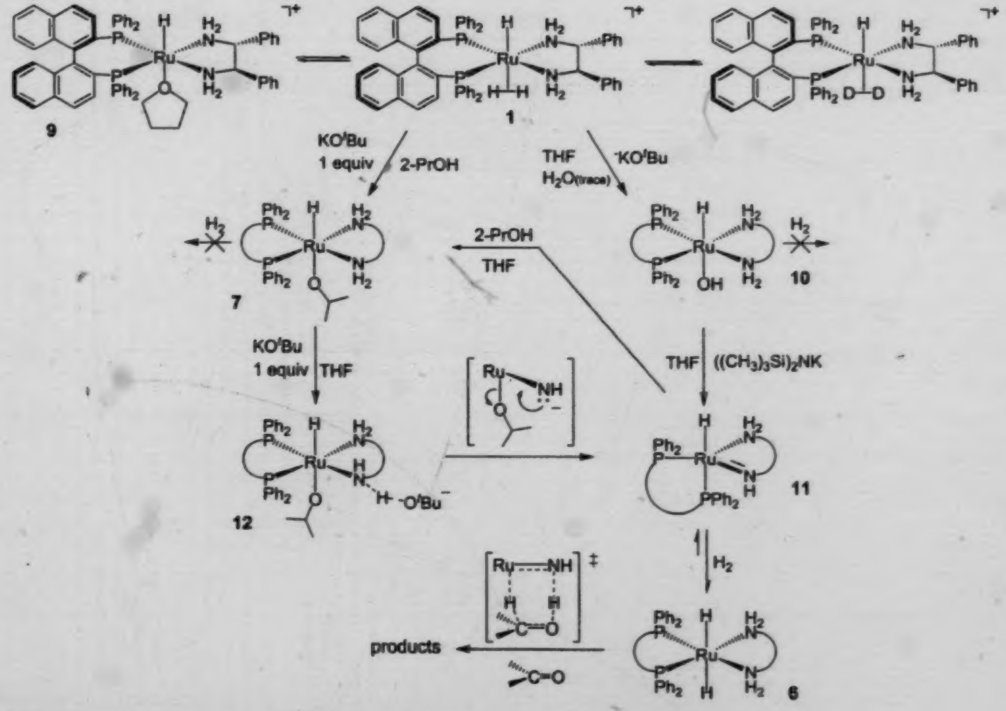
9
1
KO^tBu
1 equiv
2-PrOH
THF
H2O(trace)
KO^tBu
7
2-PrOH
THF
10
KO^tBu
1 equiv
THF
THF
((CH3)3Si)2NK
12
11
H2
6
products
C=O

[illegible]heme 5.1: Observed reactivity of the putative intermediates.

6. This result was the first conclusive identification of the actual proposed dihydride catalyst. It is likely that this proceeds through the formation of the amide **11**, which then reacts with H_2 to form **6**. This hypothesis was investigated by reacting the solvento compound **9** with the stronger more hindered base $((CH_3)_3Si)_2NK$ to form the amide **11** (Scheme 5.1 middle right). The amide **11** subsequently reacts with H_2 to form the dihydride **6**. The turnover limiting step is proposed to be the addition of H_2 to the amide **11** to produce **6**. My observations show, however, that H_2 addition to the amide **11** occurs at high rates at -80 °C. The amide **11** also reacts rapidly with 2-PrOH to form the 2-propoxide compound **7**. This results show that any amide **11** formed during a

catalytic hydrogenation will quickly react with the 2-PrOH solvent to form the 2-propoxide **7**. Therefore it is possible that the hydrogen addition is turnover limiting in the presence of excess base because the steady-state concentration of **11** is low during the catalytic hydrogenation.

To investigate the enantioselctive step the dihydride **6** was reacted with one equiv of acetophenone. The dihydride **6** is formally an 18e- complex, yet it reacts quickly with acetophenone -80 °C. The product of the addition reaction is the alkoxide compound *trans*-[Ru((*R*)-BINAP)(H)(PhCH(CH_3)O)((*R,R*)-dpen)] (**14**), and not the amide. The amide will react quickly with alcohols (*vide supra*) to form the corresponding alkoxide, so it is possible that 1-phenylethanol simply reacted with amide to produce the alkoxide. To investigate this possibility trapping experiments were performed to determine if the amide was formed during the addition step (Scheme 5.2). There was no evidence, however, for the formation of either **7** or **6** as trapping products. These results show that the amide did not form as a distinct species in solution. It is possible compound **11** forms directly *via* the pericyclic 6-membered species proposed for the bifunctional addition (Scheme 5.3 top). This removes electron density from Ru through the hydride to the carbonyl carbon. The loss of electron density allows access to the Ru center by the ketone to undergo a concerted hydride insertion through a transition state like that shown in Scheme 5.3. Species such as **14** rapidly undergo the base-assisted intramolecular alkoxide elimination to form **11** at -80 °C (Scheme 5.3, **14**→**11**). The amide **11** reacts rapidly with H_2 at -80 °C to form **6** (Scheme 5.3, **11**→**6**). Therefore it is possible that the catalytic

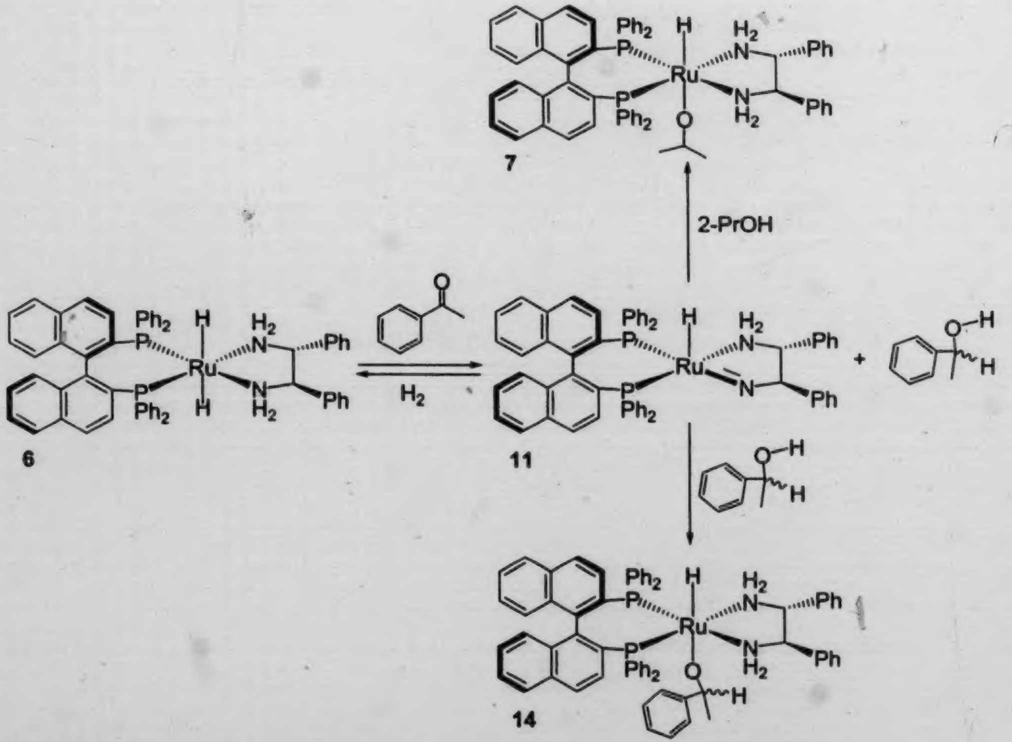

Scheme 5.2: Possible route for the formation of 1-phenylethoxide **14**.

hydrogenation proceeds through the sequence of steps **6→14→11** in the presence of base. These steps are all rapid at -80 °C, and so they are kinetically competent as a mechanism for the catalytic hydrogenation.

The dihydride **6** reduces acetophenone to 1-phenylethanol in THF with low *ee*. This result shows that either the enantioselectivity is lower in THF than in 2-PrOH, or the reaction is reversible, or both. Futher, the dihydride **6**, and the amide **11**, both react with enantiopure (*R*)-1-phenylethanol to form racemic 1-phenylethanol. This result clearly shows that the reaction is reversible under my conditions *via* a net β-hydride elimination of the alkoxide **14**. Compound **14** reacts with 2-PrOH to form the 2-propoxide **7**. If this exchange reaction is faster than the β-hydride elimination in **14**, then the *ee* should be higher in the presence of 2-PrOH. Indeed the dihydride **6** reduces acetophenone with higher

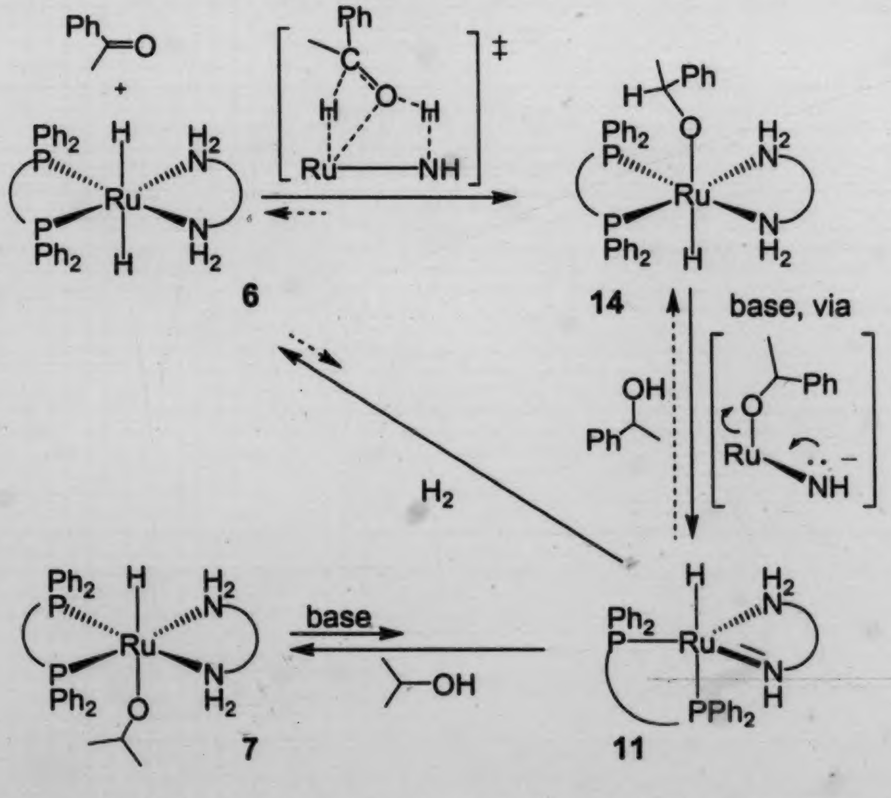

Ph
O
+
Ph2
H
H2
P
N
Ru
P
N
Ph2
H
H2
6
Ph
C
H
O
H
Ru
NH
‡
H
Ph
Ph2
O
H2
P
N
Ru
P
N
Ph2
H
H2
14
base, via
OH
Ph
O
Ph
Ru
NH
H2
Ph2
H
H2
P
N
Ru
P
N
Ph2
O
H2
7
base
OH
H
H2
Ph2
P
Ru
N
H
PPh2
11

Scheme 5.3: Proposed route for the formation of observed intermediates.

ee in the presence of 2-PrOH. Futher, the racemization of (*R*)-1-phenylethanol is hindered in the presence of 2-PrOH. Therefore, the step **6**→**14** mimics an irreversible process in the presence of 2-PrOH by the formation of **7**, and that this preserves the *ee* of the product alcohol (Scheme 5.3 bottom).

Future Work

My experiments present the possibility that the direct product of the addition is the alkoxide **14**. An alternate possibility is that the dihydride **6** reacts with acetophenone to form an amide-alcohol adduct *via* a hydrogen bond between the alcohol OH and the amide N, which then collapses to the alkoxide **14** without the formation product alcohol and amide as distinct species.[3e] If the amide-alcohol adduct collapses to the alkoxide faster than hydrogen bond breaking to form amide and alcohol, then the intermolecular trapping experiments performed in this study cannot distinguish between these two mechanistic possibilities. Intramolecular trapping experiments, however, using a ketone substrate that upon reduction would form a symmetrical diol species may provide information about the formation of the Ru-alkoxide species. For example, 1,4-cycolhexanedione could be partially reduced by $NaBD_4$ in EtOH-d_6 to form 4-hydroxy-d_2-cyclohexanone. The 4-hydroxy-d_2-cyclohexanone could then be reduced by **6** in THF at low temperature to form the Ru-alkoxide species. If the reduction occurs *via* a concerted process as I propose, then only Ru-4-hydroxy-d_2-cyclohexanoxide is formed (Scheme 5.4 right). If, however, the Ru-alkoxide forms *via* an amide-alcohol adduct then a mixture of Ru-4-hydroxy-d_2-cyclohexanoxide and Ru-4-hydroxy-cyclohexanoxide-d_1 is formed (Scheme

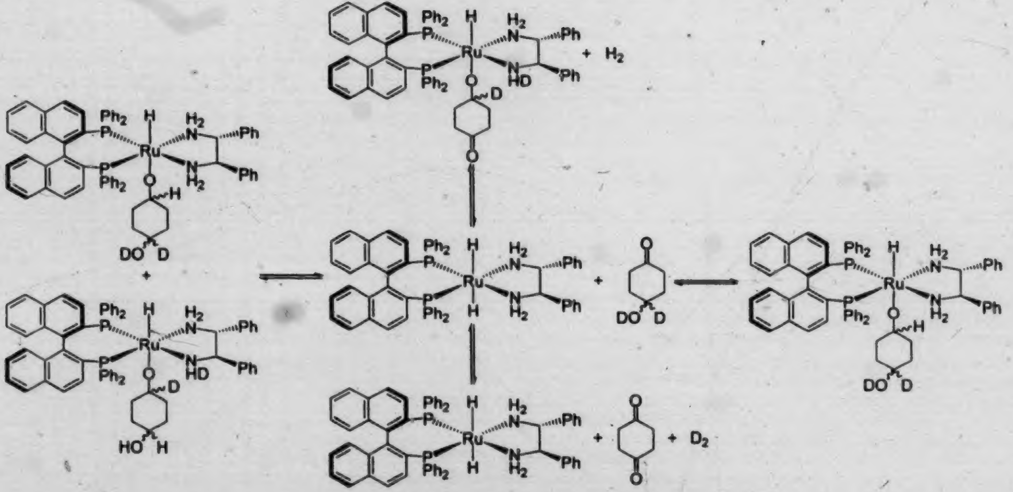

Scheme 5.4: Proposed intramolecular trapping experiments.

5.4 left). This experiment is complicated by several factors. Since the reduction is reversible, the 4-hydroxy-d_2-cyclohexanone may be oxidized to 1,4-cycolhexanedione (Scheme 5.4 bottom). The 1,4-cycolhexanedione would be reduced by **6** to form a Ru-alkoxide, but would provide no information about the pathway of formation. Additionally, I found that the Ru-alkoxide species readily exchange with alcohols in solution. Therefore, there may still be a mixture of Ru-4-hydroxy-d_2-cyclohexanoxide and Ru-4-hydroxy-cyclohexanoxide-d_1 if the exchange reaction is rapid, even if the reduction occurs *via* a concerted process. One possible solution would be to perform the experiments in the absence of excess base since this would slow the rate of exchange. Further, if a catalyst can be made where the hydride is *trans* to a ligand with a weaker trans influence but still remain catalytically active, then perhaps the rates of the Ru-alkoxide formation and alkoxide exchange steps may be slow enough at low temperature to gain additional information.

The amide **11** reacts rapidly with H_2 at -80 °C to form the dihydride **6**. Previous kinetic studies, however, indicate that this reaction is the TLS in the catalytic cycle.[2a] The amide reacts reversibly with 2-PrOH to form the inactive Ru-2-propoxide compound as a catalyst resting state. In 2-PrOH solvent, the equilibrium favors the Ru-2-propoxide compound. Therefore, varying the amount of 2-PrOH may change the rate dependence on H_2. Further kinetic studies are required to determine whether the rate dependence on H_2 is caused by a low steady state concentration of the amide due to the presence of 2-PrOH.

I showed that the presence of 2-PrOH has a beneficial effect on the product *ee*. The rate of product formation, however, may be slower due to the formation of the inactive Ru-2-propoxide compound. The ideal amount of 2-PrOH required to maintain a high *ee*, while maximizing the rate of product formation, needs to be determined. Catalytic hydrogenations in various THF/2-PrOH solvent mixtures may give information about the amount of 2-PrOH that is required. The dihydride catalyst **6** can be prepared at low temperature in THF, and added to the ketone substrate dissolved in different THF/2-PrOH solvent mixtures. Subsequent determination of the *ee* and rate of reaction will demonstrate the ideal amount of 2-PrOH.

Deuterium labeling studies may provide useful information about the product formation step. Specifically, the kinetic isotope effect (KIE) could distinguish between a concerted metal-ligand bifunctional and a stepwise product formation pathway. To gain mechanistic information the KIE when the

Ru-H's and the dpen N-H's are exchanged for deuterium individually, and when both the Ru-H's and N-H's are exchanged for deuterium, needs to be investigated. The relative rates of the proton versus deuterium isotopologues can then be compared to determine the individual and overall KIE's. If the product of the individual KIE's is equal to the overall KIE, then product formation occurs *via* the bifunctional mechanism. If, however, the overall KIE is equal to one of the individual KIE then product formation occurs *via* a stepwise mechanism.

Measuring the KIE upon deuteration of the ruthenium catalyst is complicated by several factors. I found that the dihydride **6** reacts rapidly with one equiv of acetophenone, even at -80 °C making it nearly impossible to determine the relative rates of reaction. It may be possible to circumvent this complication by using a larger, less reactive substrate such as acetonapthone. A larger problem is controlling the deuteration of the ruthenium catalyst. The reaction between the amide and H_2 to form the dihydride is a reversible process. Therefore there will be deuterium scrambling amongst the Ru-H's and N-H's. The deuterium scrambling would make the observed KIE largely meaningless since it would be difficult to discern which isotopologue was responsible for the reduction of the ketone. It may be more practical to measure the KIE's of the reverse process, *i.e.* the oxidation of an alcohol to form a ketone, to gain mechanistic information. For example, the 1-phenylethanol isotopologues $C_6H_5CH(OH)CH_3$ (Scheme 5.5 top), $C_6H_5CD(OH)CH_3$ (Scheme 5.5 bottom), $C_6H_5CH(OD)CH_3$ (Scheme 5.5 right), and $C_6H_5CD(OD)CH_3$

(Scheme 5.5 left) can be reacted with the amide, and the relative rates of acetophenone production can be determined. Similar to the KIE of the hydrogenation reaction, if the product of the individual KIE's is equal to the overall KIE, then there is direct evidence for a bifunctional mechanism. If, however, the product of the individual KIE's does not equal the overall KIE, then a stepwise mechanism is inferred. One complication is that the hydrogen produced during this reaction must be removed to avoid hydrogenation of the acetophenone.

The dihydride **6** is a very active hydrogenation catalyst. Therefore it may be used to hydrogenate other substrates containing polar bonds such as aldehydes, esters and imines. Subsequent mechanistic investigations may provide further insight into the catalytic cycle. The amide **11** is also a very reactive species. It heterolytically cleaves both H-H, and O-H bonds, to form dihydride, and Ru-alkoxide, respectively. Therefore, it may be possible to

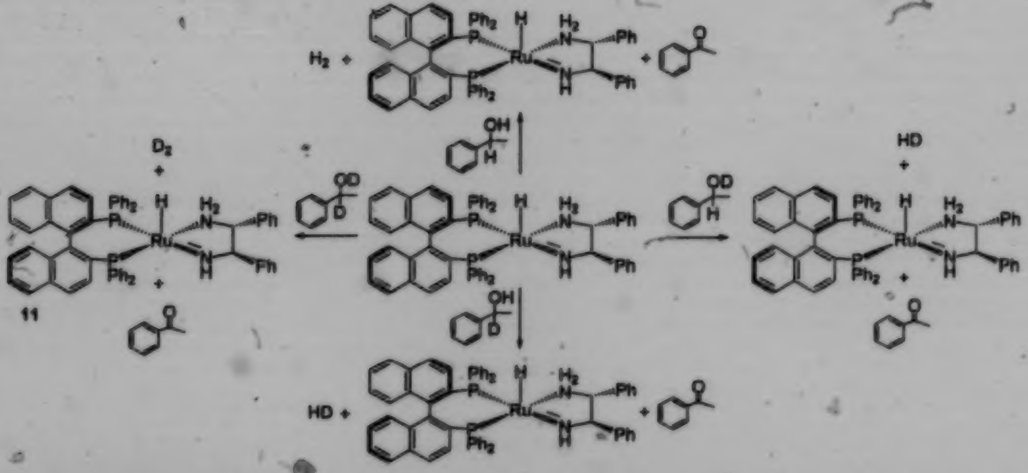

Scheme 5.5: Proposed reactivity for the oxidation of deuterium-labeled 1-phenylethanol.

develop new catalytic reactions using **11** to cleave other bonds to afford new products.

Overall, this work is the most detailed mechanistic investigation of the hydrogenation of ketones using the Noyori *et al.*'s catalyst system, *trans*-[Ru((*R*)-BINAP)$(H)_2$((*R*,*R*)-dpen)] (**6**). These studies represent the first conclusive identification, and full characterization, of the putative intermediates in the catalytic cycle. Additionally, I have shown that the reduction of ketones is reversible, and that 2-PrOH solvent inhibits the reverse process and preserves the high *ee* of the product alcohol. Futher, these studies indicate that the reduction step may not occur *via* the metal-ligand bifunctional mechanism as originally proposed, but rather through a concerted process to form a Ru-alkoxide compound. Computational studies in collaboration with other groups may determine if the concerted formation of **14** is an energetically feasible process.

References

(1) For reviews see (a) Noyori, R.; Yamakawa, M.; Hashiguchi, S. *J. Org. Chem* **2001**, *66*, 7931-7944. (b) Noyori, R.; Kitamura, M.; Ohkuma, T. *Proc. Natl. Acad. Sci U.S.A* **2004**, *101*, 5356-5362. (c) Noyori, R.; Sandoval, C. A.; Muñiz, K.; Ohkuma, T. *Phil. Trans. R. Soc. A.* **2005**, *363*, 901-912. (d) Muñiz, K. *Angew. Chem. Int. Ed.* **2005**, *44*, 6622-6627. (e) Gladiali, S.; Alberico, E. *Chem. Soc. Rev.* **2006**, *35*, 226-236. (f) Samec, J. S. M.; Bäckvall, J.-E.; Andersson, P. G.; Brandt, P. *Chem. Soc. Rev.* **2006**, *35*, 237-248. (g) Ikariya, I.; Blacker, A. J. *Acc. Chem. Res.* **2007**, *44*, 1300-1308. (h) Ito, M.; Ikariya, T. *Chem. Commun.* **2007**, *48*, 5134-5142. (i) Morris, R. H. In *Handbook of Homogeneous Hydrogenation*; de Vries, J. G., Elsevier, C. J., Eds.; Wiley-VCH: Weinheim, 2007; Vol. 1, p 45. (j) Ohkuma, T.; Noyori, R. In *Handbook of Homogeneous Hydrogenation*; de Vries, J. G., Elsevier, C. J., Eds.; Wiley-VCH: Weinheim, 2007; Vol. 3, p 1105.

(2) (a) Sandoval, C. A.; Ohkuma, T.; Muniz, K.; Noyori, R. *J. Am. Chem. Soc.* **2003**, *125*, 13490-13503. (b) Ohkuma, T.; Sandoval, C. A.; Srinivasan, R.; Lin, Q.; Wei, Y.; Muniz, K.; Noyori, R. *J. Am. Chem. Soc.* **2005**, *127*, 8288-8289.

(3) (a) Abdur-Rashid, K.; Faatz, M.; Lough, A. J.; Morris, R. H. *J. Am. Chem. Soc.* **2001**, *123*, 7473-7474. (b) Abdur-Rashid, K.; Clapham, S. E.; Hadzovic, A.; Harvey, J. N.; Lough, A. J.; Morris, R. H. *J. Am. Chem. Soc.* **2002**, *124*, 15104-15118. (c) Clapham, S. E.; Hadzovic, A.; Morris, R. H. *Coord. Chem. Rev.* **2004**, *248*, 2201-2237. (d) Abbel, R.; Abdur-Rashid, K.; Faatz, M.;

Hadzovic, A.; Lough, A. J.; Morris, R. H. *J. Am. Chem. Soc.* **2005**, *127*, 1870-1882. (e) Hadzovic, A.; Song, D.; MacLaughlin, C. M.; Morris, R. H. *Organomettalics* **2007**, *26*, 5987-5999.

(4) (a) Casey, C. P.; Singer, S. W.; Powell, D. R.; Hayashi, R. K.; Kavana, M. *J. Am. Chem. Soc.* **2001**, *123*, 1090-1100. (b) Casey, C. P.; Johnson, J. B. *J. Am. Chem. Soc.* **2005**, *127*, 1883-1894. (c) Casey, C. P.; Johnson, J. B.; Singer, S. W.; Cui, Q. *J. Am. Chem. Soc.* **2005**, *127*, 3100-3109. (d) Casey, C. P.; Bikzhanova, G. A.; Cui, Q.; Guzei, I. A. *J Am. Chem. Soc.* **2005**, *127*, 14062-14071. (e) Casey, C. P.; Bikzhanova, G. A.; Guzei, I. A. *J Am. Chem. Soc.* **2006**, *128*, 2286-2293.(f) Casey, C. P.; Clark, T. B.; Guzei, L. A. *J. Am. Chem. Soc* **2007**, *129*, 11821-11827. (g) Casey, C. P.; Beetner, S. E.; Johnson, J. B. *J. Am. Chem. Soc.* **2008**, *130*, 2285-2295.

(5) Hedberg, C.; Kallstrom, K.; Arvidsson, P. I.; Brandt, P.; Andersson, P. G. *J. Am. Chem. Soc.* **2005**, *127*, 15083-15090.

(6) (a) Baratta, W.; Chelucci, G.; Gladiali, S.; Siega, K.; Toniutti, M. Z.; Zangrando, E.; Rigo, P. *Angew. Chem. Int. Ed.* **2005**, *44*, 6214-6219. (b)Baratta, W.; Siega, K.; Rigo, P. *Chem. Ur. J.* **2007**, *13*, 7479-7486.

(7) (a) Hamilton, R. J.; Leong, C. G.; Bigam, G.; Miskolzie, M.; Bergens, S. H. *J. Am. Chem. Soc.* **2005**, *127*, 4152-4153. (b) Hamilton, R. J.; Bergens, S. H. *J. Am. Chem. Soc.* **2006**, *128*, 13700-13701.

(8) (a) Johnson, J. B.; Bäckvall, J.-E. *J. Org. Chem.* **2003**, *123*, 7681-7684. (b) Åberg, J. B.; Samec, J. S. M.; Bäckvall, J.-E. *Chem. Commun.* **2006**, 2771-2773. (c) Samec, J. S. M.; Éll, A. H.; Åberg, J. B.; Privalov, T.; Eriksson, L.;

Bäckvall, J.-E. *J. Am. Chem. Soc.* **2006**, *128*, 14293-14305. (d) Privalov, T.; Samec, J. S. M.; Bäckvall, J.-E. *Organometallics* **2007**, *26*, 2840-2848.

(9) (a) Yamakawa, M.; Ito, H.; Noyori, R. *J. Am. Chem. Soc.* **2000**, *122*, 1466-1478. (b) Handgraaf, J. –W.; Reek, J. N. H.; Meijer, E. J. *Organometallics*, **2003**, *22*, 3150-3157. (c) Handgraaf, J. –W.; Meijer, E. J. *J. Am. Chem. Soc.* **2007**, *129*, 3099-3103. (d) Tommaso, D. D.; French, S. A.; Catlow,C. R. A. *J. Mol. Struct. (THEOCHEM)* **2007**, *812*, 39-49. (e) Comas-Vives, A.; Ujaque, G.; Lledos, A. *Organometallics* **2007**, *26*, 4135-4144. (f) Tommaso, D. D.; French, S. A.; Zanotti-Gerosa, A.; Hancock, F.; Palin, E. J.; Catlow, C. R. A. *Inor. Chem.* **2008**, *47*, 2674-2687. (g) Leyssens, T.; Peeters, D.; Harvey, J. N. *Organometallics* **2008**, 27, 1514-1523.

Appendix 1: NMR spectra.

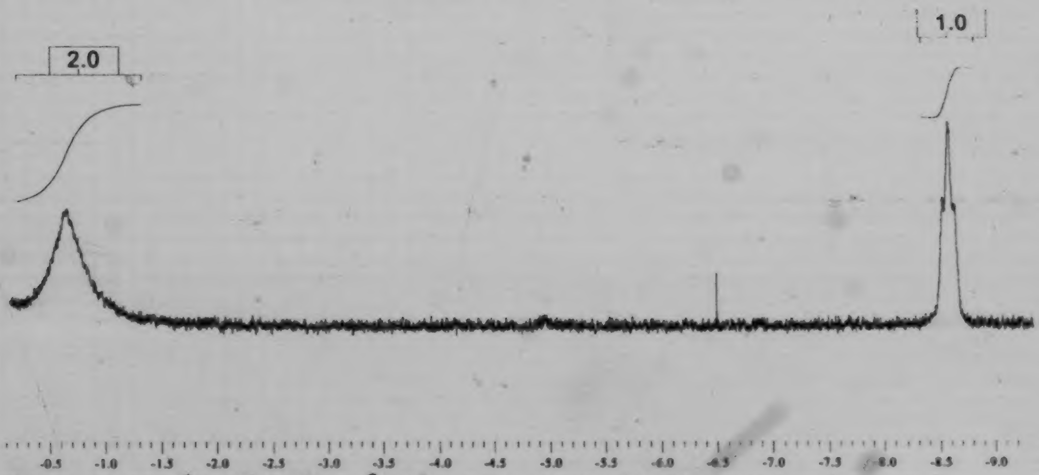

Figure A1.1: ^{1}H NMR Ru–η^2-H_2 and Ru–H signals for complex **1**.

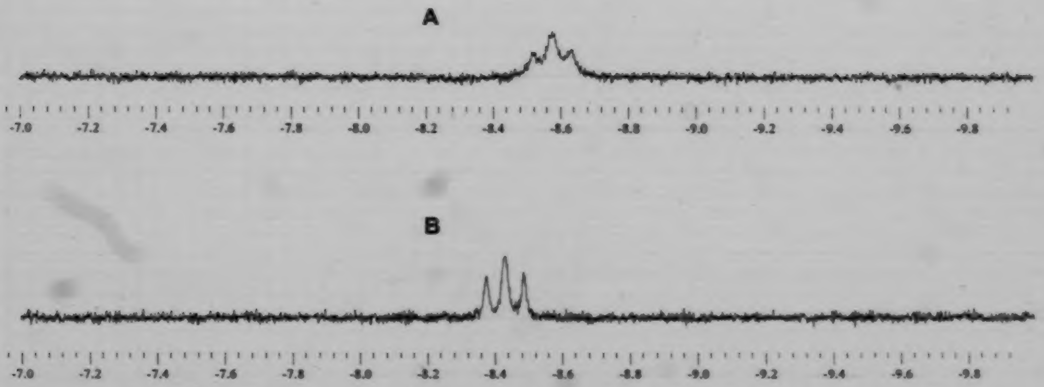

Figure A1.2: (A) ^{1}H NMR Ru–H signal trans to η^2–H_2 in complex **1**. (B) ^{1}H NMR Ru–H signal trans to η^2–D_2 in complex **89**, prepared by bubbling D_2 through solutions of **1** at -60 °C.

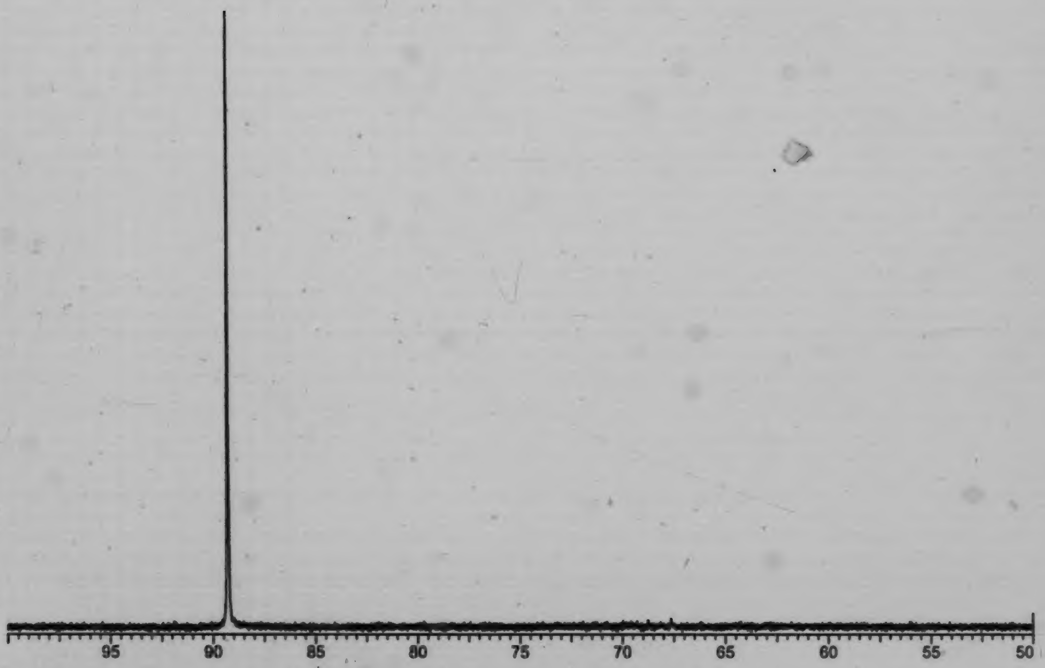

Figure A1.3: $^{31}P\{^1H\}$ NMR spectrum of **6** at –60 °C.

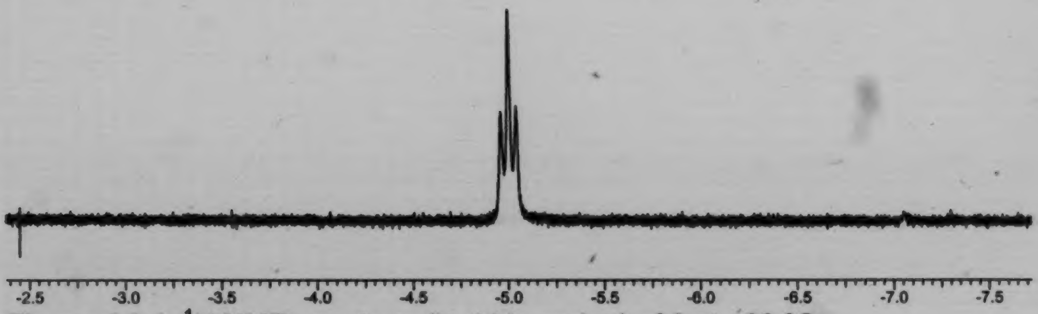

Figure A1.4: ^{1}H NMR spectrum (hydride region) of **6** at –60 °C.

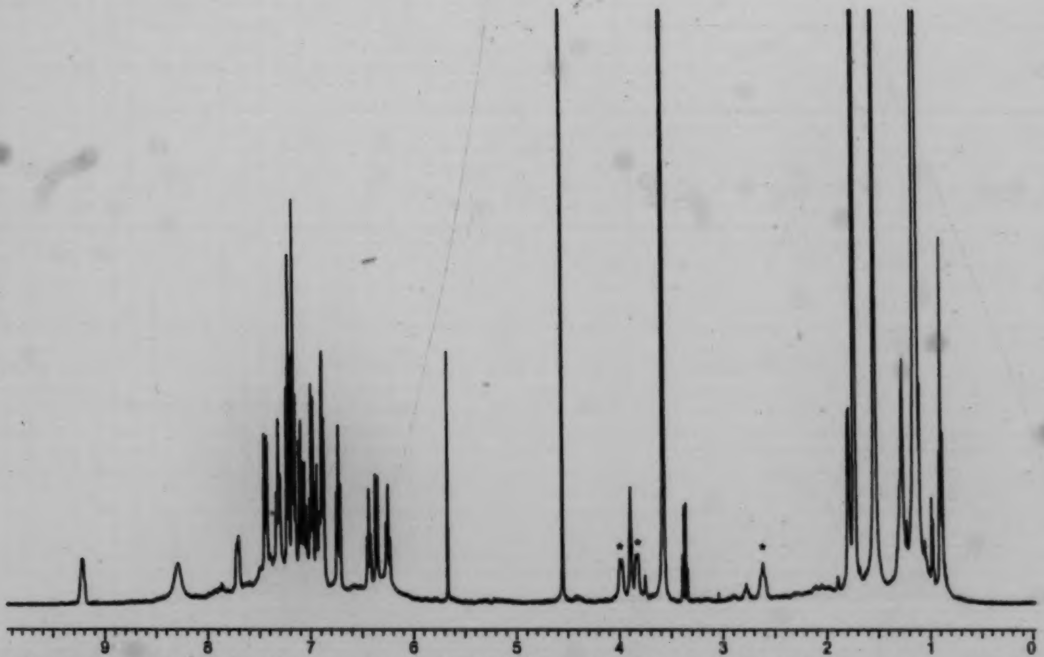

Figure A1.5: ^{1}H NMR spectrum (0 to 10 ppm) of **6** at –60 °C. The non-aromatic peaks assigned to **6** are marked with an asterisk. The remaining peaks are due to residual protons in the deuterated solvent, the added base, H_2, cyclooctane and cyclooctene (produced during hydrogenation of the precursor [Ru(BINAP)((1-5-η)-C_8H_{11})](BF_4), and traces of diethyl ether, hexanes, or CH_2Cl_2, if present.

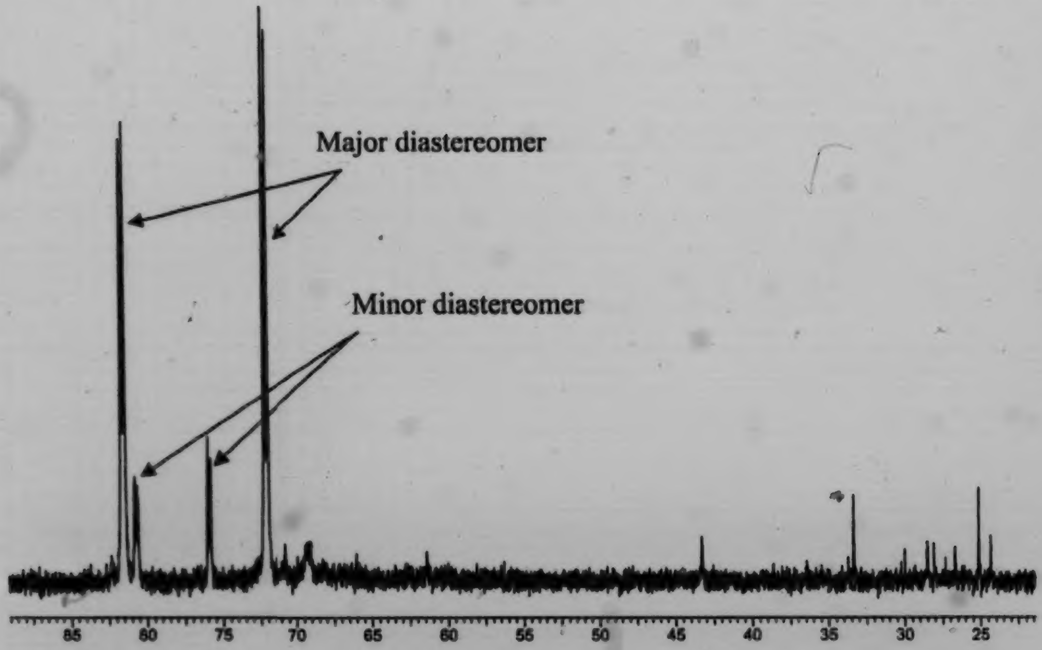

Figure A1.6: $^{31}P\{^{1}H\}$ NMR spectrum of **11** at –60 °C. The remaining, small peaks are from decomposition products formed during the hydrogenation of the precursor [Ru(BINAP)((1-5-η)-C_8H_{11})](BF_4).

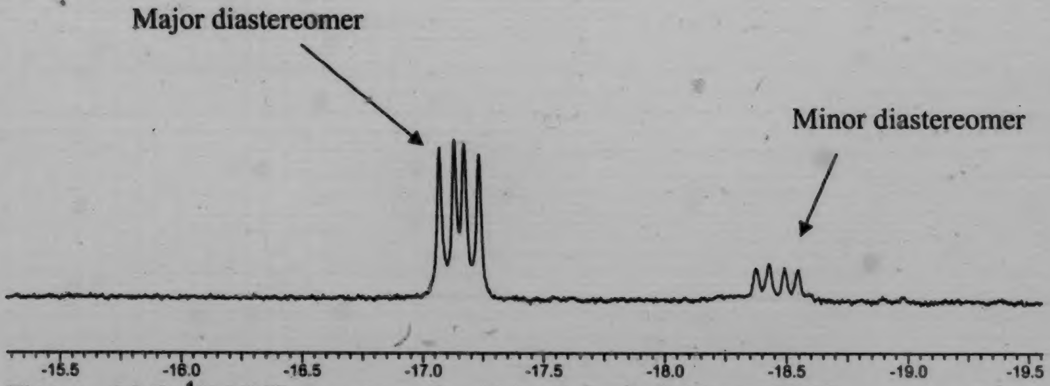

Figure A1.7: ^{1}H NMR spectrum (hydride region) of **11** at –60 °C.

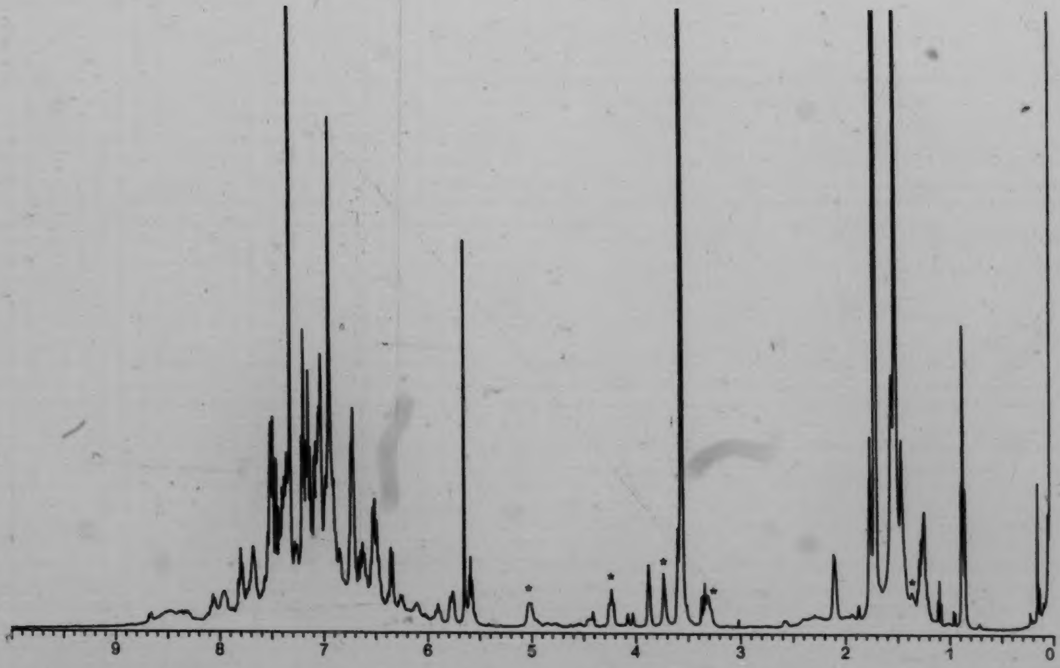

Figure A1.8: ^{1}H NMR spectrum (1 to 10 ppm) of **11** at –60 °C. The non aromatic peaks assigned to the major diasteromer are marked with an asterisk. The remaining peaks are due to residual protons in the deuterated solvent, the added base, H_2, cyclooctane and cyclooctene (produced during hydrogenation of the precursor [Ru(BINAP)((1-5-η)-C_8H_{11})](BF_4), and traces of diethyl ether, hexanes, or CH_2Cl_2, if present.

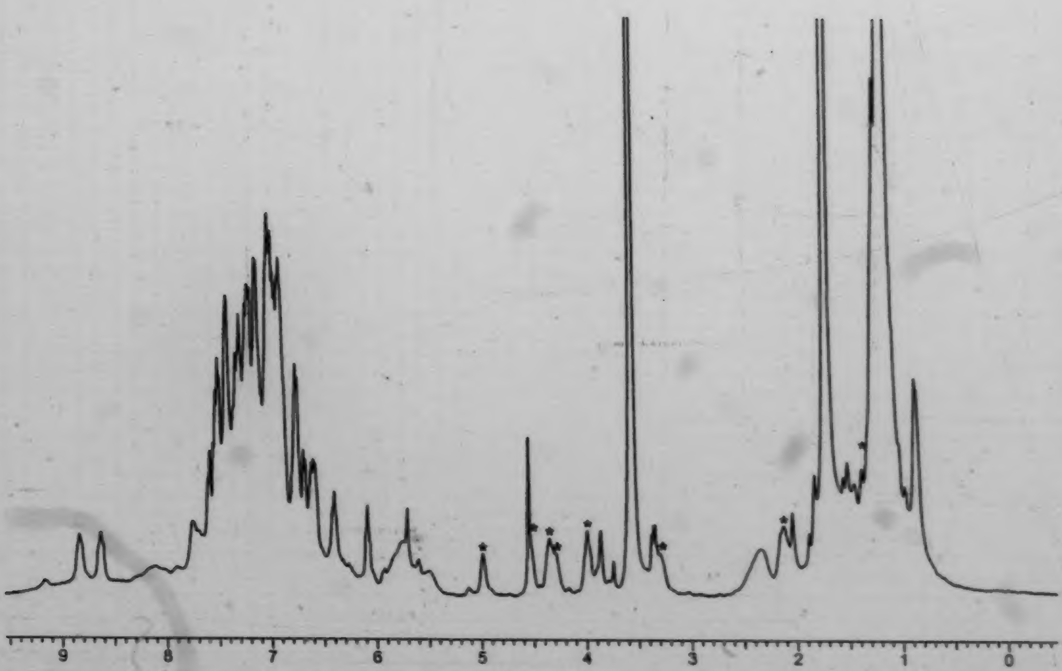

Figure A1.9: ^{1}H NMR spectrum (-1 to 10 ppm) of **14** at –80 °C. The non-aromatic peaks assigned to **14** are marked with an asterisk. The remaining peaks are due to residual protons in the deuterated solvent, the added base, H_2, cyclooctane and cyclooctene (produced during the hydrogenation of the precursor [Ru((*R*)-BINAP)((1-5-η)-C_8H_{11})](BF_4), and traces of diethyl ether, hexanes, or CH_2Cl_2, if present.

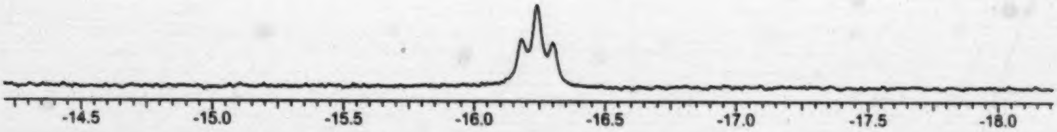

Figure A1.10: ^{1}H NMR spectrum (hydride region) of **14** in the presence of ~1.5 equiv of excess base at –80 °C. Neither the dihydride **6** nor the amide **11** were detected.

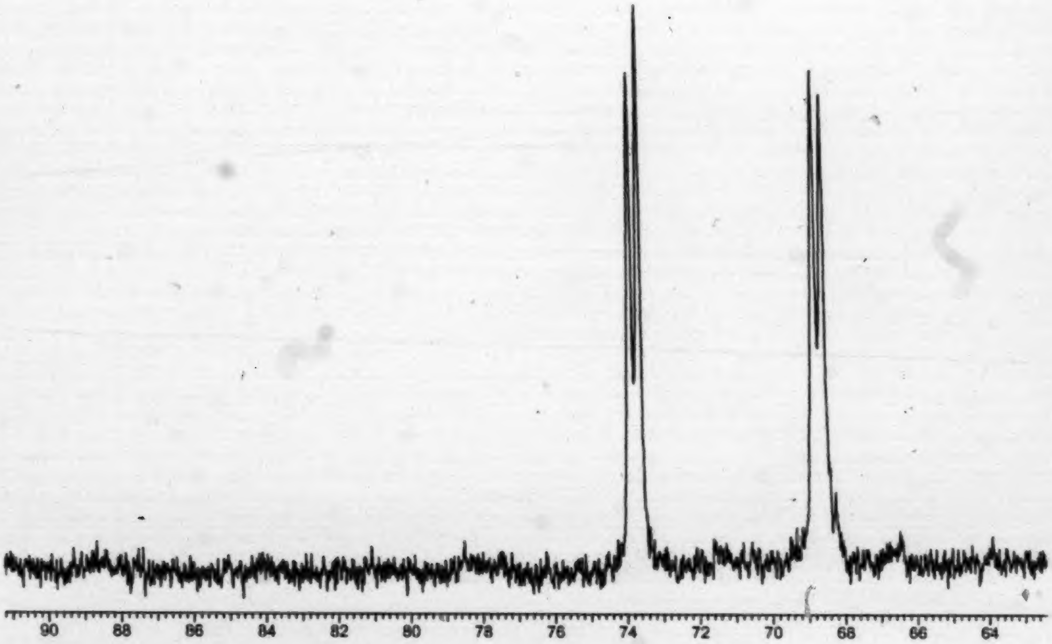

Figure A1.11: $^{31}P\{^{1}H\}$ NMR spectrum of **14** at –80 °C.